STRUCTURAL GEOMETRY OF THRUST FAULTING IN THE BAKER MOUNTAIN AND PANOLA QUADRANGLES, SOUTHEASTERN OKLAHOMA

By

JUSTIN EVANS

Bachelor of Science

Oklahoma State University

Stillwater, Oklahoma

1995

Submitted to the Faculty of the
Graduate College of the
Oklahoma State University
in partial fulfillment of
the requirements for
the Degree of
MASTER OF SCIENCE
July, 1997

STRUCTURAL GEOMETRY OF THRUST FAULTING IN THE BAKER MOUNTAIN AND PANOLA QUADRANGLES, SOUTHEASTERN OKLAHOMA

Thesis Approved:

Ibrahim Cemen
Thesis Advisor

Eric M. Rivers

Casey J. Stewart

Thomas C. Collins
Dean of Graduate College

ACKNOWLEDGMENTS

I would like to extend my deepest thanks to my committee chair, Dr. Ibrahim Cemen. His advice, knowledge, and guidance have been a great help throughout this study. I would also like to thank my other committee members, Dr. Zuhair Al-Shaieb for his help and expertise as well as for the use of lab equipment to finish this study, and to Dr. Gary Stewart for advice, guidance, and editing.

My thanks also go out to Jeff Ronck and Syed Mehdi for their help, and viewpoints when mine got narrow. I also want to thank Dr. Jim Puckette for his help in everything from geology to life. Thank you so much. Thanks also to Catherine Price for help and support with the computers.

Thanks to Neil Suneson for OGS well log information and for unpublished map interpretations by him, C. A. Ferguson and L. R. Hemish.

Thank you Mom and Dad for your love, moral, and financial support. You always taught me to push my boundaries and look over the next horizon.

Finally, and most importantly, thank you to my wife Julie. Without your love and support I never would have been able to finish this work. This is for you.

TABLE OF CONTENTS

Chapter Page

I. INTRODUCTION 1

Statement of Purpose and Methods of Investigation 3

Previous Investigations 6

Tectonics of the Ouachita Mountains 6

Arkoma Basin 10

Red Oak Gas Field 14

II. STRATIGRAPHY OF THE ARKOMA BASIN 16

III. DIAGENESIS AND DEPOSITIONAL

ENVIRONMENT OF THE SPIRO SANDSTONE 28

DIAGENESIS 28

Detrital Constituents 28

Cements 30

Diagenetic Clays 30

Porosity 32

Diagenetic Sequence 32

DEPOSITIONAL ENVIRONMENT 35

IV. GEOMETRY OF THRUST SYSTEMS 36

THRUST SYSTEMS 36

IMBRICATE FANS 36

BREAK-FORWARD THRUST SEQUENCES 38

FAULT-BEND FOLDING 40

BREAK-BACKWARD THRUST SEQUENCES 45

DUPLEX STRUCTURES 49

BACKTHRUSTS 51

TRIANGLE ZONES 51

V. STRUCTURAL GEOLOGY 58

INTRODUCTION 58

MAJOR THRUST FAULTS 73

Winding Stair Fault 73

Choctaw Detachment 74

Ti Valley Fault 74

Pine Mountain Fault 77

Choctaw Fault 77

BASAL DETACHMENTS 79

DUPLEX STRUCTURES AND THE LOWER ATOKAN DETACHMENT 81

TRIANGLE ZONE 83

NORMAL FAULTS AND STRIKE SLIP FAULTS 84

RESTORED CROSS SECTIONS AND SHORTENING 84

VI. CONCLUSIONS 93

REFERENCES 94

APPENDIX I 99

LIST OF FIGURES

Figure Page

1. Geologic Provinces of Oklahoma 2

2. Location Map 4

3. Deviated well depth 7

4. Evolution of southern margin of North America 9

5. Stratigraphy and deposition 11

6. Depositional setting of Atoka time 12

7. Stratigraphic chart for the Arkoma Basin and Ouachita Mountains 17

8. Stratigraphic chart for Atokan time 18

9. Log signature for the Spiro sandstone 22

10. Log signature for the Cecil sandstone 24

11. Log signature for the Panola sandstone 25

12. Log signature for the Red Oak sandstone 26

13. Stratigraphic chart for Desmoinesian Series 27

14. Photomicrograph of Spiro sandstone showing detrital constituents 29

15. Photomicrograph of Spiro sandstone showing chlorite clay 31

16. Photomicrograph of Spiro sandstone showing primary porosity modification 33

17. Photomicrograph of Spiro sandstone showing compaction 34

18. Thrust systems 37

19. Break-forward thrust system 39

20. "S" shaped bending of beds in duplexes 41

21. Fault bend fold over a step in décollement 42

22. Fault end folding 43

23. Fault propagation folding 44

24. Folding styles 46

25. Kink bend folding 47

26. Break-backward thrusting 48

27. Rotation of horses due to a hindrance 50

28. Antiformal stack 52

29. Foreland dipping duplex 53

30. Back-thrust 54

31. Triangle zone (McClay, 1992) 54

32. Three end member geometries of triangle zones 56

33. Simplified triangle zone 57

34. Triangle zone from Arbenz (1984) 59

35. Triangle zone from Arbenz (1989) 59

36. Triangle zone from Hardie (1988) 60

37. Triangle zone from Milliken (1988) 60

38. Triangle zone from Camp & Ratliff (1989) 62

39. Triangle zone from Reeves et al. (1990) 62

40. Triangle zone from Perry et al. (1990) 63

41. Duplex structure from Roberts (1992) 63

42. Structural cross-section from Wilkerson and Wellman (1993) 64

43. Simplified map showing location of cross-sections and seismic lines 66

44. Balanced structural cross-section A-A' 67

45. Balanced structural cross-section B-B' 68

46. Balanced structural cross-section C-C' 69

47. Balanced structural cross-section D-D' 70

48. Balanced structural cross-section E-E' 71

49. Seismic line QM5-8 72

50. General geology and tectonic map 75

51. Northern Choctaw Fault interpretation 78

52. Structural cross-section from Sagnak (1995) 82

53. Restored cross-section A-A' 85

54. Restored cross-section B-B' 86

55. Restored cross-section C-C' 87

56. Restored cross-section D-D' 88

57. Restored cross-section E-E' 89

LIST OF PLATES

I. Balanced and Restored Cross-Section A-A' ..... In Pocket

II. Balanced and Restored Cross-Section B-B' ..... In Pocket

III. Balanced and Restored Cross-Section C-C' ..... In Pocket

IV. Balanced and Restored Cross-Section D-D' ..... In Pocket

V. Balanced and Restored Cross-Section E-E' ..... In Pocket

VI. Seismic line QM5-8 ..... In Pocket

VII. Simplified Geological Map of the Study Area ..... In Pocket

Chapter 1

INTRODUCTION

The Arkoma Basin and Ouachita Mountains are tectonic features extending through southeastern Oklahoma and west-central Arkansas (Figure 1). The mountain front of the Ouachitas extends from west-central Arkansas to southeastern Oklahoma and is separated from the Ozark Plateau by the Arkoma Basin. The Arkoma Basin is considered a foreland basin that developed as a result of compressional tectonics that formed the Ouachita Mountains. Based on structural geology and stratigraphy, the Ouachita mountains are composed of three assemblages: the frontal belt, central belt, and Broken Bow Uplift.

The frontal belt is bounded to the north by the surface exposure of the Choctaw fault and to the south by the Winding Stair fault. The belt contains imbricately thrusted, folded, and tilted Morrowan shallow-water sedimentary rocks to Atokan turbidite facies. The central belt is characterized by broad synclines separated by narrow anticlines. Mississippian and Lower Pennsylvanian turbidites are exposed throughout the belt, with the exception of pre-Mississippian rocks in the Potato Hills (Suneson and others, 1990). The Broken Bow Uplift is composed of Lower Ordovician to Lower Mississippian deep-

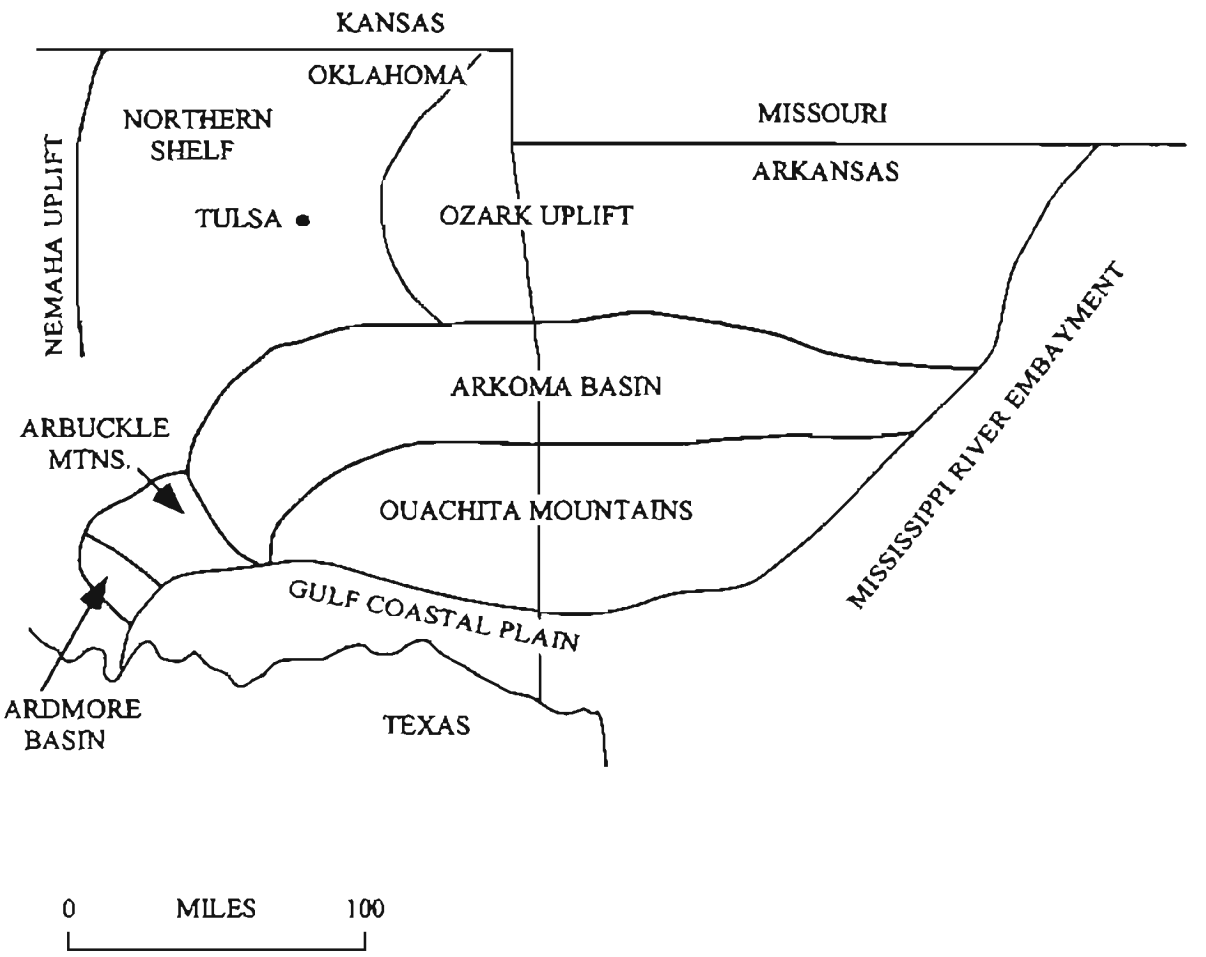

Figure 1: Major geologic provinces of eastern Oklahoma and western Arkansas (from Johnson, 1988).

water strata. In this uplift, strata are isoclinally folded as well as thrusted (Suneson and others 1990).

The Arkoma Basin is a mixed assemblage of structural styles ranging from extensional to compressional (Arbenz, 1989). In Oklahoma, the northern boundary is the southern limit of the Ozark Uplift. The southern boundary is defined by the trace of the Choctaw Fault. This bounding fault dies out in western Arkansas, where the northern and southern boundaries of the basin are defined respectively by the termination of folding to the north and the next major thrust fault to the south.

STATEMENT OF PURPOSE AND METHODS OF INVESTIGATION

The study area covers the Panola and Baker Mountain Quadrangles Oklahoma (U.S. Geological Survey, 1988 and 1989. respectively) (Figure 2). The main purpose of this study was to delineate the subsurface structural geometry of the area through the construction of balanced structural cross-sections in the Baker Mountain and Panola Quadrangles (T3N-6N, R20E) in Latimer County, Oklahoma.

In accordance with the main purpose of this study, the following information was used to prepare the necessary maps and structural cross-sections:

1) Unpublished areal geologic maps by Neil Suneson, C.A. Ferguson, and LeRoy Hemish of the Oklahoma Geological Survey were used to prepare a simplified geologic map of the study area.

2) Spontaneous potential (SP), gamma ray, and resistivity/conductivity logs obtained from

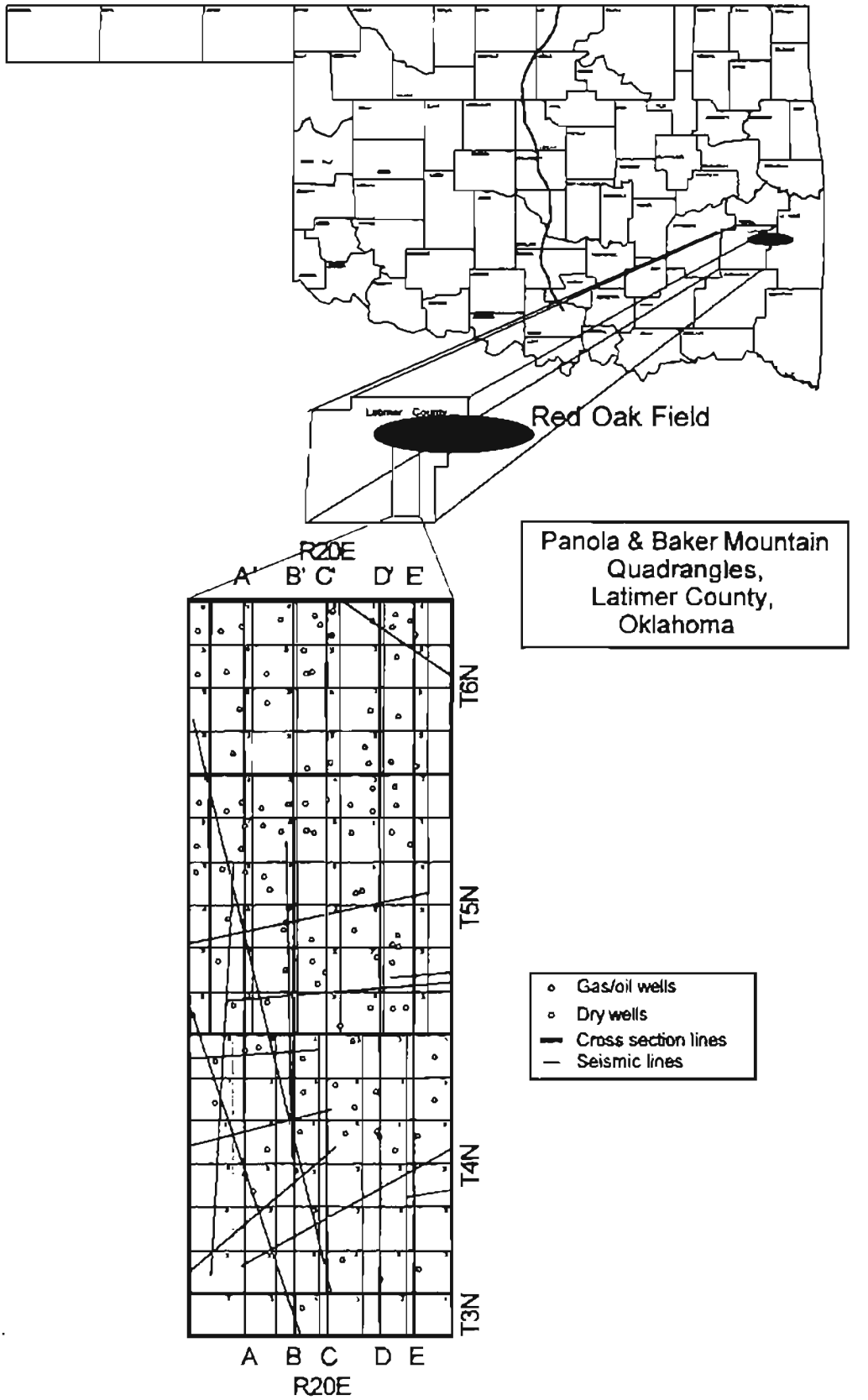

Figure 2. Location map of study area

the available well logs in both the Oklahoma City and Tulsa well-log libraries were used to locate the stratigraphic positions of the Spiro, Red Oak, Panola, Cecil and Hartshorne sandstones. These rock-stratigraphic units were extensively used in construction of the balanced structural cross-sections.

3) Scout tickets were used to locate and learn the log signatures of the rock units that were used to construct balanced structural cross-sections.

4) Seismic profiles donated by Amoco and Exxon were the documents for interpretation of subsurface structural geometry.

These data were employed to construct five balanced structural cross-sections, which were restored by the key-bed-method, based on thickness of the Spiro sandstone. The balanced cross-sections were the basis for estimation of the amount of shortening due to thrusting. Analysis of eleven thin sections from three outcrops of the Spiro sandstone within the study area were analyzed to determine sediment type, possible source, diagenesis, and porosity. X-ray diffraction was also performed on these samples to determine the types of clays in the samples.

All structural cross-sections trend more-or-less perpendicular to the axes of the major structural features. This orientation makes them "parallel" to the inferred tectonic transport direction, and they should yield the most accurate geometry. The seismic profiles used in the study had the same orientation. For the construction of the cross-sections, data concerning the Spiro, Red Oak, Panola, Cecil, and Hartshorne sandstones were interpreted from well-log signatures. Horizontal scale of the cross-sections is in 1:24,000 map scale; vertical scale is 1:12,000. These cross-sections are included as Plates

I-V, which were digitized by the Canvas program.

Oil wells in this study were assumed to have vertical boreholes, unless data about deviation were available. Where deviations were shown on scout tickets, vertical depths to formations commonly were reported as well. Where vertical depths were not reported, a simple geometric method was used to plot depths to formations (Figure 3).

The term "Spiro" used in this study and on the cross-sections actually refers to the Spiro sandstone-Wapanucka Limestone package. The Spiro sandstone and Wapanucka Limestone were not differentiated individually.

PREVIOUS INVESTIGATIONS

TECTONICS OF THE OUACHITA MOUNTAINS

The Ouachita Mountains and the Arkoma Basin are tectonic features that formed in Early and Middle Pennsylvanian. The Arkoma Basin is an elongate tectonic province that extends about 250 miles across parts of eastern Oklahoma and western and central Arkansas (Figure 1). The basin is bounded to the south by the frontal belt of the Ouachita Mountains, to the southwest by the Arbuckle Mountains, to the north by the Ozark uplift, and grades onto the Cherokee platform to the northwest (Johnson, 1988).

The formation of the Arkoma Basin has been interpreted as the result of the opening and closing of the Iapetus (the proto-Atlantic) ocean basin (Houseknecht and McGilvery, 1990). During Late Precambrian-Early Cambrian, a major episode of rifting opened an ocean basin along the southern margin of North America (Figure 4a). The

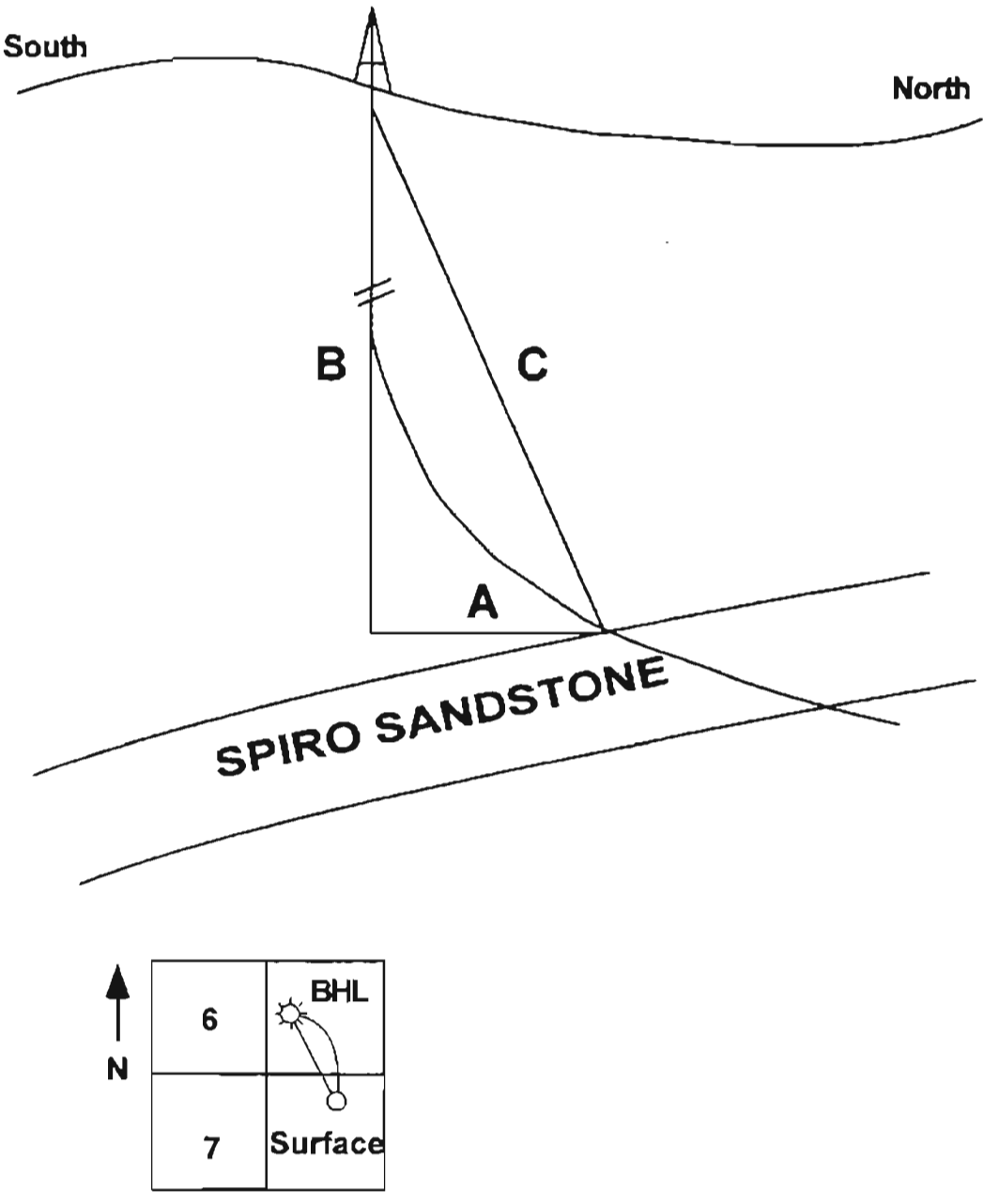

Figure 3. Simplified model for figuring depth in deviated wells.

southern margin of North America became a passive continental margin. The shelf system that formed adjacent to this passive margin persisted until Middle Paleozoic (Figure 4b).

Sediments deposited on the shelf include Cambrian through lower Atokan. These include deep and shallow marine as well as nonmarine sandstones, shales, and carbonates. To the south, deeper water environments received sheet sands, dark shales, deep-water limestones, and some submarine-fan-complex sediments. These deeper-water sediments can now be found in the Ouachita Mountains with the deepest water sediments in the core of the frontal Ouachitas as a result of extensive thrusting (Houseknecht and McGilvery, 1990).

During the Devonian or Early Mississippian, the Iapetus ocean began to close as a subduction zone formed beneath a southern continental mass referred to as Llanoria (Figure 4c). The presence of the subduction zone is evidenced by the widespread metamorphic event in the Lower Devonian, and locally abundant amounts of volcanic debris in the form of flysch sedimentary rocks within the Mississippian Stanley Shale (Houseknecht, 1986). Subsurface Mississippian volcanic rocks in the Sabine Uplift to the south of the Ouachitas suggest a magmatic arc that developed on the northern margin of Llanoria, as a part of the subduction zone complex.

The northward advancing accretionary prism scraped sediments off of the subducting plate during Early Mississippian to earliest Atokan time (Figure 4c). Continued subduction along the northern margin of Llanoria closed the proto-Atlantic (Iapetus) ocean by early Atokan time (Figure 4d). The southern margin of the North American continent underwent flexural bending as the accretionary prism was obducted

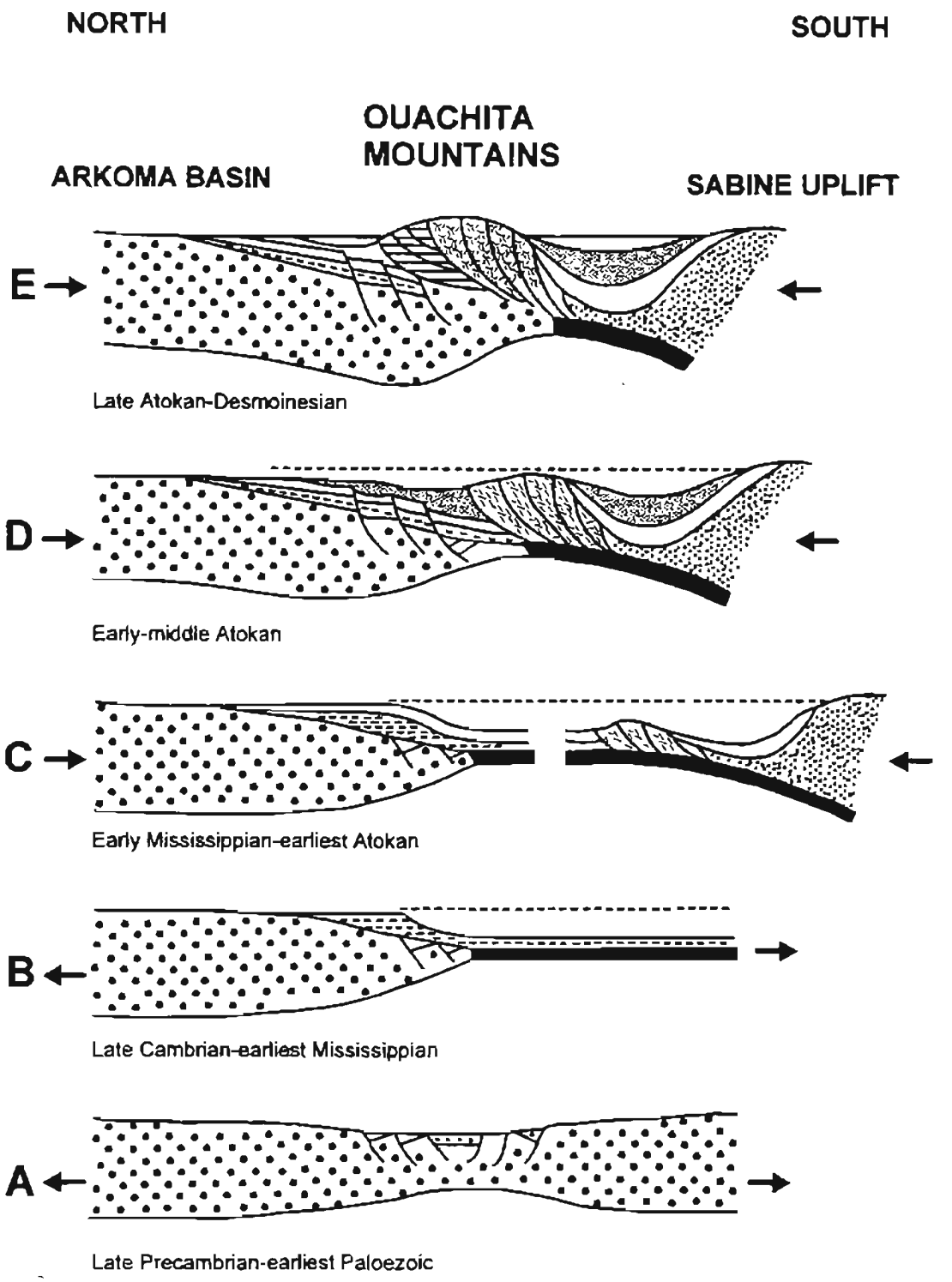

Figure 4: Diagrammatic evolution of southern margin of North America (From Houseknecht and Kacena, 1983)

onto the continent (Houseknecht, 1986). Although the continent was undergoing compressional forces, the flexure caused normal faulting in the foreland. This faulting can be explained by tensional forces that resulted from the upwarping of land in response to loading and compression to the south (Houseknecht, 1986). The normal faults generally strike subparallel to the Ouachita orogenic belt, and most are downthrown to the south, offsetting both crystalline basement and overlying Cambrian trough sediments. Due to the normal faulting, subsidence and sedimentation were increased as the Arkoma foreland basin was formed (Houseknecht and McGilvery, 1990). Contemporaneous subduction and the deposition of lower through middle Atokan shales and sandstones resulted in marked variation in thickness across faults (Figure 5) (Houseknecht and McGilvery, 1990).

By late Atokan time, foreland-style thrusting became prevalent as the accretionary prism moved northward (Figure 4d and 4e). Flysch sediments were shed off of the accretionary prism and flooded the basin during its early stages (Sutherland, 1988). Shallow marine, deltaic, and fluvial sedimentation occurred in this basin (Figure 6). The structural configuration of the Arkoma-Ouachita system has remained relatively undisturbed since the Desmoinesian, although minor thrusting and folding did occur after the Desmoinesian (Figure 4e) (Houseknecht and Kacena, 1983).

ARKOMA BASIN

The Arkoma basin was first classified as a foreland basin by Buchanan and Johnson (1968). Arbenz (1989) studied the frontal Ouachita belt as well as the Arkoma basin and documented an assemblage of structural styles. He suggested that the southern two-thirds

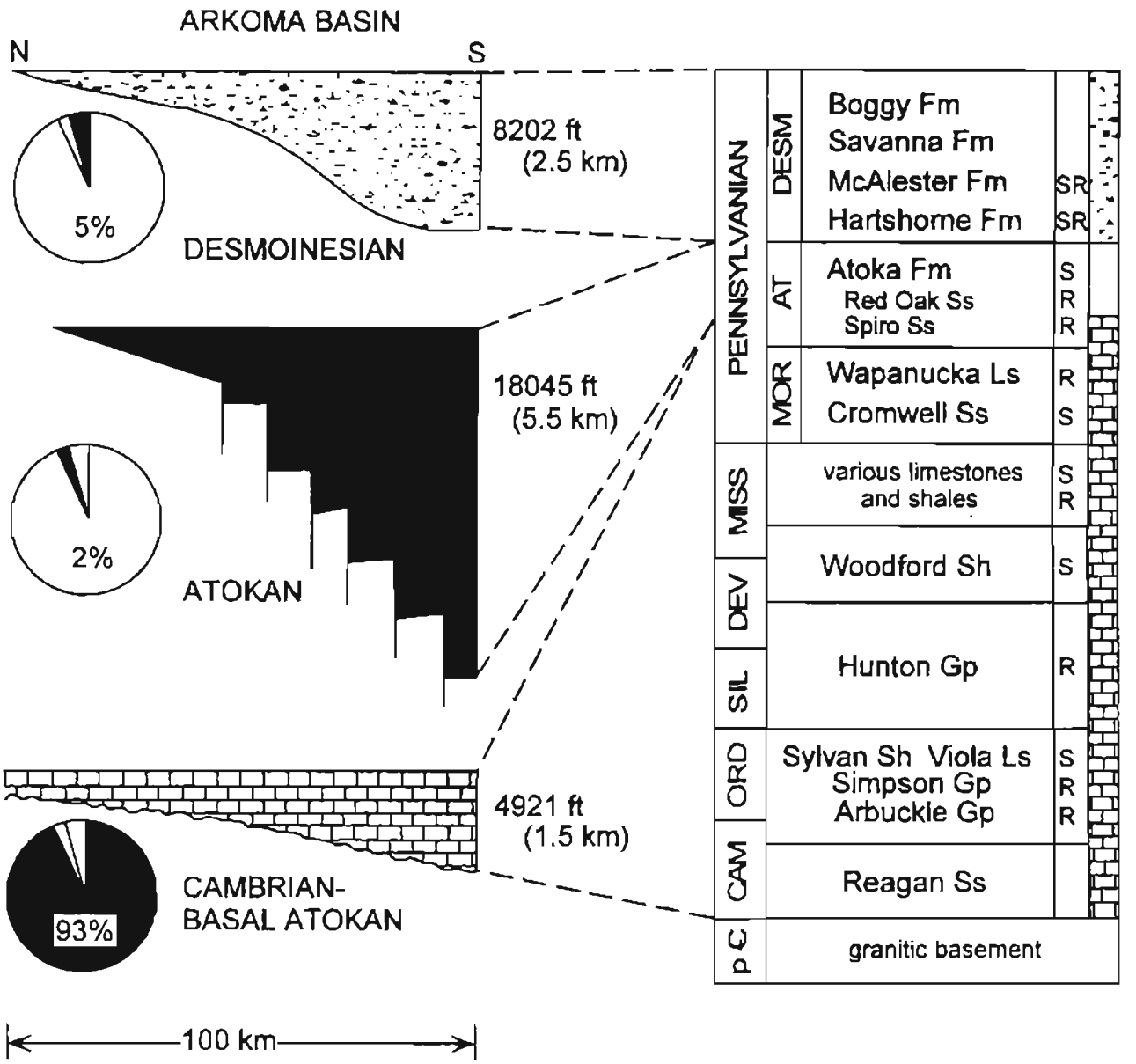

Figure 5. General stratigraphy of Oklahoma portion of the Arkoma Basin. Pie charts indicate percentage of total time for each depositional event (From Houseknecht and McGilvery, 1990).

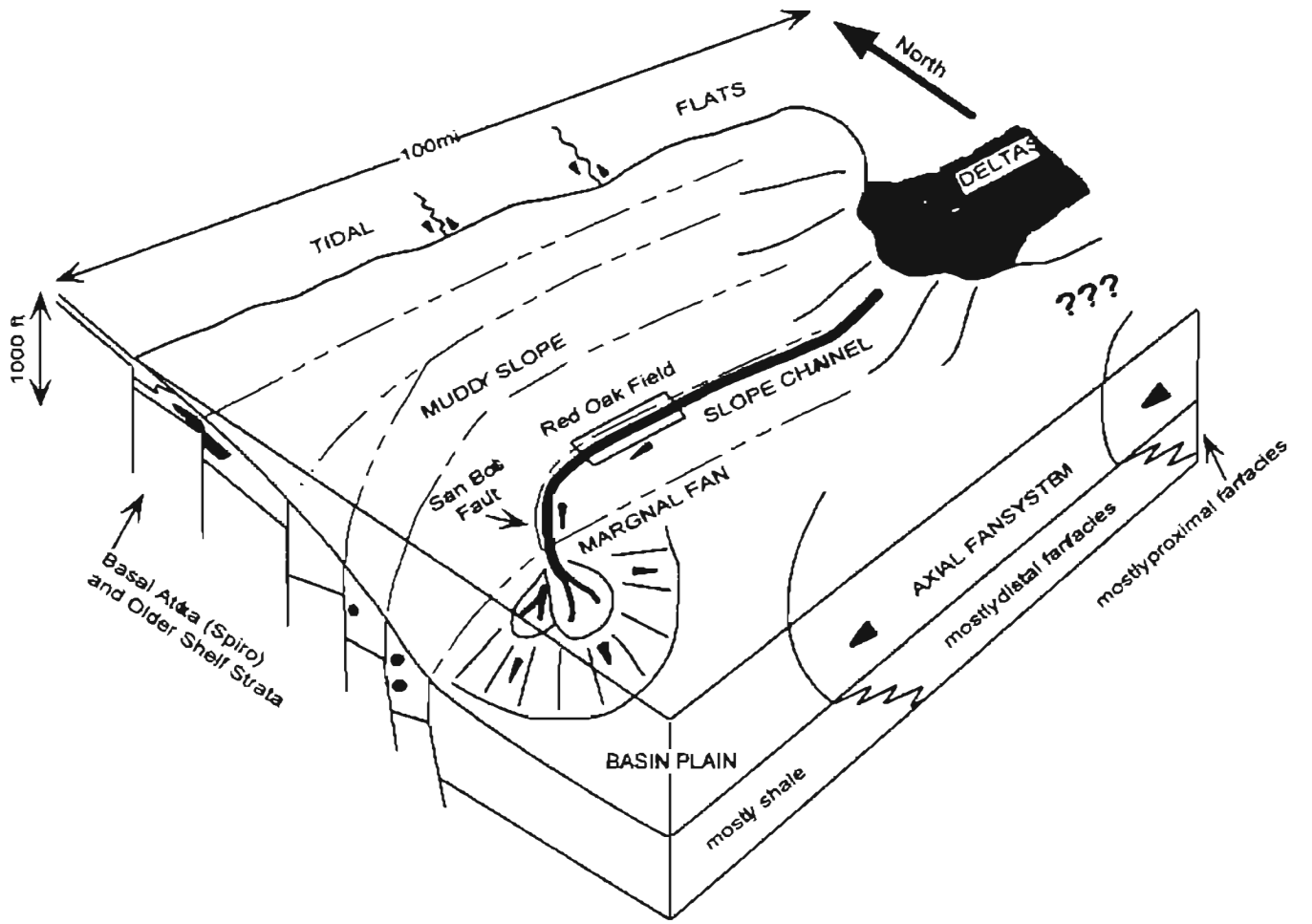

Figure 6. Reconstruction of depositional system in which Atoka strata were deposited in the Arkoma basin (from Houseknecht and McGilvery, 1990; modified from Houseknecht 1986).

of the basin was dominated by a thin-skinned compressional fold belt detached from the underlying block-faulted Lower Atokan and older rocks. The northern third of the basin is dominated by the San Bois Syncline (Figures 44-48 and Plates I-V). Arbenz (1989) also observed that the Choctaw fault dies out into western Arkansas, leaving an interpreted boundary between the Ouachita mountains and the Arkoma basin.

An extensional fault system that displaced the Atokan and pre-Atokan Paleozoic rocks has been documented by Buchanan and Johnson (1968) and Berry and Trumbley (1968). Throw on these faults is generally down-to-the-south and displaces the crystalline basement (Arbenz, 1989). Abrupt increase in thickness of sedimentary rock, as well as the presence of turbidite facies suggest that these fault blocks were active during Atokan sedimentation. However, Arbenz (1989) cited olistostromal (flysch sedimentation) evidence that the faults could have been active during Mississippian time. Offset along a normal fault would create conditions for gravity-flow sedimentation to form. Reactivation of thrust blocks would have given thrust faults an easy place through which to propagate (Suneson and Ferguson, 1988). The presence of a triangle zone marking the transition from the Frontal Ouachitas to the Arkoma Basin was proposed by Hardie (1988), Perry and Suneson (1990), and Mazengarb (1995).

From 1992-1995, the Spiro sandstone and the structural geology of the Arkoma Basin in the Wilburton gas field area were studied by a group from Oklahoma State University with a grant from the Oklahoma Center for Advancement in Science and Technology (OCAST). The present study is a continuation of the OCAST project. The structural group in the OCAST project concluded that a triangle zone exists in the

Wilburton area. This zone is bounded by the Choctaw Fault to the south, the Carbon Fault to the north, and is floored by the Lower Atokan Detachment (Al-Shaieb et al., 1995; Cemen et al., 1994, 1995, 1997; Akthar, 1995; and Sagnak, 1996.

Below the Choctaw fault is a system of thrusts called the Gale-Buckeye Thrust System. Wilkerson and Wellman (1993) suggested that the Gale-Buckeye system was formed as a break-forward thrust sequence.

RED OAK GAS FIELD

The northernmost section of this study area (T6N-R20E) is located in the Red Oak gas field (Figure 2). The field was established in 1912 when the Gladys Belle Oil Company encountered gas within sandstone of the Hartshorne Formation. Gladys Belle Oil did no more drilling in the area after a limited development effort. In 1928, LeFlore County Gas and Electric Company drilled 55 wells in the Brazil anticline. Production from these wells was mainly from the Hartshorne sandstone, but also from the Booch sandstones of the McAlester Formation, which lies next above the Hartshorne. The deepest wells drilled at this time came within a few hundred meters of the Red Oak sandstone (Houseknecht and McGilvery, 1990).

Several gas fields were developed just to the north of the Red Oak Field along the Milton anticline. Production in this area came from the Spiro sandstone. In 1959, Midwest Oil Corporation drilled a discovery well into the deep Atokan Spiro sandstone. The Midwest Oil Corporation No. 1 Orr, in Section 8, T6N, R22E, encountered a sandstone at 7190 ft and produced 6.3 mmcf of gas per day on a 2 inch choke. The reservoir was the Red Oak sandstone (Houseknecht and McGilvery, 1990). The Spiro

sandstone was encountered at 11,510 ft. By 1962, gas reserves of the Red Oak field were estimated at 1.1 tcf (Houseknecht and McGilvery, 1990).

Major structural features within the field include the San Bois normal fault and the thrust-cored Brazil anticline. In the deeper subsurface are many blind thrust faults. These are high-angle faults, but become listric with depth, where they grade into bedding planes within lower Atokan shales.

CHAPTER 2

STRATIGRAPHY OF THE ARKOMA BASIN

The Arkoma Basin is composed of a thick assemblage of strata ranging in age from Cambrian to Pennsylvanian (Figure 7). As Cambrian through Mississippian rocks are related to the pre-foreland basin history; they will be covered briefly. The Pennsylvanian is represented by Morrowan, Atokan, and Desmoinesian strata. Exposed within the basin in Oklahoma are strata of Atokan and Desmoinesian age. In this chapter, descriptions of Cambrian through Mississippian rocks are based on descriptions of these systems in the Arbuckle Mountains by Ham (1978) and by Johnson (1988). Whether rocks younger than Pennsylvanian were deposited in the Arkoma basin is unknown.

Proterozoic granite, rhyolite, and metamorphic rocks are believed to make up the basement of the basin (Figure 7). The Upper Cambrian Timbered Hills Group overlies the basement. It is composed of the Reagan Sandstone and the Honey Creek Limestone. The Reagan Sandstone is a transgressive sandstone that was widespread, but not deposited on local "highs" (Johnson, 1988). The Honey Creek Limestone is a thin bedded, trilobite-rich, pelmatozoan limestone (Ham, 1978).

The Arbuckle Group conformably overlies the Timbered Hills Group. The

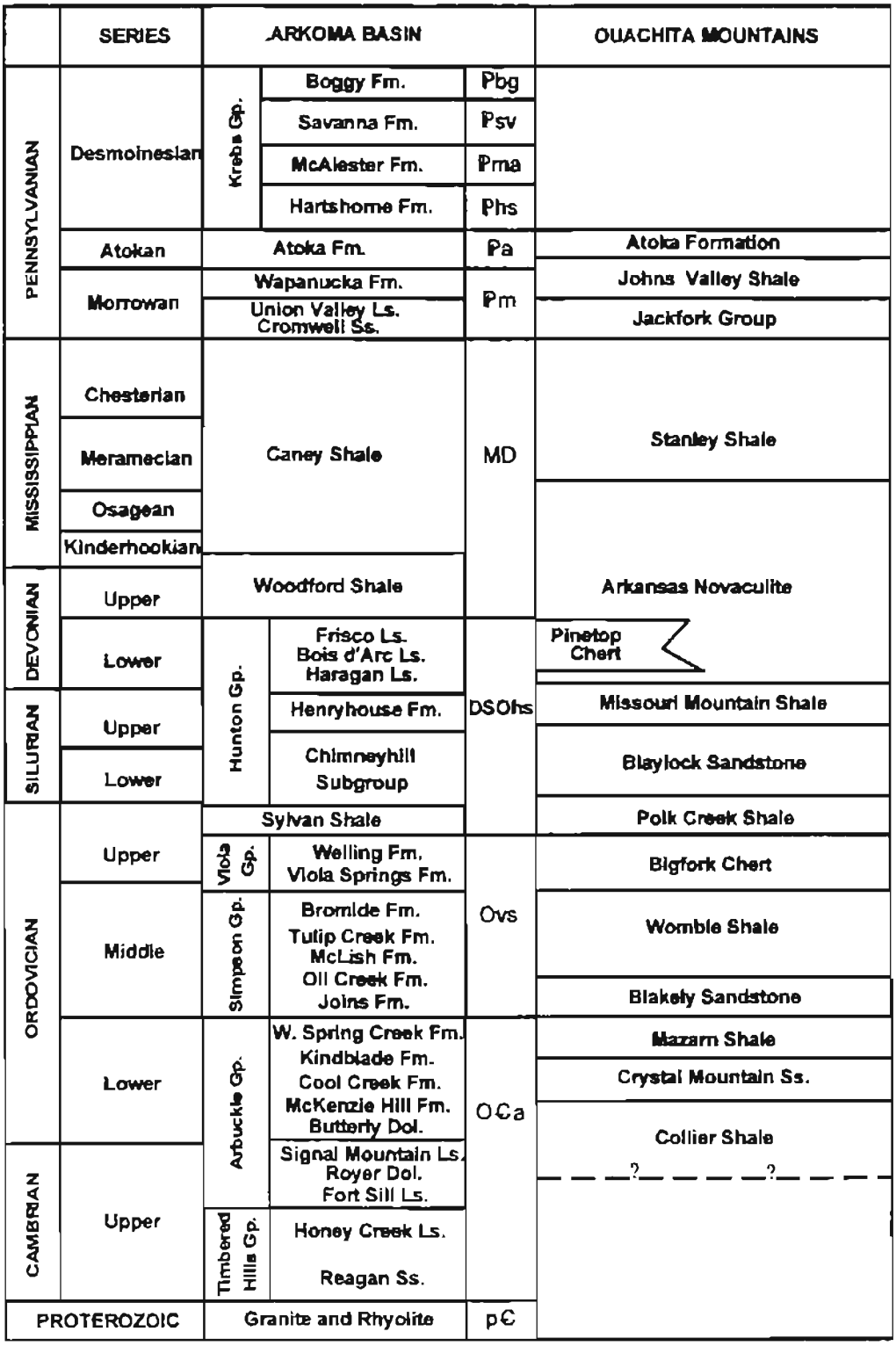

Figure 7: Stratigraphic chart for the Arkoma Basin and the Ouachita Mountains (from Johnson, 1988).

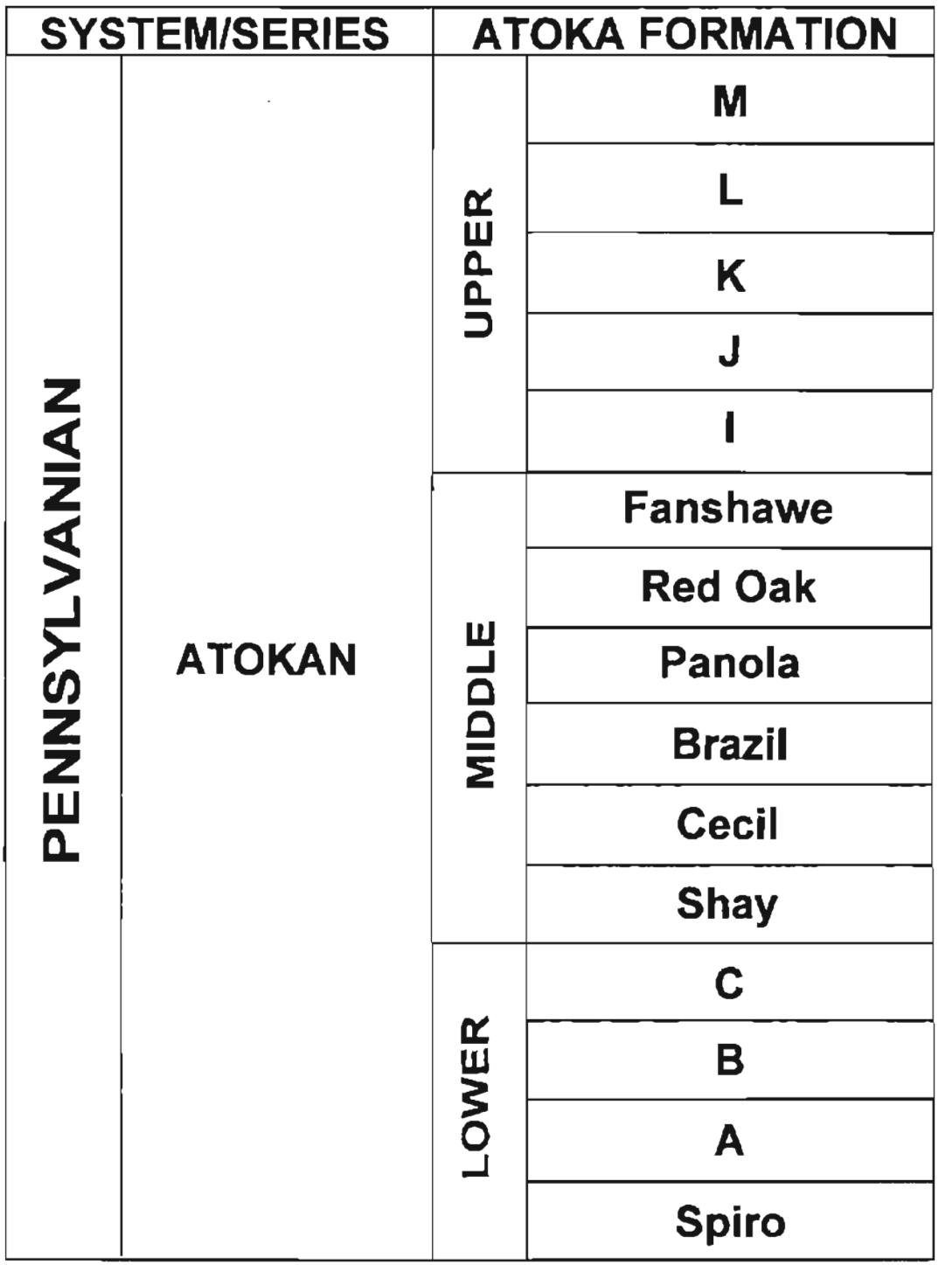

Figure 8: Stratigraphic chart, Atokan strata, informal rock-stratigraphic units, Arkoma Basin.

Arbuckle ranges in age from Upper Cambrian to Lower Ordovician (Ham, 1978). The lower part of the Arbuckle Group is composed of the Fort Sill Limestone, Royer Dolomite, and Signal Mountain Limestone (Figure 7). The upper part of the Arbuckle Group contains the Butterly Dolomite, McKenzie Hill Formation, Cool Creek Formation, Kindblade Formation, and West Spring Creek Formation. These are all shallow-marine sedimentary rocks, and are rich in fossils, including trilobites, brachiopods, mollusks, pelmatozoans, sponges, and near the top, graptolites (Ham, 1978).

Overlying the Arbuckle Group is the Simpson Group of the Middle Ordovician (Figure 7). The Simpson Group records a fundamental change in depositional environment from that of the Arbuckle Group. The group is predominantly composed of skeletal calcarenites, skeletal carbonates, mudstones, sandstones, and shales. In ascending order, rock stratigraphic units of the Simpson Group are the Joins Formation, Oil Creek Formation, McLish Formation, Tulip Creek Formation, and Bromide Formation. In shelf areas the group is composed mostly of limestones (Ham, 1978).

The Viola Group conformably overlies the Simpson Group and is composed of the Viola Springs Formation and the Welling Formation (Figure 7). The Viola Group consists of several limestone facies, including nodular chert-rich mudstones, packstones, porous grainstones, wackestones, and dolomitized wackestones (Sikes, 1995). The Upper Ordovician Sylvan Shale unconformably overlies the Viola Group. It is greenish gray shale with well developed laminations, and it contains graptolites and chitinozoans (Ham, 1978).

The Hunton Group of Lower Silurian to Lower Devonian age conformably

overlies the Sylvan Shale (Figure 7). The base is characterized by Ordovician oolites. The Chimneyhill Subgroup and Henryhouse Formations are Silurian skeletal mudstones and skeletal calcarenties. Overlying these are the Devonian Haragan, Bois d' Arc, and Frisco Limestones which are predominantly skeletal mudstones and calcarenites (Ham, 1978).

The Upper Devonian to Lower Mississippian (Kinderhookian) Woodford Shale unconformably overlies the Hunton Group (Figure 7). The Hunton is composed of dark fissile shale, beds of vitreous chert, and siliceous chert (Ham, 1978).

The Caney Shale, which overlies the Woodford Shale, is Lower and Middle Mississippian dark gray fissile shale that contains phosphatic nodules at some localities. The lowermost occurrence of siderite or clay-ironstone beds within the sequence marks the boundary between the Caney and the informal Springer Shale unit. Based on spores and pollens within the Springer, it is Late Mississippian (Chesterian) in age (Ham, 1978).

Pennsylvanian (Morrowan) strata unconformably overlie Mississippian rocks. Morrowan strata in the Arkoma basin are shelf-like sediments even though they contain large amounts of sandstone. Time-equivalent units within the Ouachita frontal belt are the Jackfork Group and the Johns Valley Shale (Figure 7) which were deep marine flysch sediments (Johnson, 1988). Within the Arkoma basin, Morrowan rocks are the Cromwell sandstone, Union Valley Limestone, and the Wapanucka Formation. The Cromwell sandstone and Union Valley Limestone were deposited during a series of transgressions and regressions and are composed of several discontinuous limestones and sandstones separated by shales (Sutherland, 1988). The Wapanucka Formation conformably overlies the Union Valley Limestone. It is composed of shale and limestone. The Wapanucka is

marked by continuous sedimentation in a shallowing-upward sequence that is marked by reversals. Within the eastern half of the study area, the Wapanucka is exposed at some places along the Choctaw fault.

The Atoka Formation of the Atokan Series was deposited unconformably on the Wapanucka Formation. The Atoka Formation is, by far, the thickest formation within the basin, ranging from several hundreds of feet to about 20,000 feet (Johnson, 1988). The division between lower, middle and upper Atokan is based on the effects of syndepositional normal faults within the basin (Johnson, 1988). Deposition in the basin from Cambrian to Mississippian time resulted in only about 1.5 km of deep-water sediments. During the Atokan, nearly 5.5 km of sand, limestone, and shale were deposited as the result of increase in accommodation space within the basin due to normal faulting (Houseknecht and McGilvery, 1990). Shale composes most of the Atokan rocks. Sandstone, siltstone, and some thin coal beds comprise the rest of the Atokan Formation. Most sandstone units are not continuous, being the result of fluvial and deltaic processes across the sometimes exposed shelf (Sutherland, 1988).

The lower Atokan is represented by the Spiro sandstone (Figure 8) and a thin marine shale. An example of the well-log signature of the Spiro is shown in Figure 9. Faunal evidence suggests that the boundary between Morrowan and Atokan ages lies within this 20-40 foot shale (Houseknecht and McGilvery, 1990). The Spiro sandstone is the record of deposition in a broad delta complex with distal channels, tidal channels, and shallow water with interfingered marine sandstone bars and carbonates (Houseknecht, 1983). Detrital constituents of the Spiro were derived from the north and northeast.

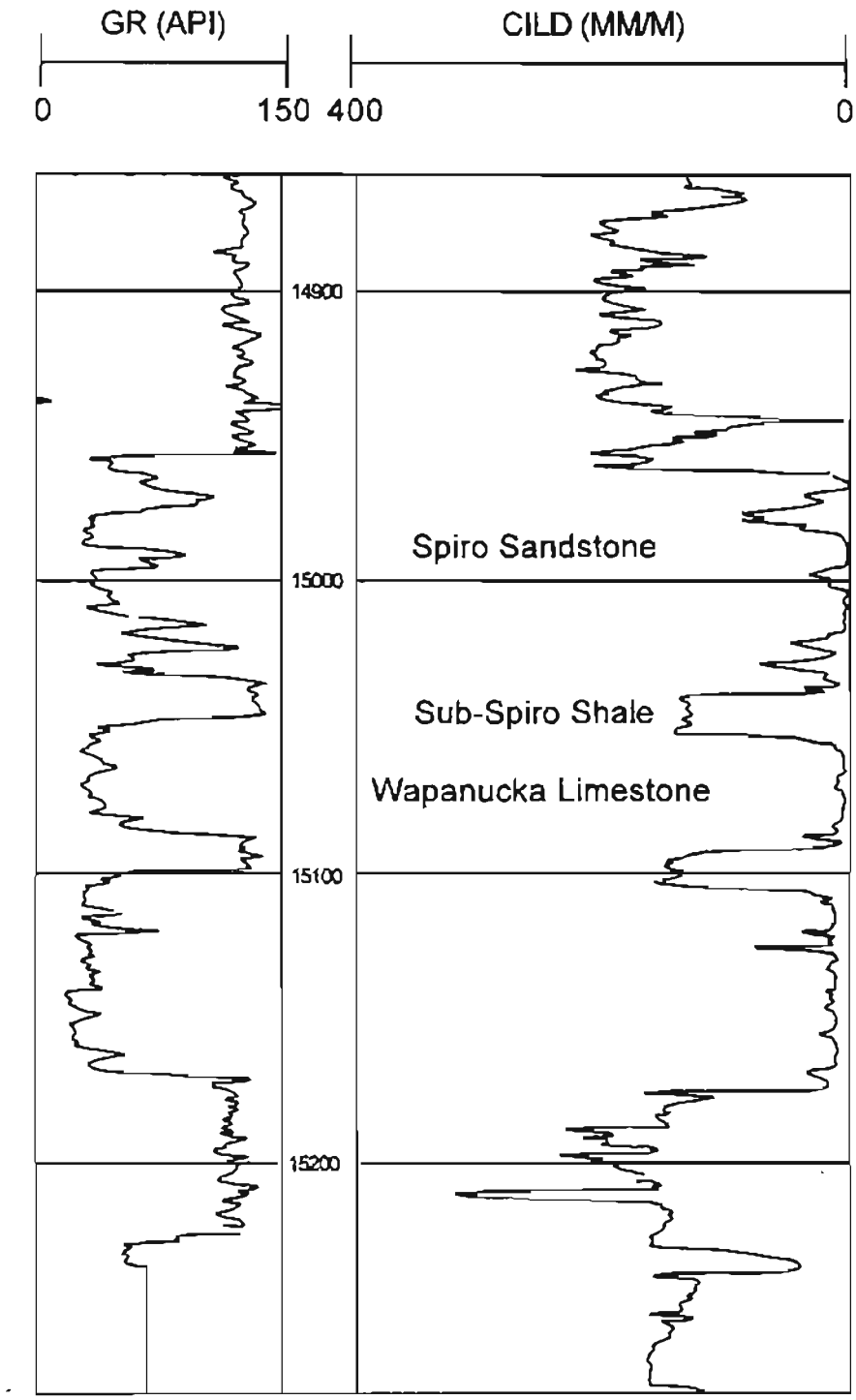

Figure 9. Log signature of the Spiro Sandstone. (AnSon Corp., No.1-28 Turney, Sec 28, T5N R20E)

The Middle Atokan section is composed of the Shay, Cecil, Panola, Red Oak, and Fanshawe sandstones within a thick shale sequence. Examples of wire-line log signatures of the Cecil, Panola, and Red Oak sandstones are shown in Figures 10-12 respectively. According to Vedros and Fisher (1978), the Red Oak sandstone was deposited as gravity-flow sediments and possibly formed a submarine fan at the base of the slope caused by the San Bois growth fault (shown in Figure 6) (Houseknecht and McGilvery, 1990). Sediments were derived from the eastern uplift of the Ouachita orogenic belt (Figure 6) (Houseknecht and McGilvery, 1990). Upper Atokan strata are not cut by the normal faults that controlled sedimentation patterns within the middle Atokan. The lower shales could have compacted and absorbed the displacement along the fault, rendering the upper Atokan unfaulted (Sutherland, 1988). A cessation of normal faulting due to decreased bending of the loaded lower plate also could have left the upper Atokan unfaulted. Predominant lithologies within the upper Atoka are shallow shelf and deltaic rocks (Sutherland, 1988).

The Desmoinesian Series within the Arkoma basin comprises the Krebs, Cabaniss, and Marmaton Groups (Figure 13). Within the study area only the Krebs Group crops out. The Krebs Group is composed of the Hartshorne, McAlester, Savanna, and Boggy Formations. The Hartshorne Formation was deposited gradationally on the Atoka Formation and was deposited as a high-constructive, tidally influenced deltaic system. The overlying McAlester to Boggy Formations are comprised of fluvial/deltaic sediments deposited during a series of transgressions and regressions (Sutherland, 1988).

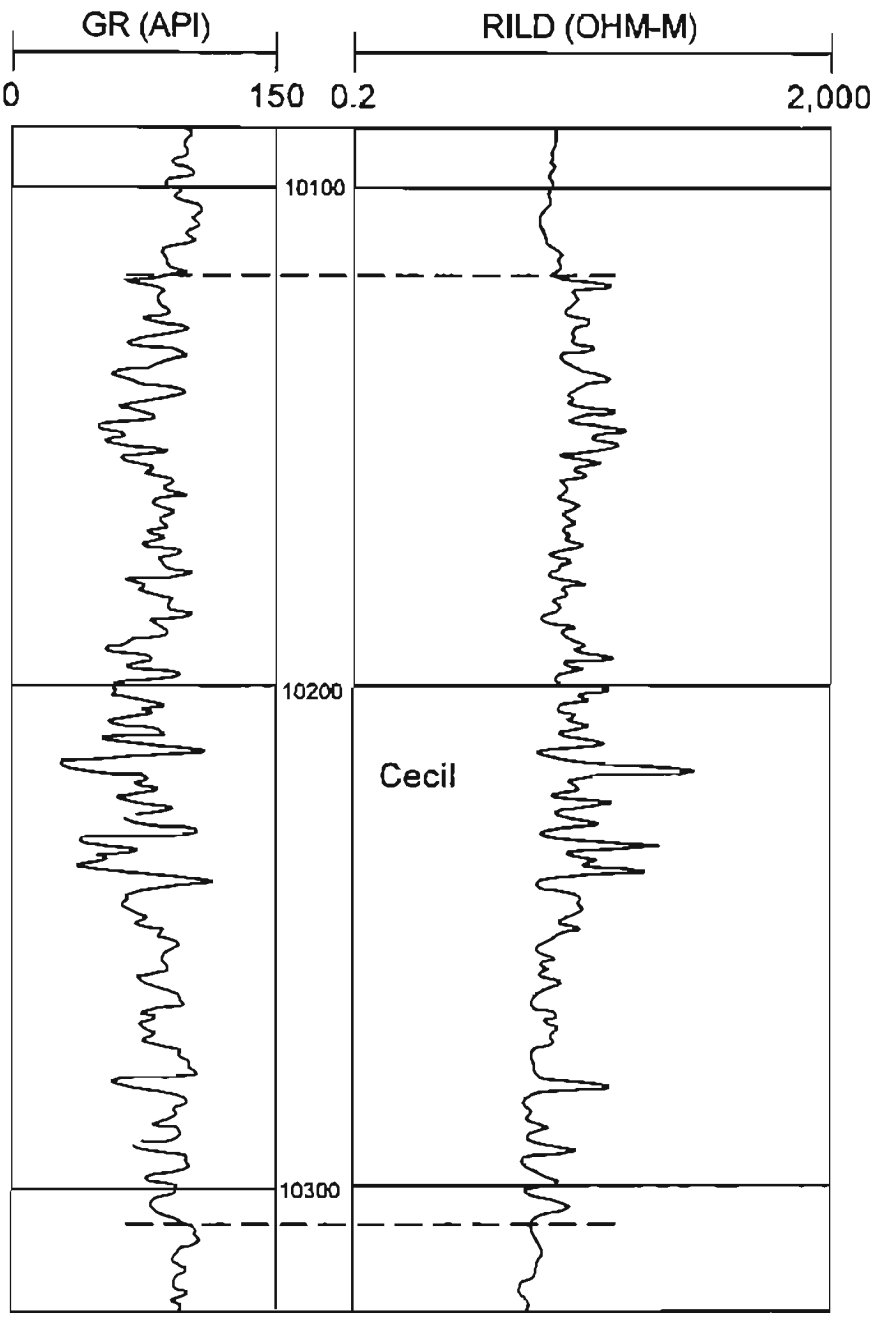

Figure 10. Log signature of the Cecil sandstone. (Austin Production Co., No. 1 Colvard Lm. , Sec. 10, T5N, R20E.)

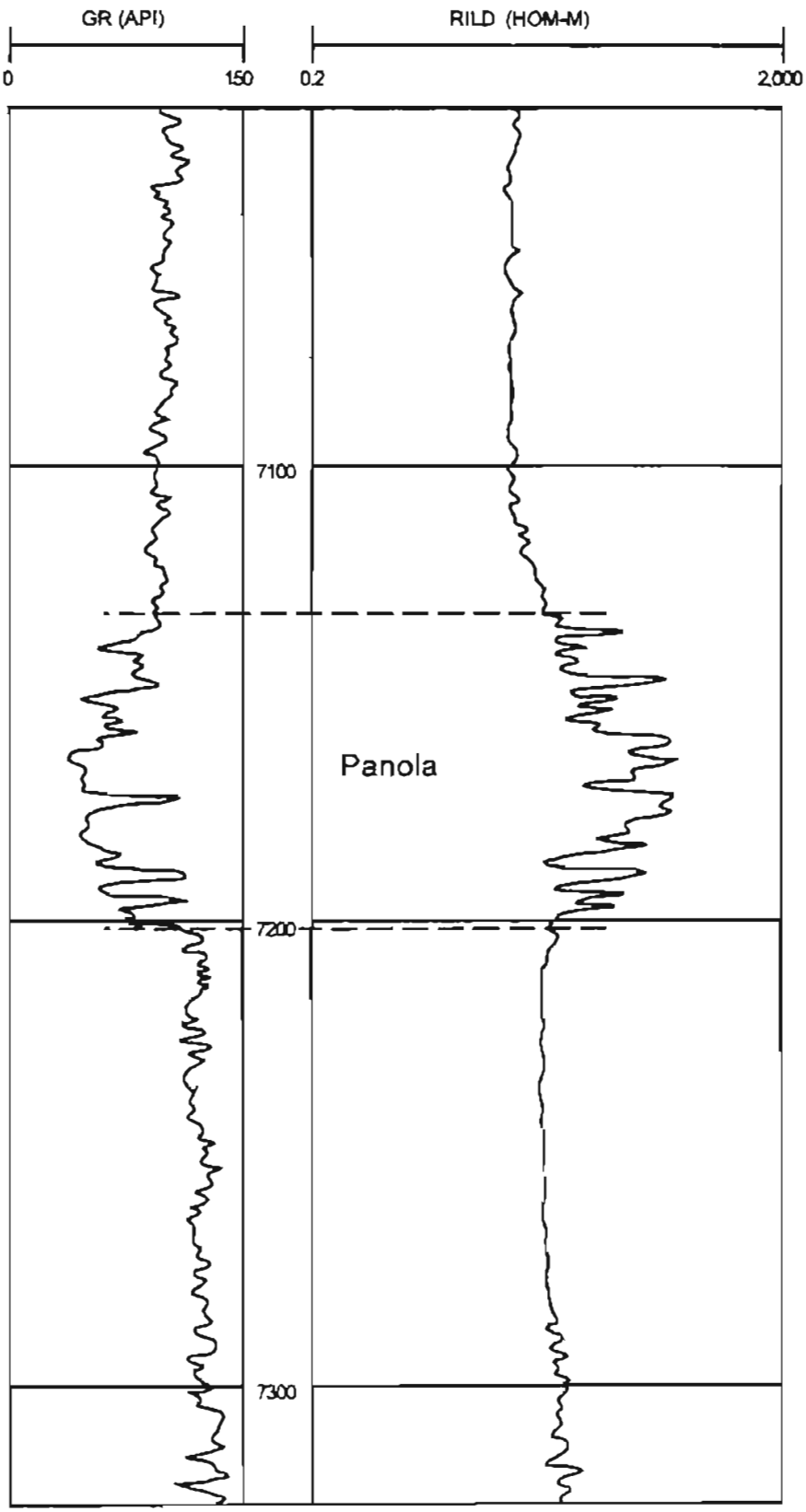

Figure 11. Log signature of the Panola sandstone. (Austin Production Co., No. 1 Colvard Lm., Sec. 10, T5N, R20E.)

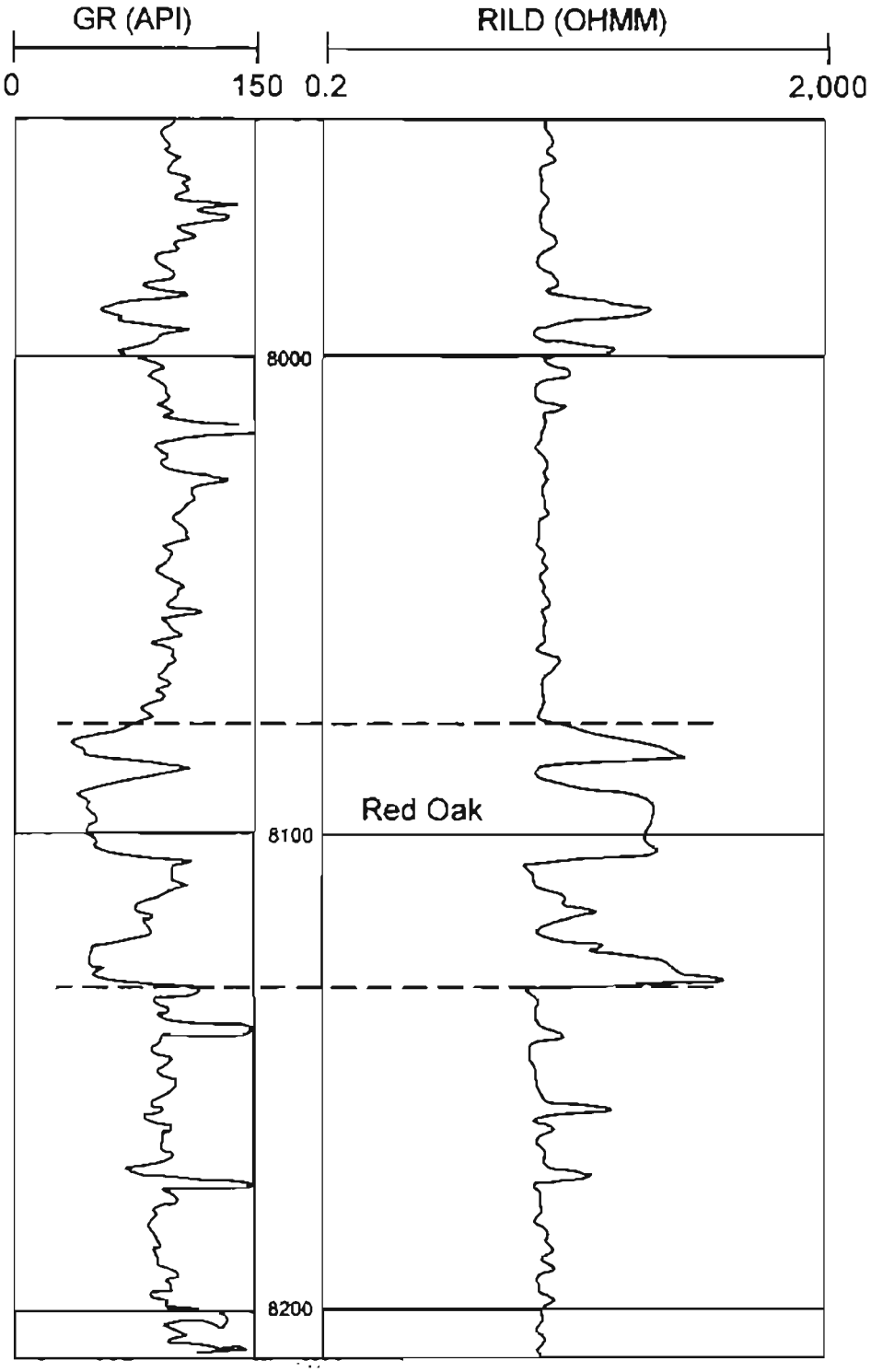

Figure 12. Log signature of the Red Oak sandstone (Unit Drilling and Exploration Co. No. 1, Hawthorne, Sec. 4, T5N, R20E).

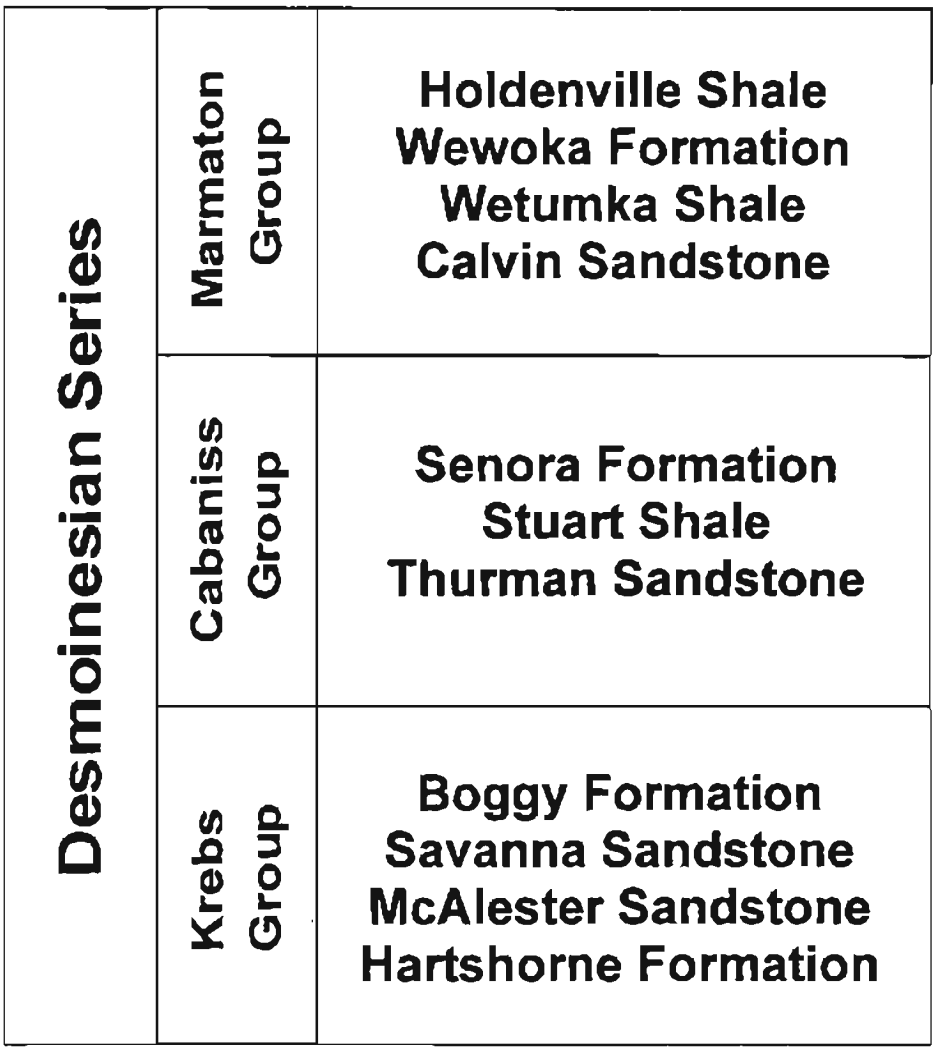

Figure 13. Stratigraphic chart showing the Desmoinesian Series

CHAPTER 3

DIAGENESIS AND DEPOSITIONAL ENVIRONMENT OF THE SPIRO SANDSTONE

DIAGENESIS

Extensive diagenetic studies on the Spiro sandstone have been done by Al-Shaieb et al. (1995), Akhtar (1995), and Sagnak (1996). The results of these studies, as well as a study of eleven thin-sections within the project area, will be given here.

DETRITAL CONSTITUENTS

Major detrital constituents of the Spiro sandstone are quartz, metamorphic rock fragments, glauconite, and skeletal fragments. Minor constituents include zircon, phosphate, muscovite, and biotite (Al-Shaieb et al., 1995). The major constituent is monocrystalline quartz, comprising approximately 90-95% of the detrital constituents of the thin sections (Figure 14). The grains exhibit straight to slightly undulose extinction, indicating compaction of the grains. The quartz grains are medium grained and moderately well sorted with rounded to subrounded shapes. The other 5-10% of detrital constituents are metamorphic rock fragments and glauconite grains.

Al-Shaieb et al. (1995) and Sagnak (1996) reported skeletal debris in a study of the Pan-American No. 1 Reusch core. These bits of debris included echinoderm plates

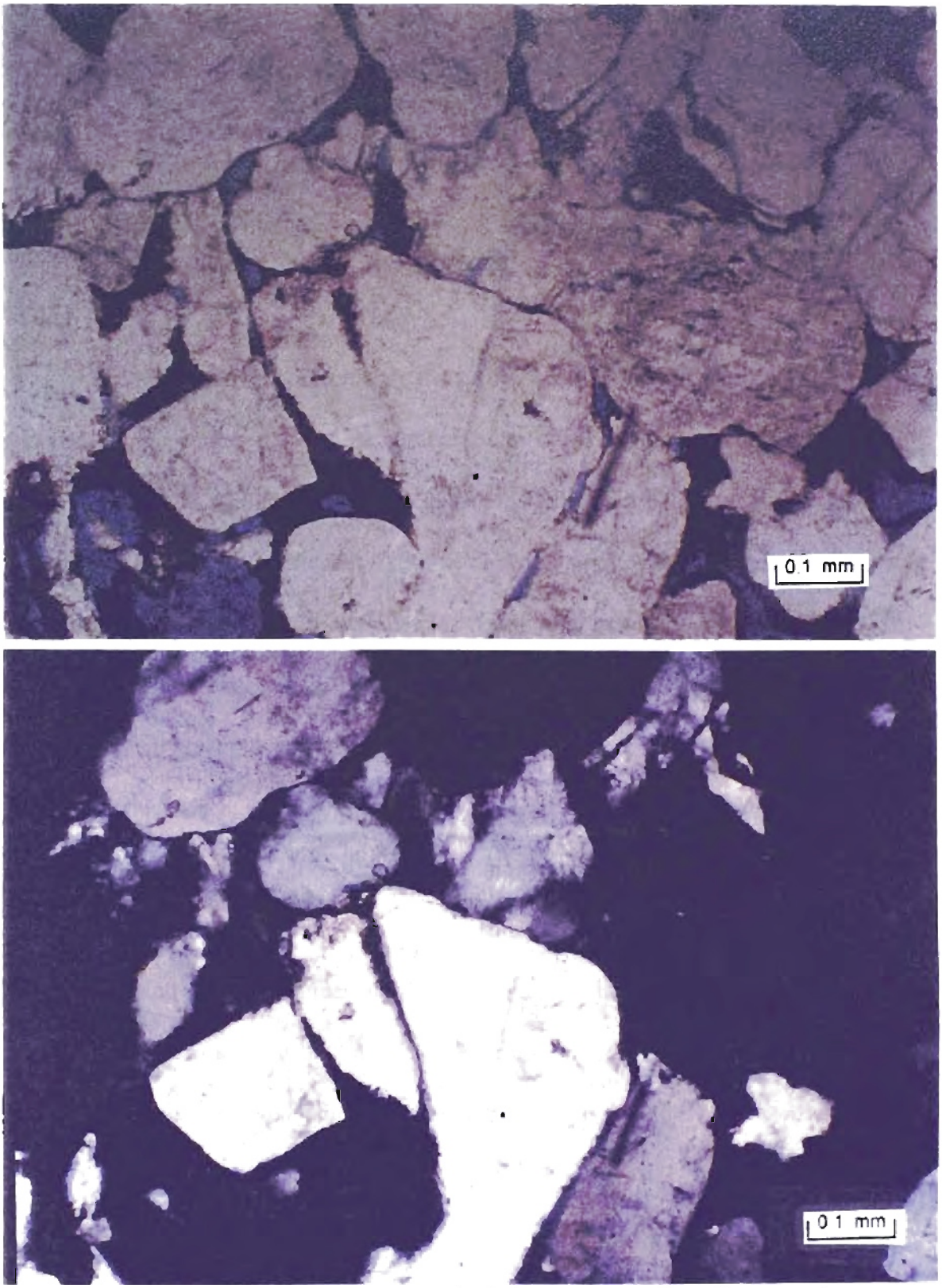

Figure 14. Photomicrograph showing detrital constituents from Spiro sandstone outcrop in NW SW NE, Sec 20, T5N, R20E.

and spines, bryozoans, and trilobites. These debris have been mostly replaced by calcite. Some of the skeletal debris altered to collophane, but that was uncommon. Percentages of fossils ranged from 1 to 25%. Al-Shaieb et al. (1995) and Sagnak (1996) documented ostracodes, fusulinids, and coral fragments as well.

CEMENTS

Silica and carbonate cements are the primary cements in the Spiro. Silica forms as syntaxial quartz overgrowths. These are marked by dust rims on the quartz grains. Al-Shaieb et al. (1995), Akthar (1995), and Sagnak (1996) indicate the dust rims to be chlorite or chamosite (iron chlorite). Thin-section and x-ray diffraction analysis indicated that chlorite, and not chamosite, was the clay type within this study area (Figure 15). In the footwall of the Choctaw fault, chamosite acts to prevent the formation of quartz overgrowths and preserves primary porosity. Samples examined in this study were from locations at the surface, within the hanging wall of the Choctaw fault. Absence of chamosite in the hanging wall resulted in cementation and destruction of primary porosity.

Where calcite is present, it is the dominant carbonate cement (Sagnak, 1996). Quartz grains and skeletal fragments commonly were replaced by calcite or dolomite. Dolomite is the second-most-abundant carbonate cement. If calcite were originally present in the rocks that were studied by me, it has been removed by solution.

DIAGENETIC CLAYS

Chlorite is the most abundant diagenetic clay, it occurs as grain-coatings and as individual pellets. Chlorite is typically green to brownish green. Chlorite is also present in thin sections as a pore-filling mineral.

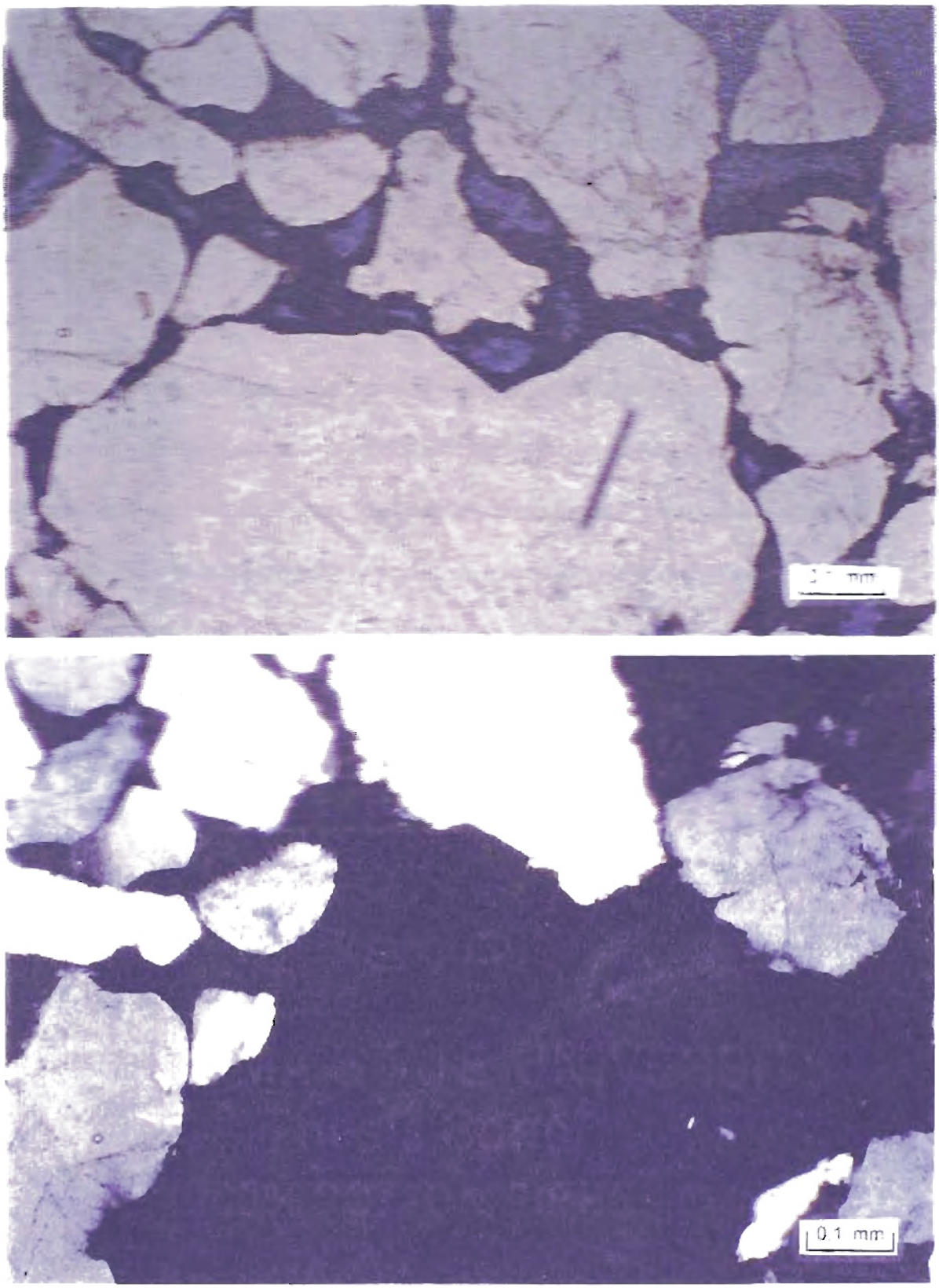

Figure 15. Photomicrograph showing chlorite as a grain-coating clay. From the Spiro sandstone, NW SW NE, Sec 20, T5N, R20E.

Montmorillonite, smectite, vermiculite, and illite also were identified in thin sections and in x-ray diffractions. These clays probably result from the breakdown of feldspars and possibly glauconite. The clay forms a pseudomatrix, indicating compaction of the grains.

POROSITY

Both primary and secondary porosity were observed in the Spiro sandstone. Primary porosity is the main porosity type, although it was modified by compaction, cementation and dissolution (Figure 16). Primary porosity was preserved in areas with clay coatings. The primary porosity provided pore-fluid migration pathways within the sandstone. Primary porosity of the Spiro sandstone in the study area is approximately 11%. The fluids partially or completely dissolved metastable constituents to produce secondary porosity (Al-Shaieb et al., 1995. Akthar, 1995, and Sagnak, 1996).

Secondary porosity is significant in the Spiro sandstone. It appears as moldic porosity and as oversized and elongated pores. Secondary porosity was documented by Al-Shaieb et al. (1995) as being volumetrically as significant as primary porosity.

DIAGENETIC SEQUENCE

Diagenesis of the Spiro sandstone in the Arkoma Basin of Oklahoma was studied in depth by Lumsden et al. (1971), Al-Shaieb (1988), Al-Shaieb et al. (1995), Akthar (1995), Sagnak (1996), and was also dealt with in this study. Diagenesis of the Spiro sandstone began shortly after deposition, just below the sediment-sea water interface. In chamosite-rich

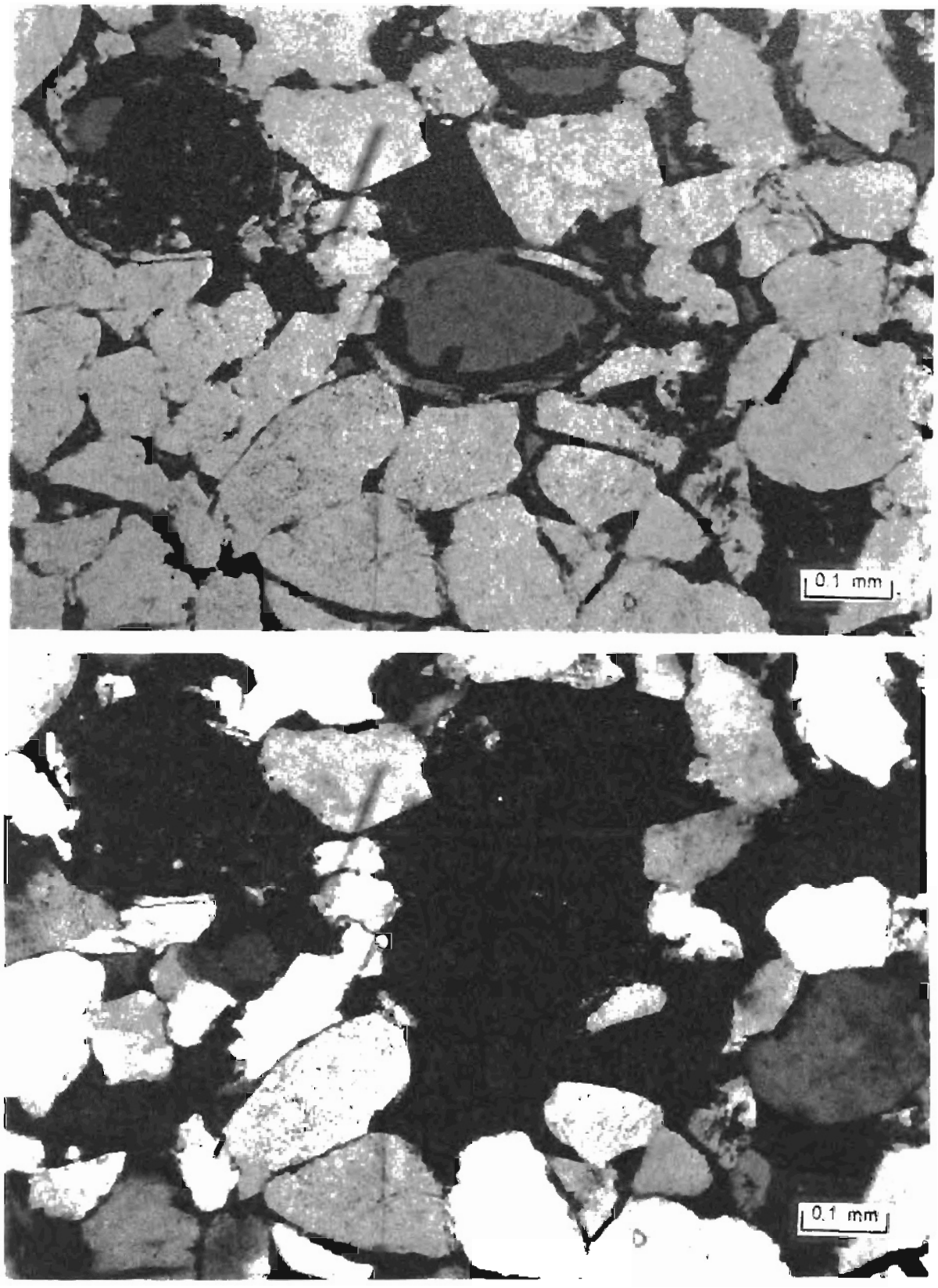

Figure 16. Primary porosity modified by compaction, cementation, and dissolution. From the Spiro sandstone, NW SW NE, Sec 20, T5N, R20E.

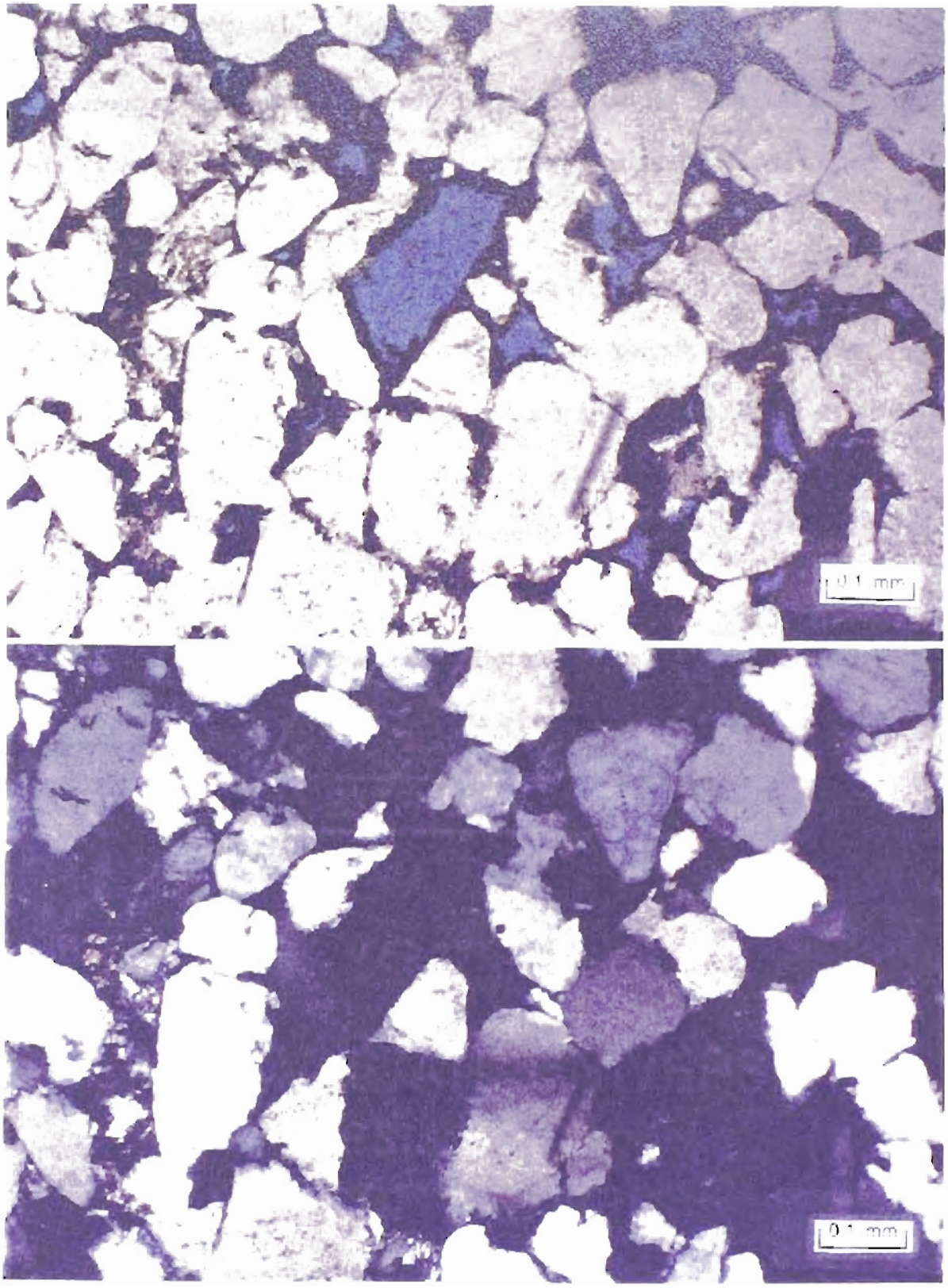

Figure [illegible] Photomicrograph showing [illegible] texture in Jurassic Entrada sandstone
[illegible] Spiro sandstone, NW SW NE Sec 20, T5N, R20E

areas, quartz grains were coated thickly with diagenetic chamosite. With increasing depth of burial, primary porosity was diminished slightly due to compaction (Figure 17) (Al-Shaieb et al., 1995).

In areas with little chamosite, quartz overgrowths significantly decreased primary porosity. The formation of calcite cement further decreased porosity. Deeper burial allowed for thermal maturation of organic materials into hydrocarbons. Fluids, rich in hydrogen ions and acidic (Al-Shaieb et al., 1995), moved through pore spaces, dissolving metastable constituents and forming secondary porosity.

DEPOSITIONAL ENVIRONMENT

Studies of outcrops and cores, and documentation of sedimentary structures by Akhtar (1995) and Sagnak (1996) resulted in the interpretation that the Spiro sandstone was deposited in a shallow marine environment (Figure 5). The Spiro is marked by medium scale trough cross-bedding with flow structures. Glauconite within the unit suggests shallow marine deposition. Al-Shaieb et al. (1995) and Sagnak (1996) indicated that burrows exist within a sub-Spiro shale. Houseknecht (1987), Lumsden et al. (1971), and others suggested that sedimentary structures within the Spiro indicate a fluvial depositional environment. Chamosite led Porrenga (1967) to suggest a shallow marine environment. Sutherland (1988) concluded from this evidence as well as from his own findings that the Spiro sandstone was deposited in a tidal-flat environment; other evidence included interchannel deposits of fine grained sand and shale organized into ripple-bedded and thoroughly bioturbated sequences.

CHAPTER 4

GEOMETRY OF THRUST SYSTEMS

THRUST SYSTEMS

Where several thrust faults form in the same area they are collectively termed a "thrust system". Individual thrusts can be linked by connecting splays. Thrust systems are composed of individual thrust sheets that stack on top of each other. Thrust faults in a thrust system branch off a common sole thrust. According to Boyer and Elliott (1982), the thrust sheets stack like "roof tiles" that all dip in the same general direction. The branching thrusts will take one of two general structures: imbricate fan or duplex structure (Figure 18).

IMBRICATE FANS

"Imbricate fan" refers to the shape of the thrust faults as they branch off the sole thrust. Fans form either in front, or towards the foreland, of the leading thrust or behind the leading thrust, towards the hinterland. If the maximum slip is toward the foreland, the fan is said to be a "leading imbricate fan". If the maximum slip is toward the hinterland, the fan is called a "trailing imbricate fan" (Figure 18). Boyer and Elliott (1982) stipulated that all imbricate fans are of the leading type. They suggested that when a thrust sheet

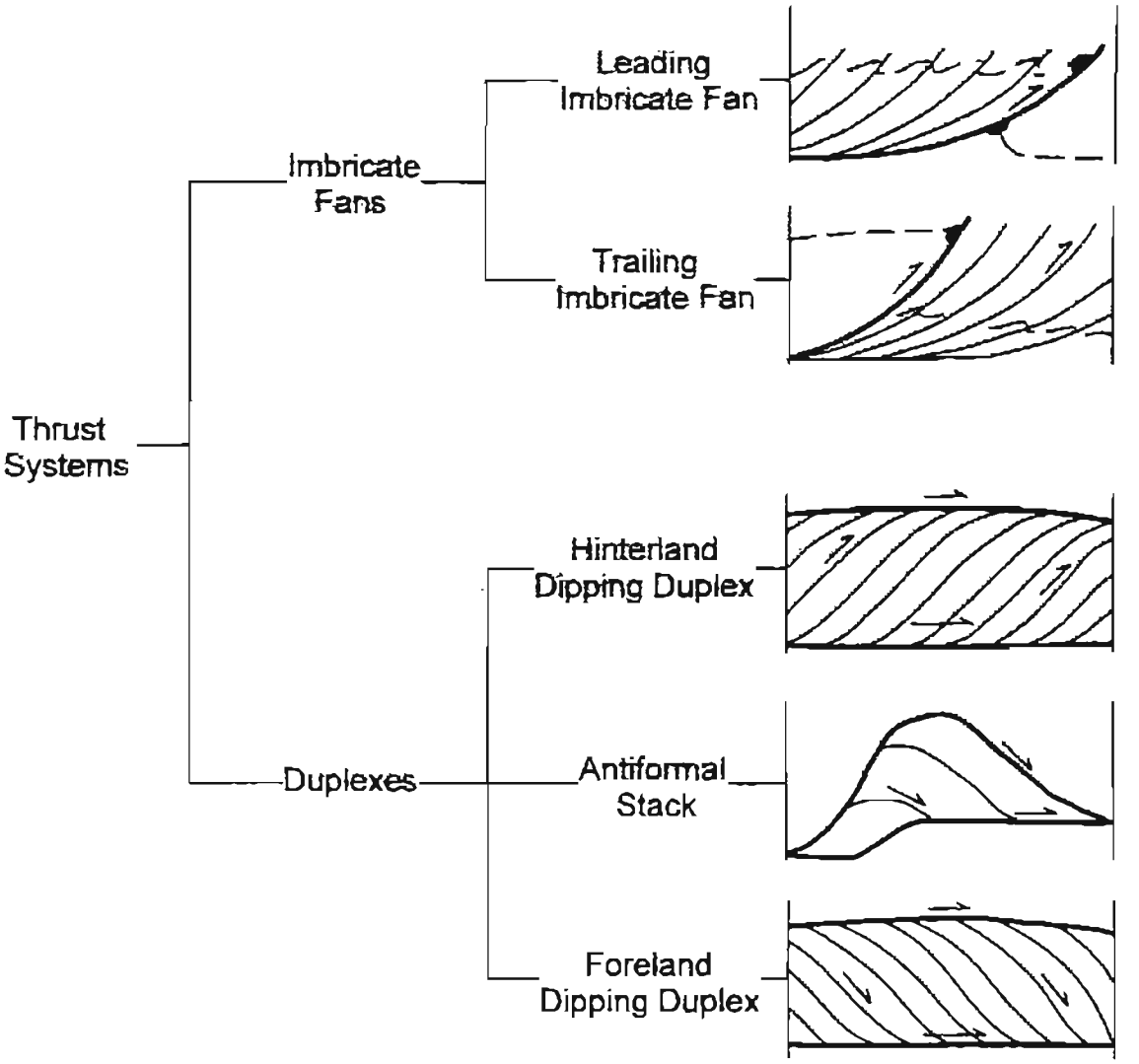

Figure 18. Thrust systems (from Boyer and Elliott, 1982).

forms, it will slip upwards until strain is no longer strong enough to push it. At this point, a new thrust sheet forms in front of it. This is termed a "break-forward thrust sequence" Boyer and Elliott (1982). As subsequent thrusts formed, each would be located farther in the foreland than the previous fault. This model works well in most cases. However, exceptions have been pointed out in the literature, notably by Butler (1987).

BREAK-FORWARD THRUST SEQUENCES

A break-forward sequence begins as a leading imbricate system. Faulting follows the ramp and flat geometry proposed by Rich (1934). Thrust faults will propagate almost horizontally through incompetent strata (evaporites, shales, etc.). Where the thrust encounters a competent bed (sandstone, limestone, etc.) it forms a ramp at about 30° to the horizontal. The thrust continues at this angle until it has cleared the competent bed (Rich, 1934). Where the footwall ramp ends and the thrust sheet is pushed onto the flat, the thrust sheet folds into an anticlinal form. Commonly, beds within a horse form an anticline-syncline pair with the anticline in the headwall and the syncline in the footwall. The term for the overlapping of duplex structures is "piggy-back" thrusting (Boyer and Elliott, 1982). Therefore, break-forward sequences are also referred to as piggy-back thrust sequences. Figure 19 shows the evolution of the simplest case of break-forward thrusting. As the thrust propagates upward through the competent bed it forms a ramp structure. The resulting horse "rides" up the ramp and slips along the flat at the top of the ramp. The horse develops an anticlinal form on its leading edge as the original hanging wall bends over onto the flat (Figure 19b). With folding comes increased friction along the thrust. When the coefficient of friction overcomes the thrusting force, the thrust

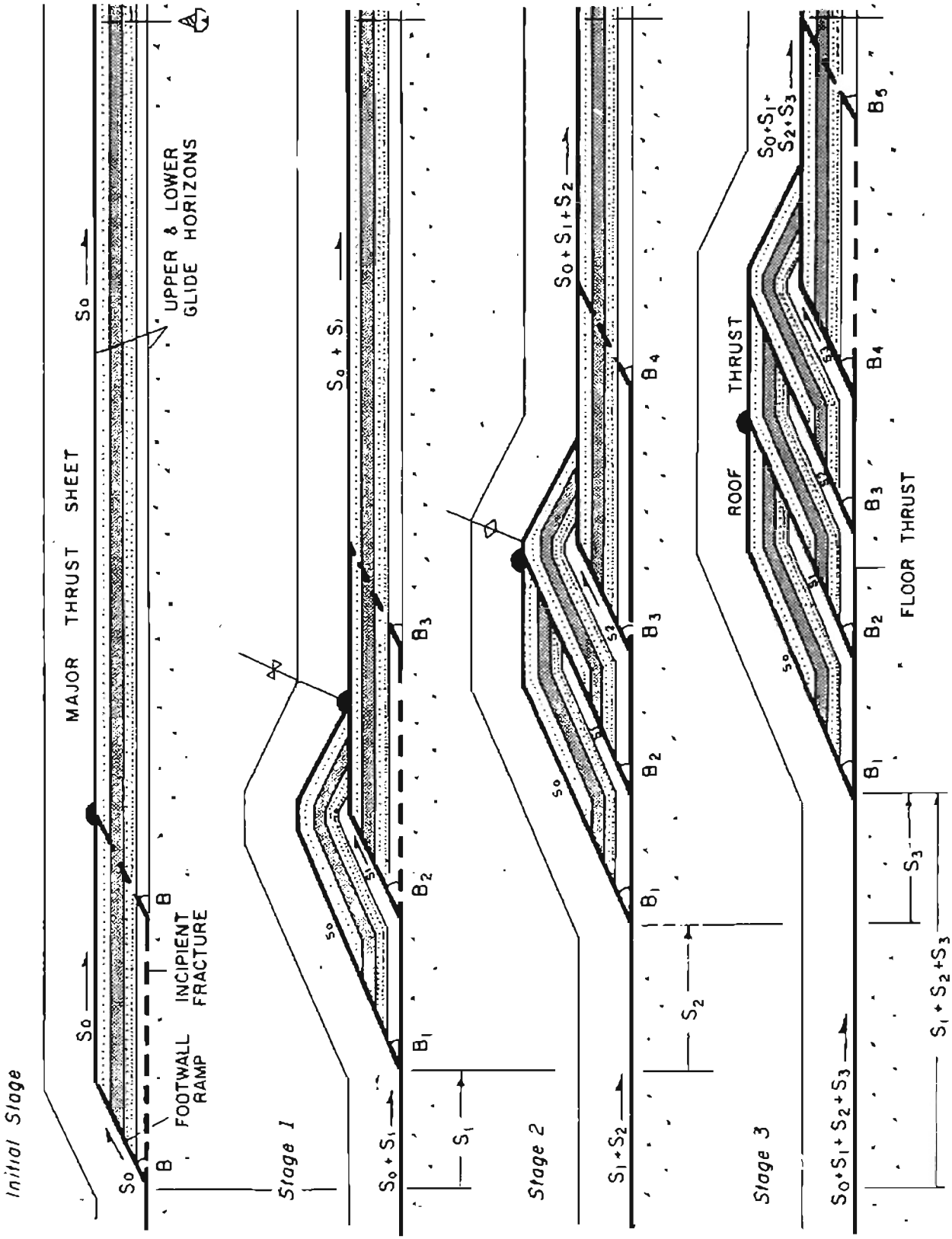

Figure 19. Evolution of a break-foreward thrust sequence (from Boyer and Elliott, 1982)

becomes inactive. At this point a new ramp forms in the foreland. This stacking of duplexes continues throughout the thrust sheet (Figure 19d).

FAULT-BEND FOLDING

Suppe (1983) proposed that if a fault surface is not planar, one of the fault blocks must be distorted as it slips past the other. As the thrust sheet moves over a ramp and onto the flat, folding of the horse results in a rollover (Figure 19d). Folding can also occur after the horse forms. As the hanging wall slides along the footwall, the areas of the beds that contact the faults tend to bend in the direction of the motion. As the imbricate thrusts overlap, the truncated pieces of the beds will fold on both ends causing an "S" shape (Figure 20). Folding can also occur beyond the tip line in a blind imbricate thrust. The stresses that cause faulting get dissipated over the length of the thrust in order to overcome friction and the strength of unbroken rock. Eventually the strain is not great enough to overcome the strength of the rock into which the fault is propagating. At this point, it is common for elastic and plastic deformation to occur. The result is an anticlinal fold around the tip line of the thrust sheet (Figure 22).

Suppe (1983) termed this folding style fault-bend folding. Fault bend folding is the process of bending of hanging wall fault blocks as they ride over a non-planar fault surface (Woodward et al., 1985). Suppe recognized three classes of fault-related folds. These include: "(1) buckling caused by compression above a bedding-plane décollement" (Figure 21), "(2) fault-bend folding caused by bending of a fault-block as it rides over a non-planar fault surface" (Figure 22), and "(3) fault-propagation folding caused by compression in front of a fault tip during fault propagation" (Figure 23) (Suppe, 1983).

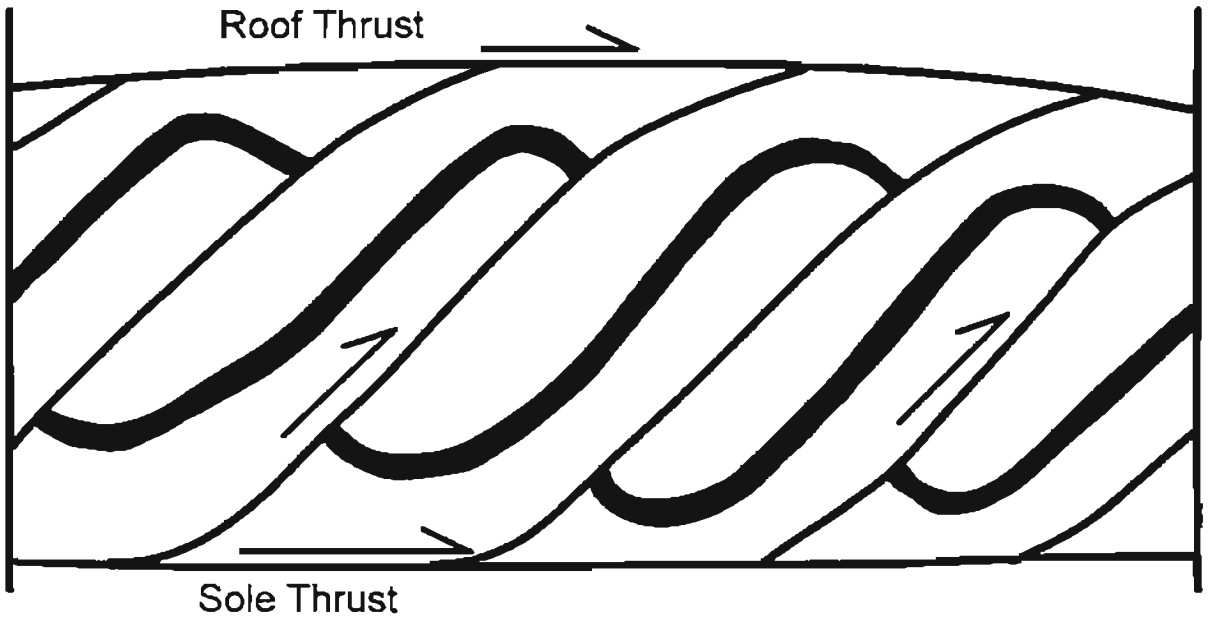

Figure 20. A duplex represented as "an imbricate family of horses," as described by Boyer and Elliott (1982).

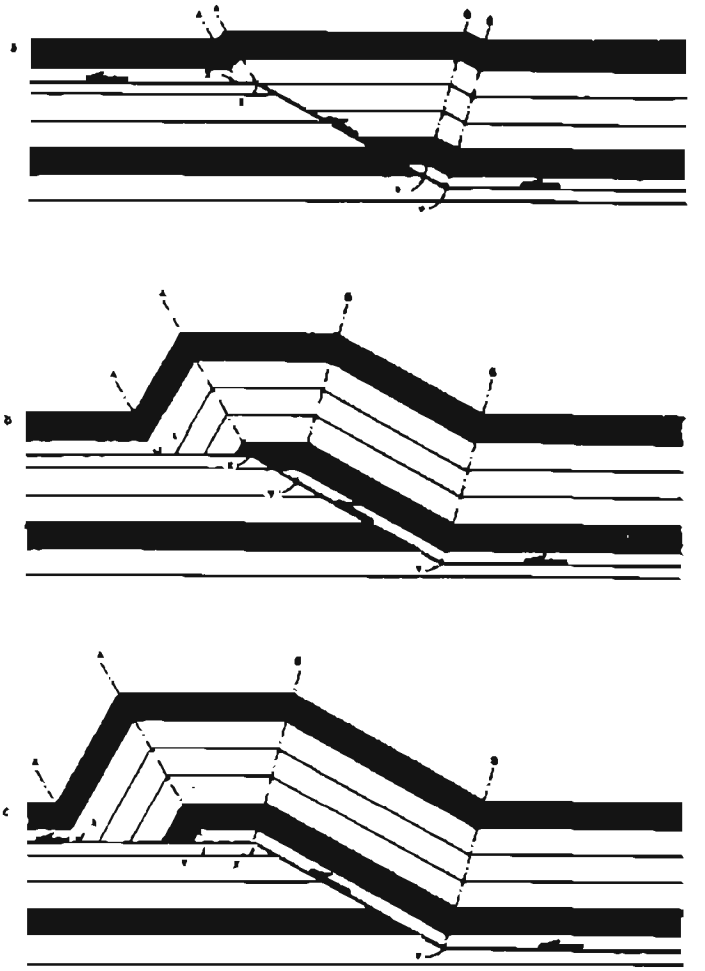

Figure 21. Schematic progressive development of a fault-bend fold as a thrust sheet rides over a step in décollement. (From Suppe, 1983.)

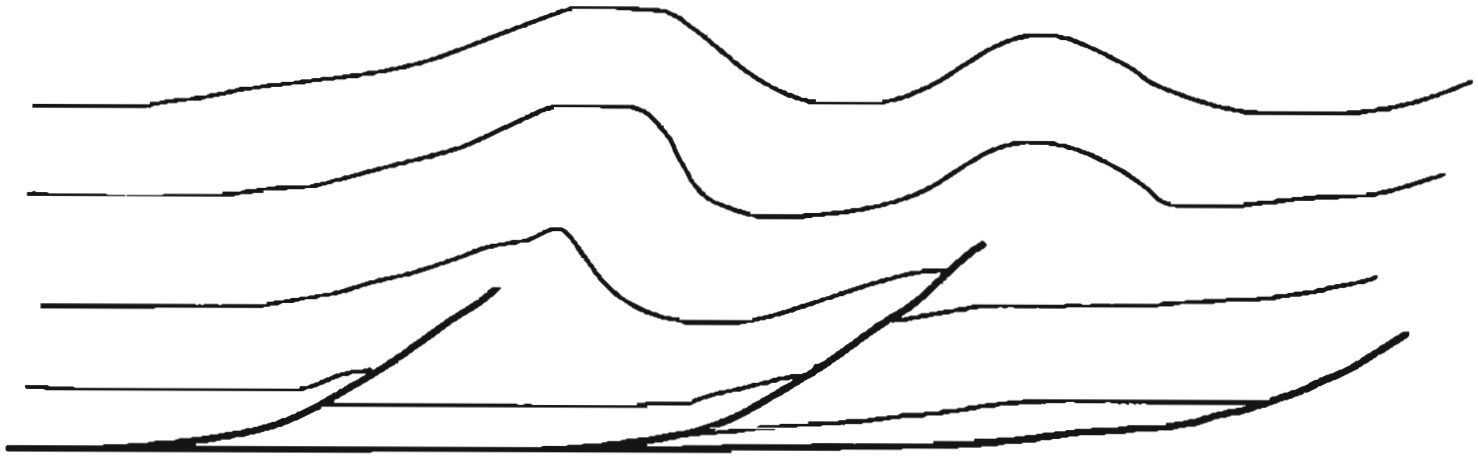

Figure 22. Stylized diagram of fault-end folding. As slip along the fault dies out, stress is transferred to the surrounding rock in the form of folding.

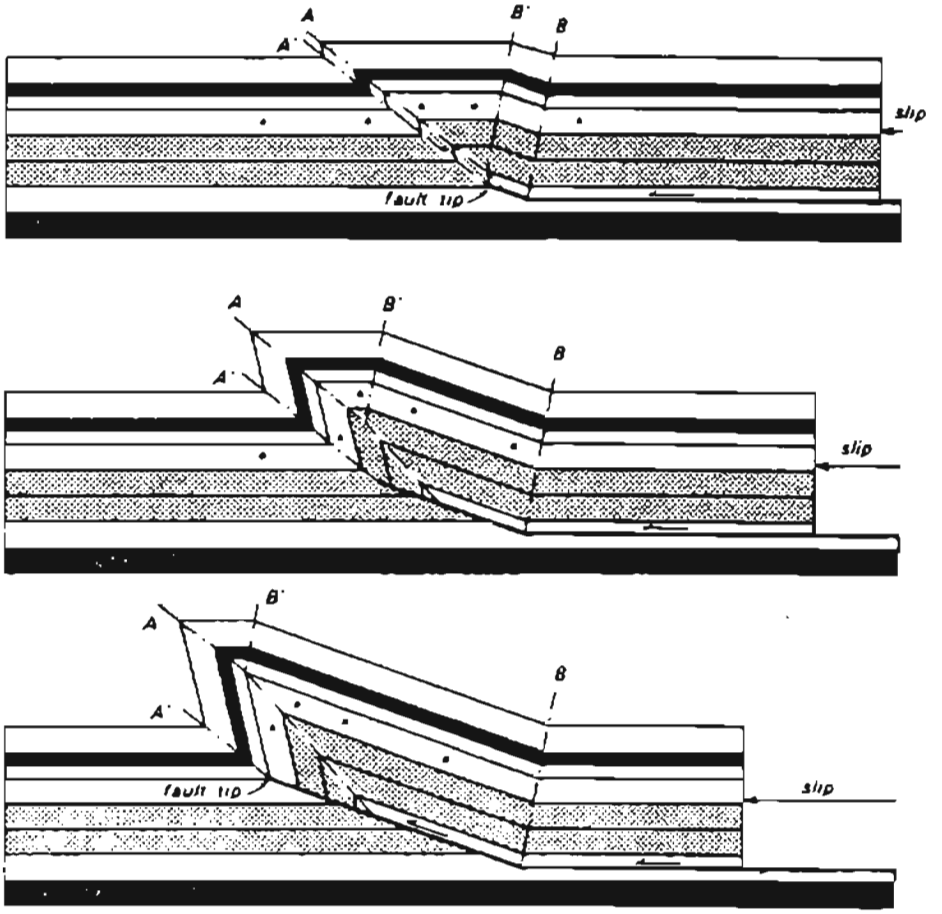

Figure 23. Schematic progressive development of a fault-propagation fold (from Suppe, 1983).

Several types of folding styles were studied by Suppe (1983). These included folds with constant bed thickness (Figure 24a), kink bend folds (Figure 24b), chevron folds (Figure 24c), box folds (Figure 24d), and concentric folds (Figure 24e). Kink and chevron folds form in brittle rock units (Suppe, 1983). Concentric folds would form in areas composed of thick shales with few structurally competent layers. This is the case within the study area. The Atoka shales comprise a very thick column of strata interlain by thin sandstones (Spiro, Cecil, Panola, Red Oak, and others). Folds have the general appearance of kink-bend or chevron folds if the entire rock sequence behaves in a brittle fashion. For this reason, Suppe (1983) stated that even concentric folds can be characterized as a nearly infinite series of kink folds (Figure 25). Suppe devised a method to analyze mathematically the dip angle of duplexes, to determine the angle of the thrust fault that formed them. This angle can be very useful in building balanced cross-sections. Duplexes have multiple angles to be measured after they fold over earlier duplexes. Analysis of the changes in angles can tell something about the shortening and shearing of the horse as it rode over the thrust.

BREAK-BACKWARD THRUST SEQUENCES

Butler (1987) examined the break-forward sequence of thrusting and pointed out that foreland-forming imbricate fans do form, but he also studied imbricate fans that he believed formed to the hinterland of the original fault. He termed these fans "break-backward thrust sequences." When the fault reaches its maximal displacement due to the changed slope of the thrust, the new thrust will form towards the hinterland (Figure 26). Subsequent thrusts will continue to form in the hinterland, due to the resistant forces in the

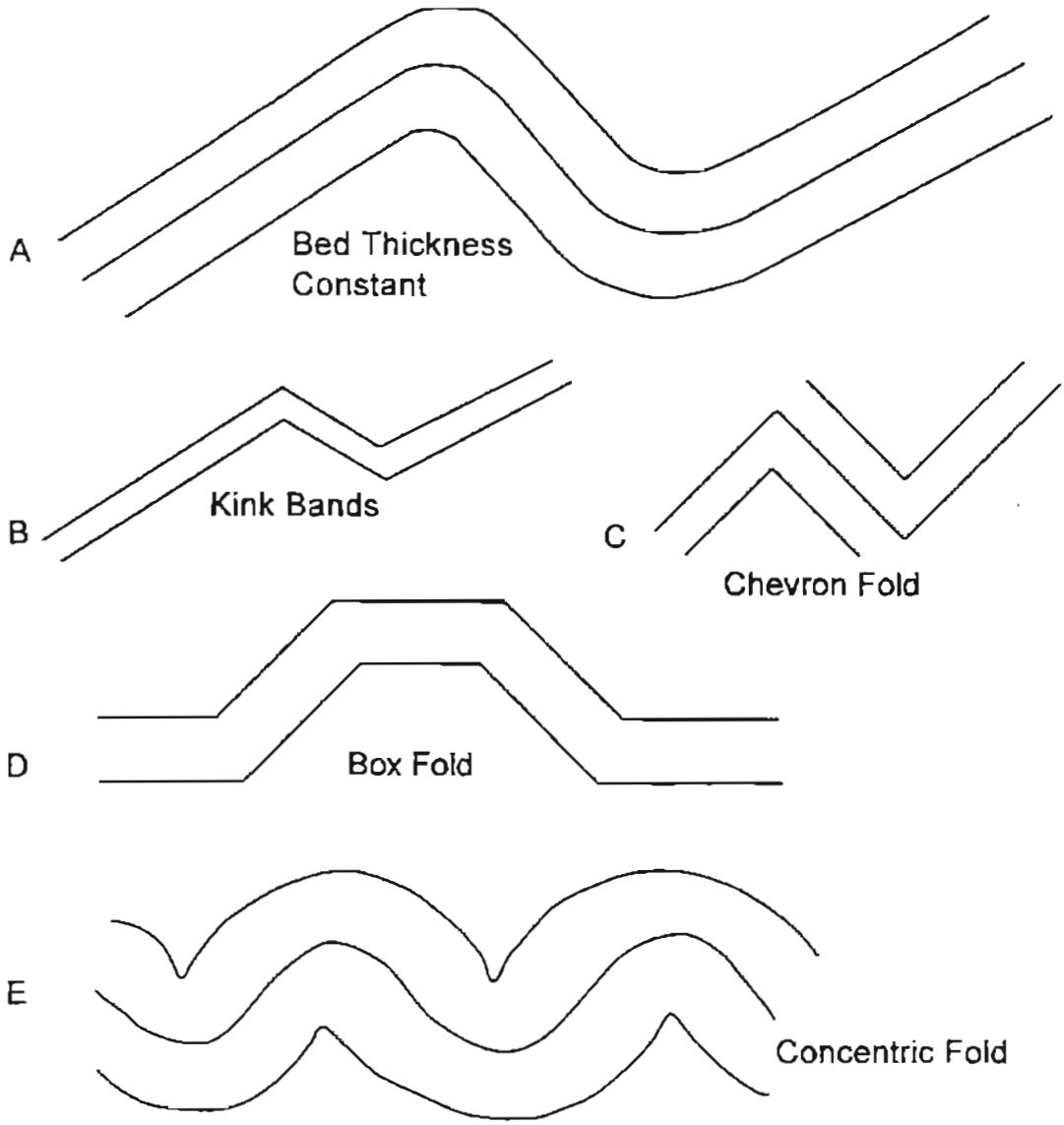

Figure 24. Folding styles. From (Woodward et. al., 1985)

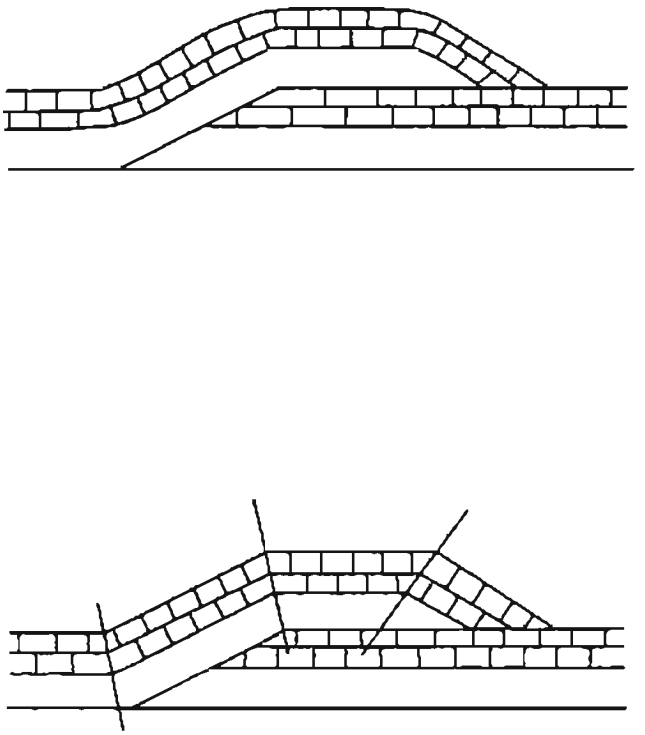

Figure 25. Folding characterized as a series of kink-bend folds, according to Suppe (1983).

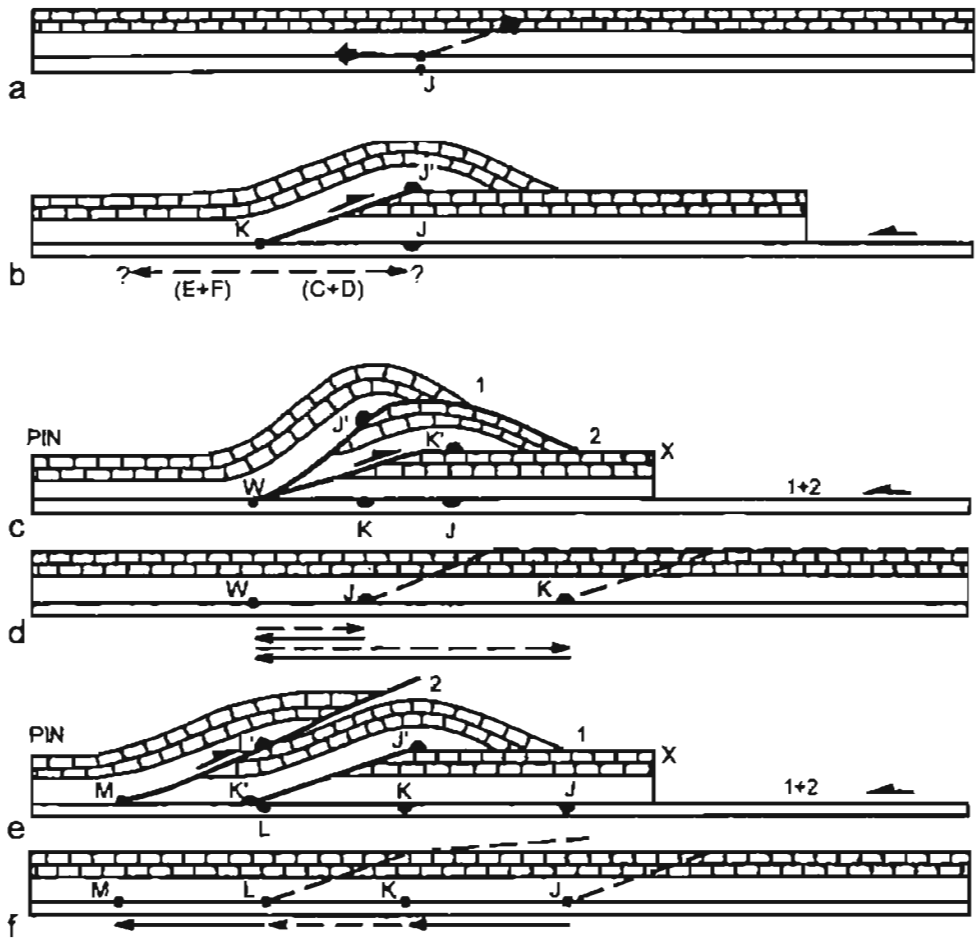

Figure26. The generation of back-thrust sequences. (a,b) Resored and balanced sections of the first thrust surface, with forward migration of the displacement front (J-K); (c,d) the development of internally piggy-back sequences of back-thrust movement where the displacement front (W) is fixed and the displacements on the back thrusts are determined by the propagated length of the lower thrust segment (e.g. W-J); (e,f) the development of internally break-back sequences by the continued forward displacement of the displacement front (J-K-L-M). (From Butler, 1982)

foreland (Butler, 1987). Break-backward regimes form in areas where a propagating thrust sheet cannot be moved forward (Figure 27). This could be the result of a thrust encountering a resistive up-thrown block, a fault escarpment, a resistive landform, or some other unmovable object (Butler. 1987). The fact that the thrust cannot propagate forward does not stop the stresses that are pushing the sheet. Where the thrust sheet encounters the hindrance, horses begin to develop. It is possible that the horses will rotate with the pressure of continued thrusting. If this happens the thrust will become deformed and motion along it ceases. The internal structures of the beds will also become deformed. Localized folding and shortening are to be expected (Butler, 1987). Eventually, as strains build, faults will form. These thrusts form in a direction opposite that of the break-forward sequence of thrusting discussed by Boyer and Elliott (1982) and Suppe (1983) (Figure 19). The ramp will orient itself in such a way as to allow the thrust sheet to undercut the horse (Figure 26). However, these duplexes will dip to the foreland, while break-forward duplexes normally dip towards the hinterland. There is still an active sole thrust, but the roof thrust is not active. Stacked duplexes and antiformal stacks are commonly in areas that have undergone break-backward thrusting (Butler, 1987).

DUPLEX STRUCTURES

Duplex structures are the other form of branching thrust faults. Boyer and Elliott (1982) defined a duplex as "an imbricate family of horses" (Figure 20). If a thrust sheet is completely bounded by branch lines the resulting form is a horse. According to Boyer and Elliott (1982), horse is an "old and useful term" that indicates a "pod" of rock or strata that is bounded by thrust faults.

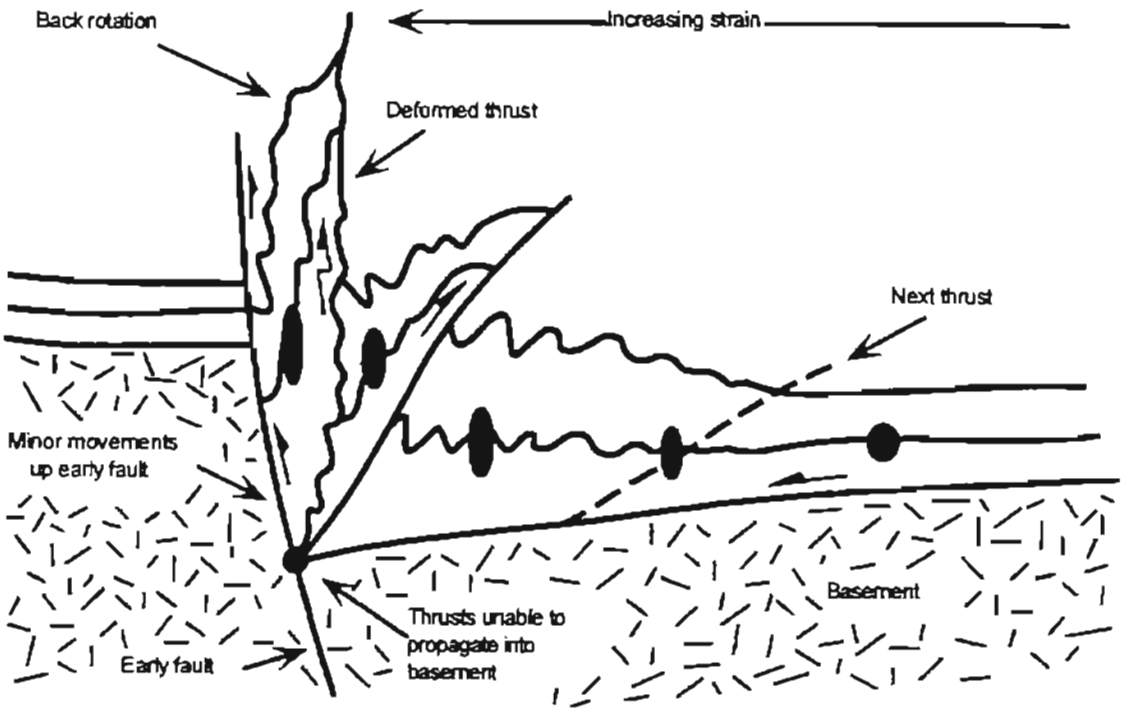

Figure 27. Rotation of horses as a propogating thrust sheet encounters a hinderance (from Butler, 1987).

If the slip along the thrust is approximately equal to the length of the horse then the branch lines will bunch up and the horses will stack (Figure 28). This is referred to as an antiformal stack (Butler, 1987). The antiformal stack derives its name from its resemblance to an anticline. As the horses are moved into position they undergo some amount of folding. In some foreland-dipping duplexes, horses do not stack neatly. Forward motion of the horse along the thrust surface may not stop when the horse overrides the ramp. If this occurs, the horse will rotate so that the part of the horse that was the hanging wall of the ramp will lie against the sole thrust. As new horses are formed and progress up the ramp, they overturn. In this model the common "shingle-stacking" of the duplexes is restored (Figure 29).

BACKTHRUSTS

Some thrust faults form in the direction opposite to regional thrust sheet-movement (Figure 30). They are termed "backthrusts"" or out-of-sequence thrust faults" by Boyer and Elliott (1982). New thrust faults either propagate upward into the thrust sheet as a breakback structure, or forward and down into the footwall in an imbricate formation (Butler, 1987). Whether backthrusts form as the result of localized binding of the thrust sheet or by some other means is still undetermined (Butler, 1987).

TRIANGLE ZONES

Near the foreland termination of a thrust sheet conflicting stresses can build up and form a backthrust (Tearpock and Bischke, 1991). McClay (1992) proposed that a triangle zone is a combination of two thrusts with opposing vergence that form a triangular zone between them (Figure 31). Price (1986) further stipulated that a triangle zone is bounded

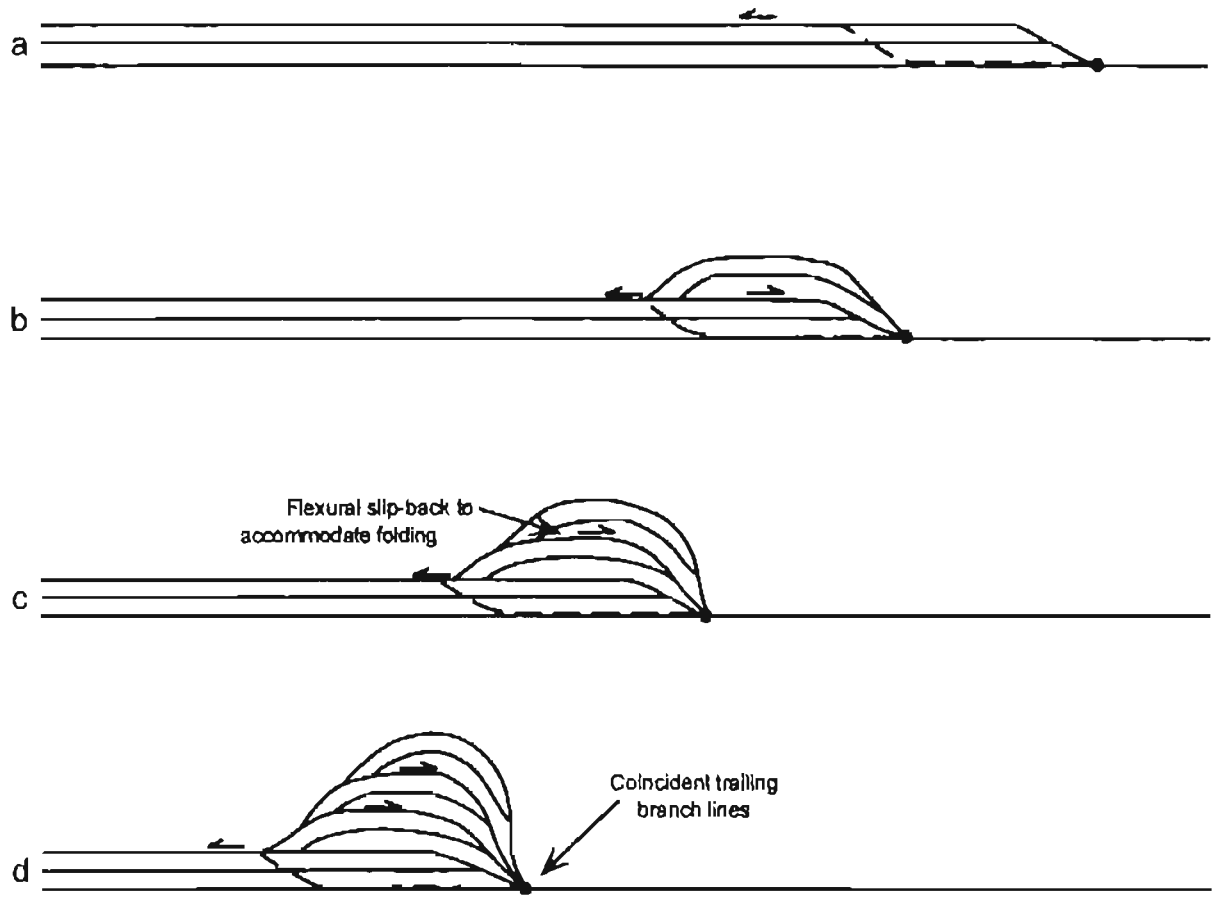

Figure 28. The sequential evolution (a-d in time) of a hypothetical antiformal stack duplex illustrated on balanced cross-sections (from Buter, 1987).

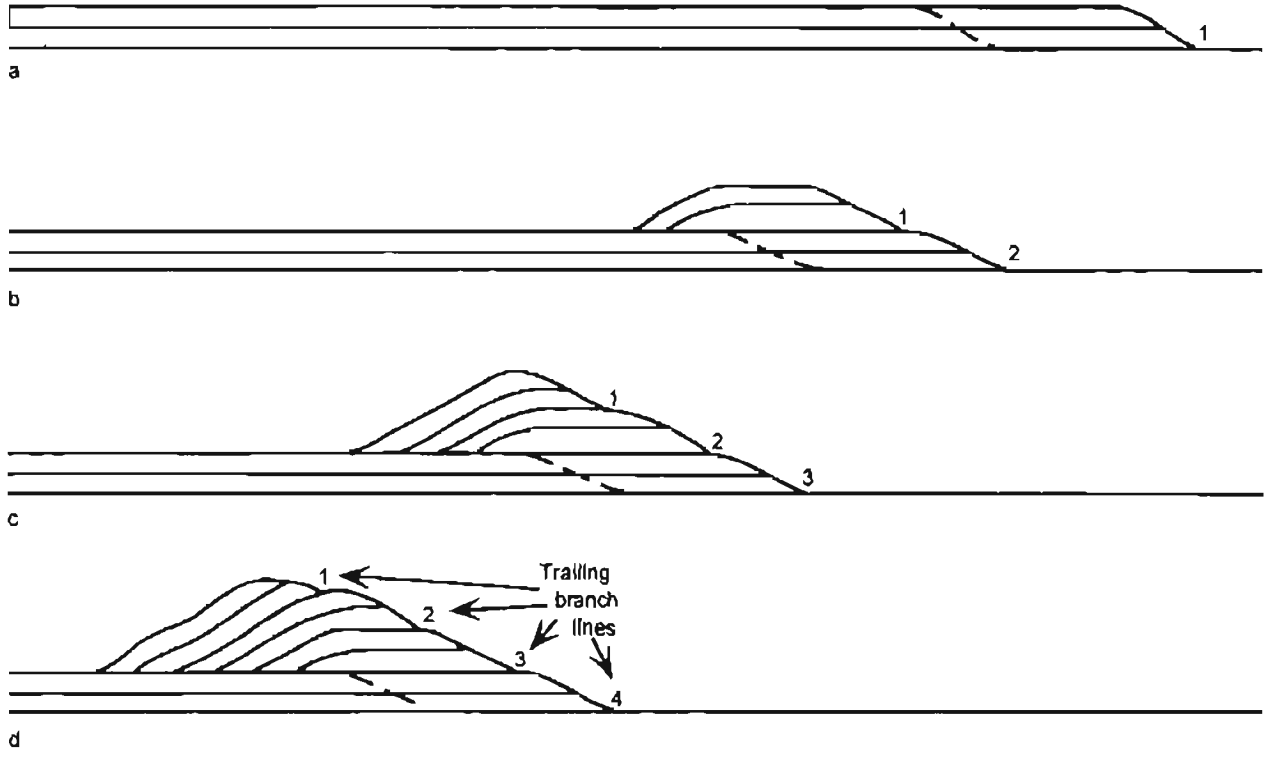

Figure 29. The sequential evolution (a-d in time) of a hypothetical foreland-dipping duplex illustrated on balanced cross-sections. The trailing branch lines are numbered in order of development (1, oldest; 4, youngest) (from Butler, 1987).

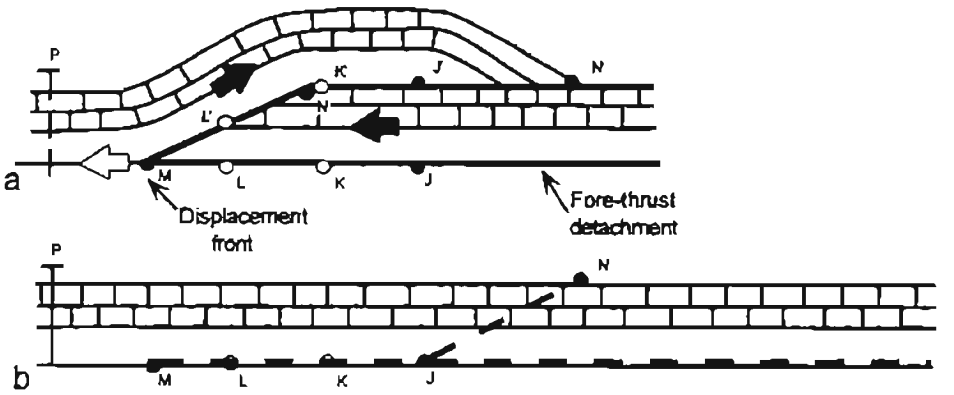

Figure 30. Displacement and propogation of a single back-thrust (a) After displacement; (b) before displacement. (Modified from Butler, 1987).

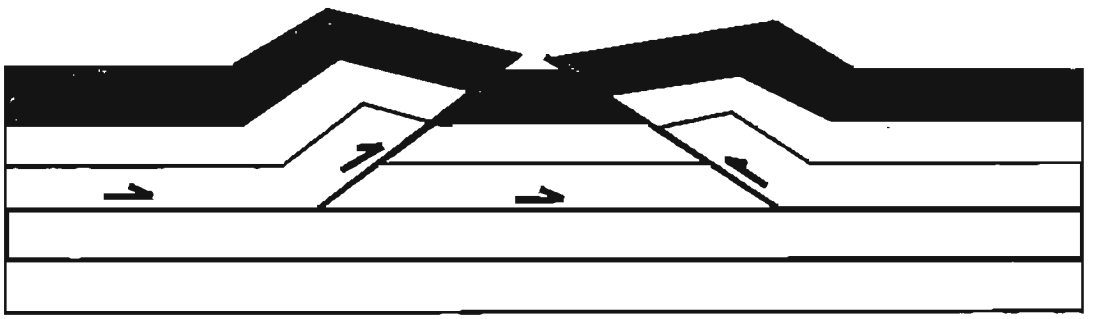

Figure 31. Triangle zone (from McClay, 1992).

below by a floor thrust. Deformation of the thrust sheet terminates at the triangle zone (Johns, 1987 and Tearpock and Bischke, 1991). Thrusting extends into the basin until stresses are weakened to the point where no new thrust forms. This commonly occurs because of a hindrance. Where the thrust sheet becomes hindered, a backthrust can form. The place where the backthrust forms on the fore-thrust is called the "zero-displacement point" (Figure 32b and 32c). Couzens and Wiltschko (1994) studied triangle zones at many places in the world, and proposed three basic types. Type one has "opposed thrusts with a symmetrical distribution above a single detachment level" (Figure 32a). Type two features "opposing thrusts with an asymmetrical distribution above a single detachment" (Figure 32b). In this case, duplexes of the propagating thrust sheet are in the footwall of the backthrust. Type three (Figure 32c) has "opposed thrusts with an asymmetrical distribution and two detachment levels" (Couzens and Wiltschko, 1994). The type two triangle zone is most commonly found in areas with no "strong structural-lithic unit," such as triangle zones in forearc basins. The triangle zone that is defined in the Wilburton area by Al-Shaieb et al. (1995), Cemen et al. (1994,1995,1997), Akthar (1995), and Sagnak (1996) (from Sagnak, 1996) is similar to the type three triangle zone of Couzens and Wiltschko (1994) (Figure 32c). Figure 33 shows a sole thrust as the base of the triangle zone whereas the final imbricate fault and the backthrust are the legs of the triangle.

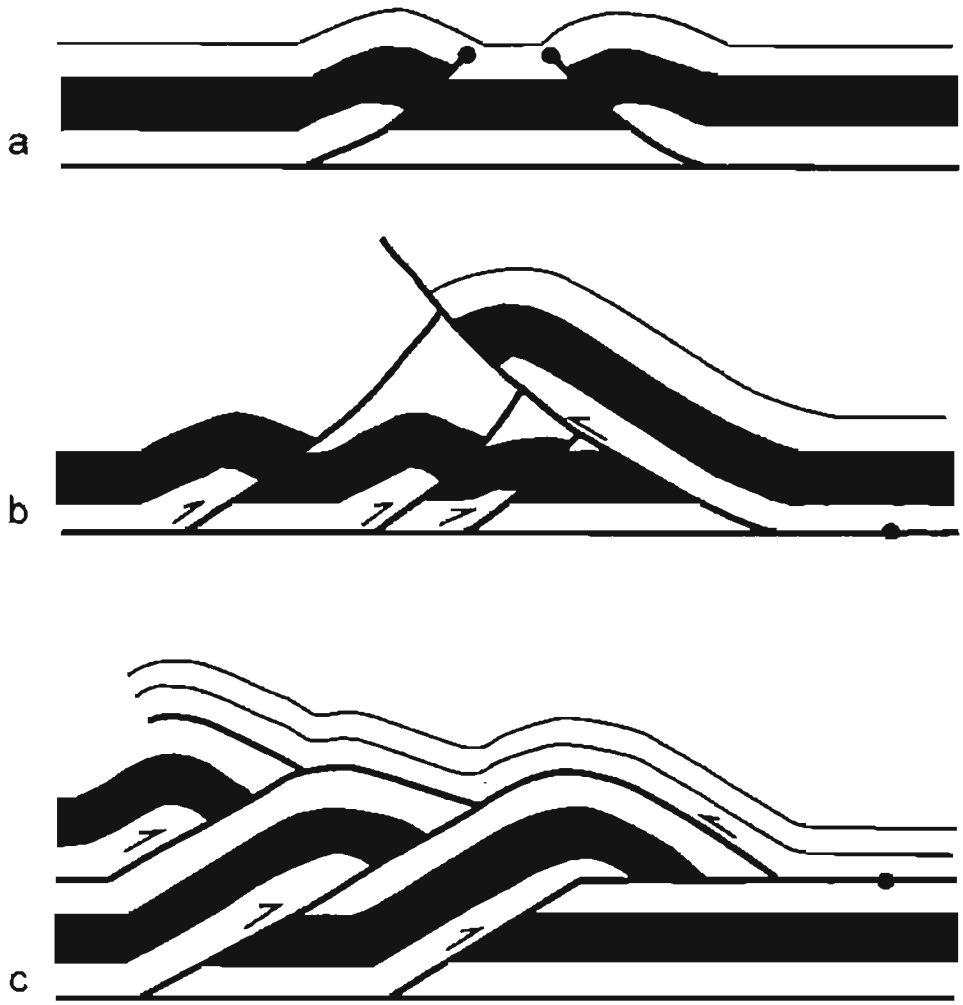

Figure 32. Three-end-member geometries of triangle zones (from Couzens and Wiltschko, 1994).

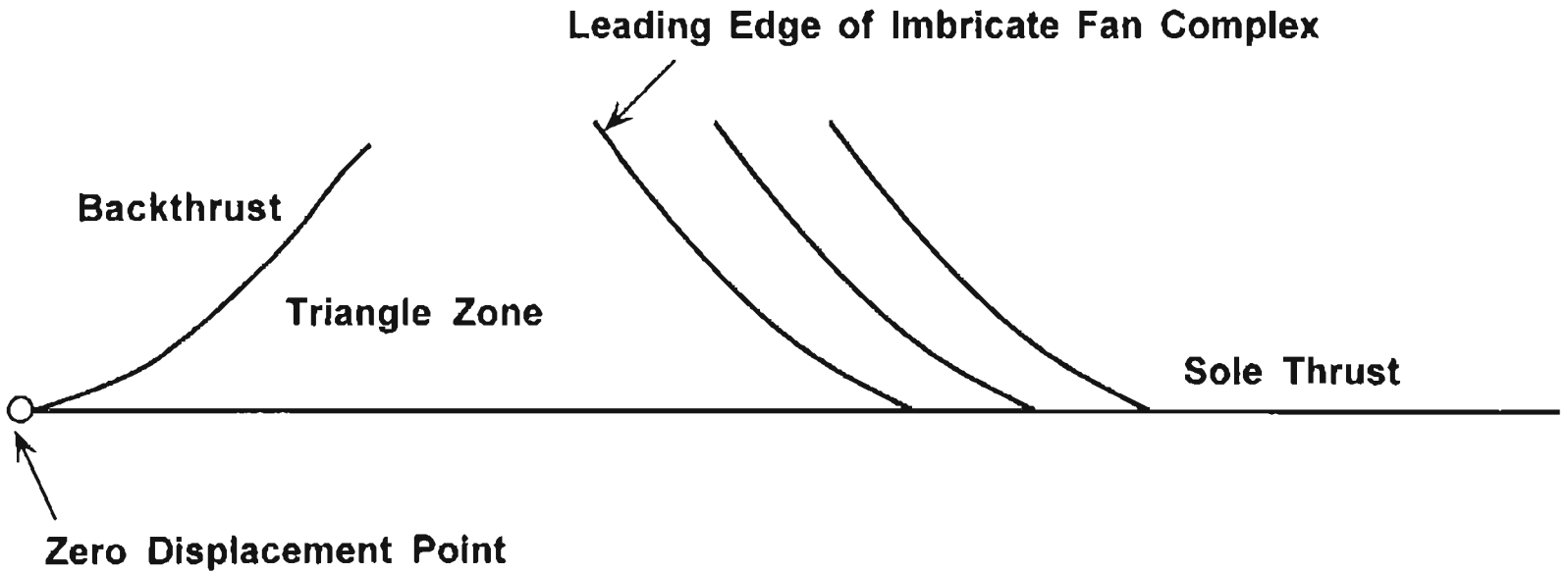

Figure. 33. The simple formation of a triangle zone. The backthrust forms in response to some resistance to thrusting. The sole thrust forms the base of the triangle and the imbricate thrustforms the third leg.

CHAPTER 5

STRUCTURAL GEOLOGY

INTRODUCTION

Structural geometry of thrust faults in the transition zone between the Ouachita Mountains and the Arkoma Basin has been debated for some time. The main debate concerning structural geometry has been over the imbricate thrusts and the presence of a triangle zone. Suneson (1995) summarized structural interpretations of the transition zone. The following paragraphs dealing with triangle zones are based on this summary.

Arbenz (1984) was the first to recognize south-dipping thrust faults, blind imbricate thrusts branching from the exposed thrust system, and deep décollement surfaces that served as the floor thrusts for the imbricate thrusts that extend into the basin (Figures 34 and 35). Arbenz interpreted the detachment surface as rising gradually northward.

Hardie (1988) was the first to apply the term "triangle zone" to the geometry of the basinward side of the transition zone (Figure 36). Based on areal geologic maps, Hardie (1988) identified the Blanco thrust, located southwest of the town of Hartshorne (east of the study area), as the "basinward roof of a relatively thick triangle zone." His cross-sections showed blind imbricate thrusts and backthrusts in the footwall of the

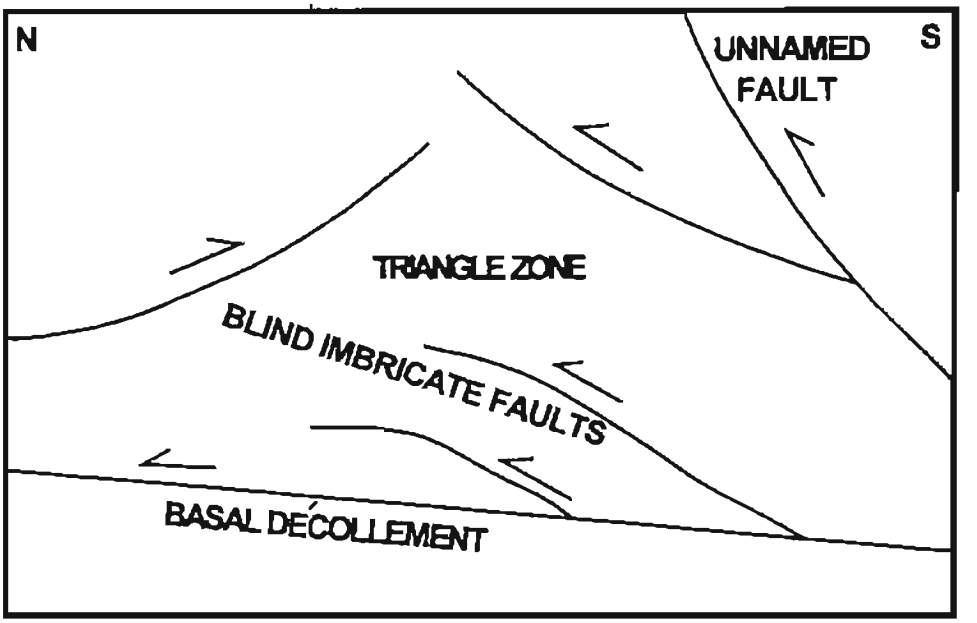

Figure 34. Triangle zone, décollement, and blind imbricate faults (From Arbenz, 1984).

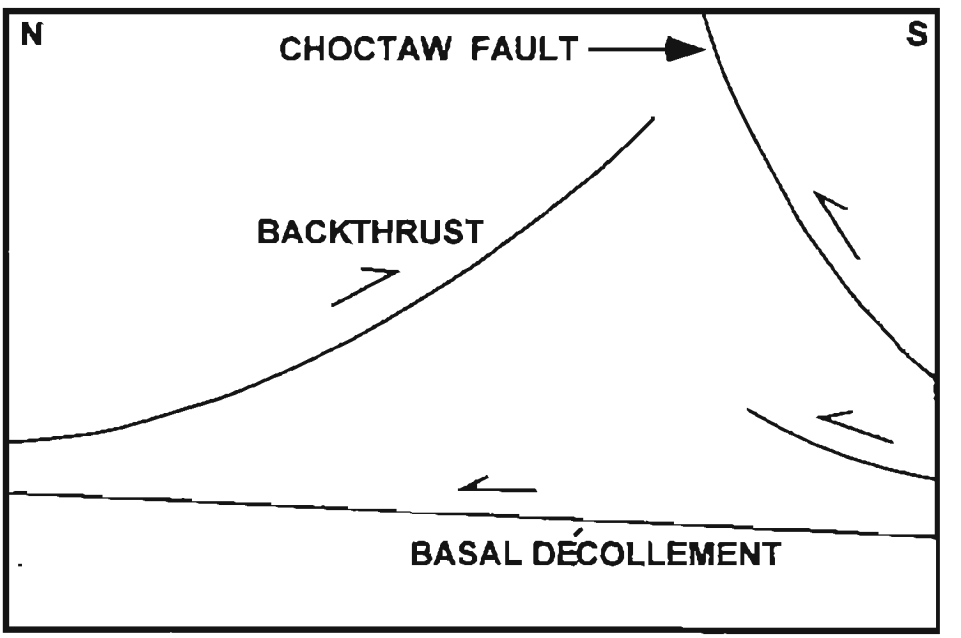

Figure 35. Triangle zone from Arbenz (1989)

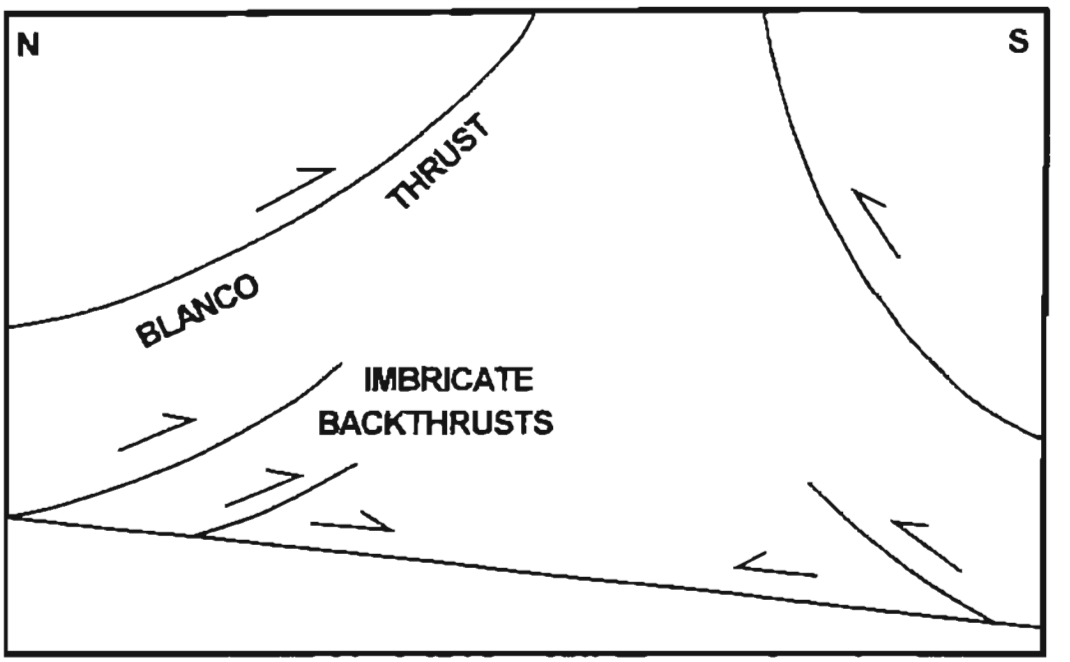

Figure 36. Sketch cross-section showing styles of deformation in the subsurface at the transition zone between the Arkoma Basin and Ouachita Mountains, as proposed by Hardie (1988) (after Suneson, 1995).

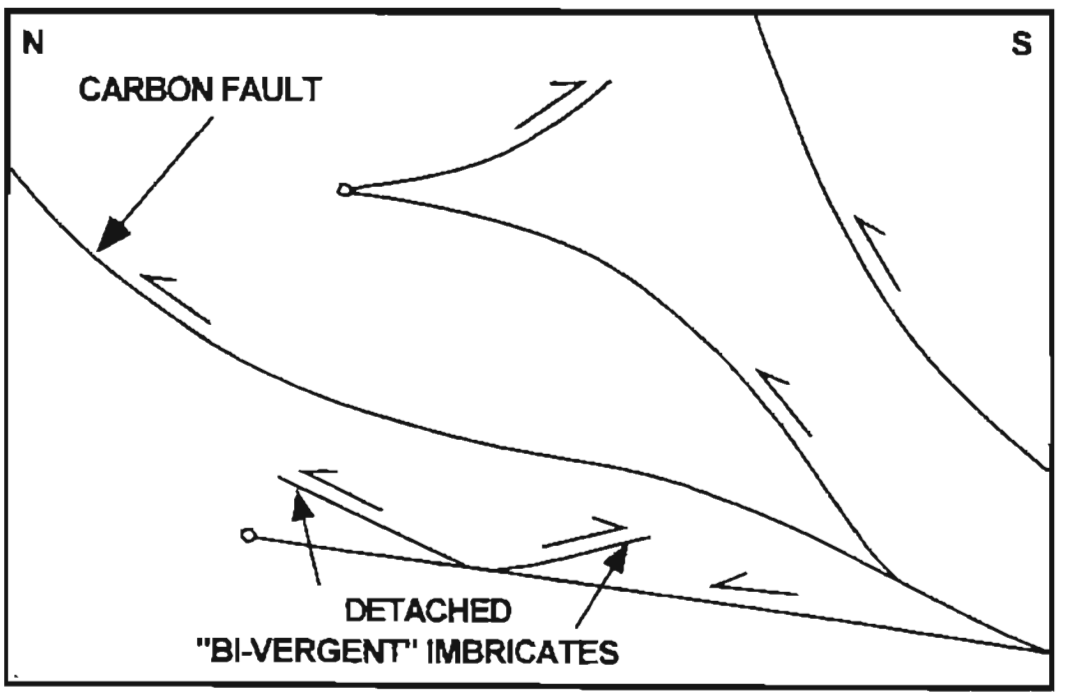

Figure 37. Sketch cross-section showing styles of deformation in the subsurface at the transition zone between the Arkoma Basin and Ouachita Mountains, as proposed by Milliken (1988) (after Suneson, 1995).

Choctaw Fault. He also mapped a basal detachment surface at the base of the Pennsylvanian Springer Formation.

Milliken (1988) interpreted a thin triangle zone floored by north-directed imbricate thrust fault (Figure 37). He also interpreted deeper structures that he termed "detached bi-vergent imbricates."

Camp and Ratliff (1989) identified a thick triangle zone floored by blind imbricate thrusts and backthrusts (Figure 38). They also suggested a deep, north-directed detachment that climbs from Mississippian shales in the south to Middle Pennsylvanian strata to the north. Their cross-section also shows imbricate backthrusts splaying off the roof backthrust of the triangle zone.

Reeves et al. (1990) interpreted a thin triangle zone floored by two north-directed duplex structures (Figure 39). They suggested that the décollement actually lies within lower Atokan strata instead of the formerly proposed Mississippian to Morrowan strata. They also showed a complex series of blind imbricate thrust faults, similar to the "detached bi-vergent imbricates" of Milliken (1988).

Perry et al. (1990) proposed a shallow triangle zone overlying a deeper triangle zone. They revised their interpretation to show that the deep triangle zone consisted of north-directed duplexes with a floor thrust and a north-directed roof thrust that gradually gets shallower within the Atoka Formation (Figure 40).

Roberts (1992) interpreted the structural geometry near Heavener, Oklahoma to be the result of underlying duplex structures instead of a triangle zone (Figure 41). He made his interpretations with seismic data and little well control. He proposed a basal

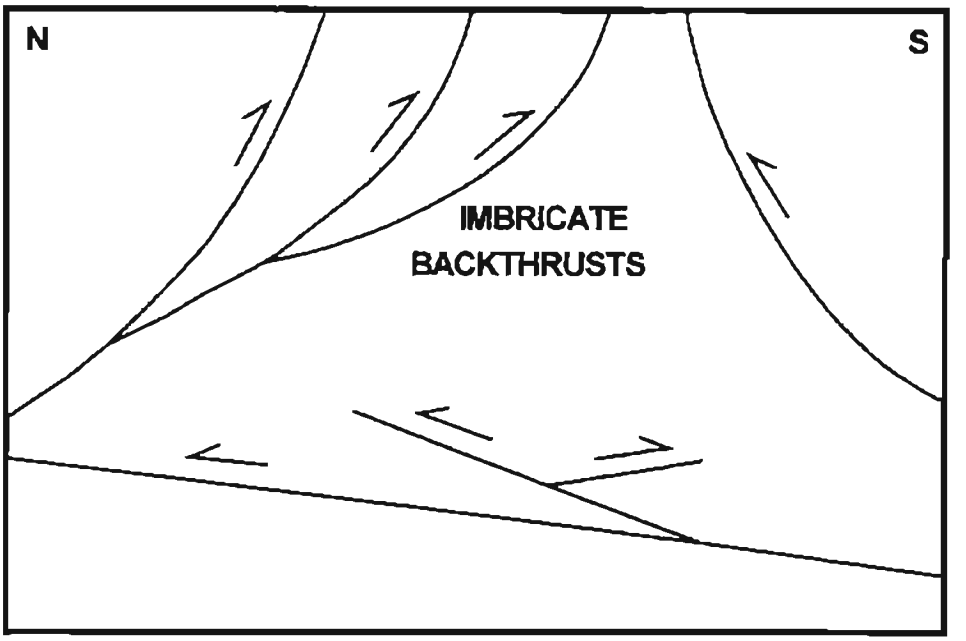

Figure 38. Triangle zone with imbricate backthrusts (from Camp and Ratliff, 1989).

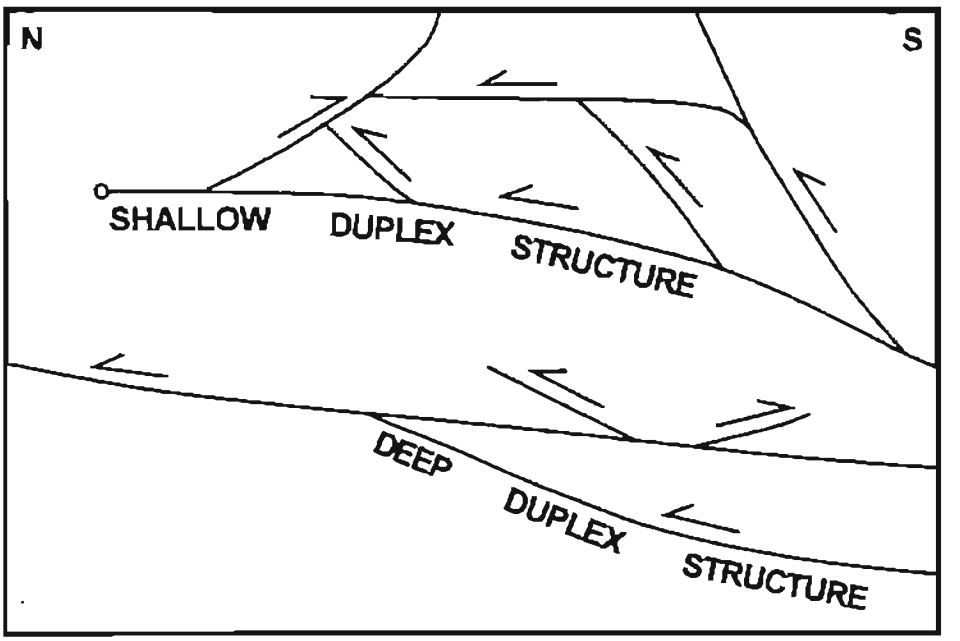

Figure 39. Triangle zone with shallow and deep duplex structures and higher level of basal detachment (from Reeves et al., 1990).

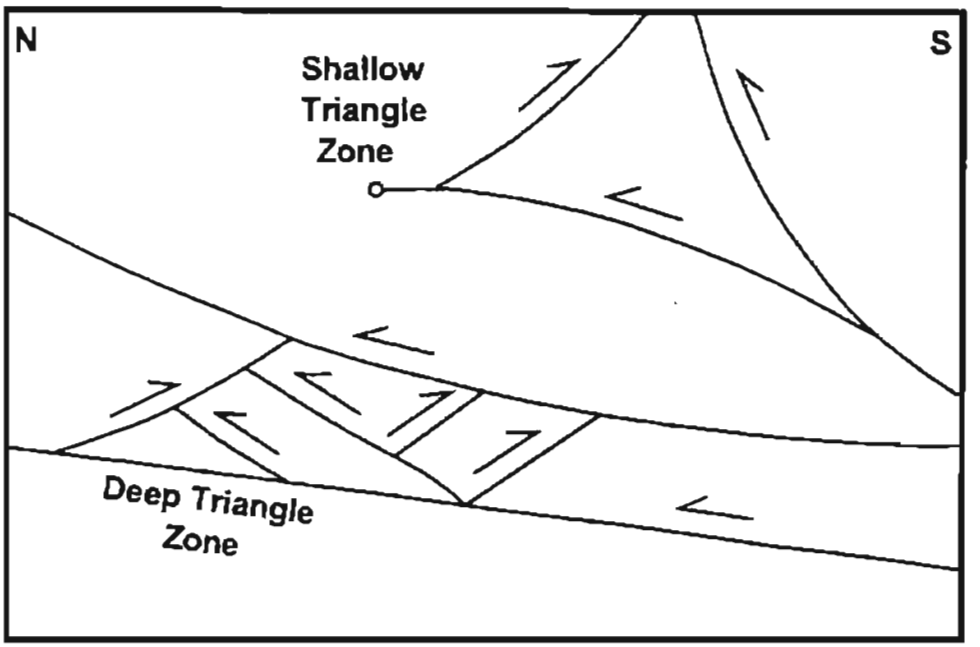

Figure 40. Note passive roof duplex and shallow and deep triangle zones (From Perry and others 1990).

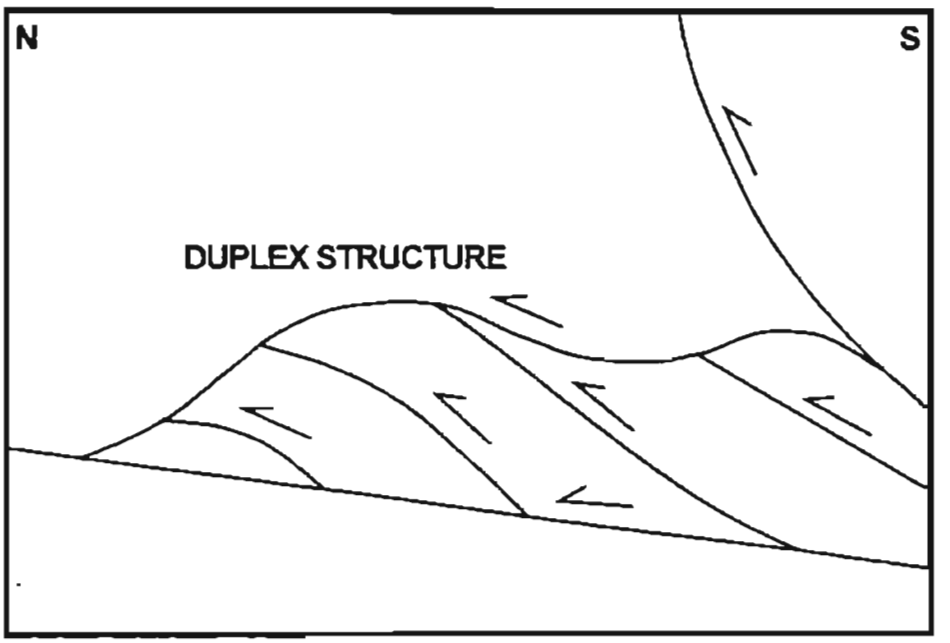

Figure 41. Note absence of triangle zone and presence of thick duplex structure (From Roberts 1992).

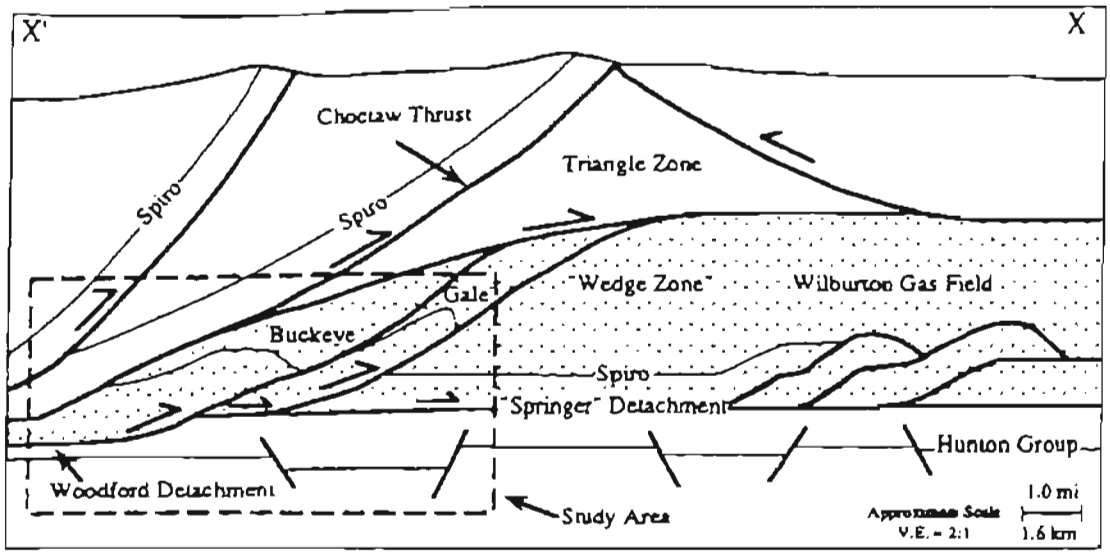

Figure 42. Schematic structural cross-section illustrating the transition from the Ouachita fold and thrust belt to the Arkoma foreland basin (after Wilkerson and Wellman, 1993).

décollement in the lower part of the Atoka Formation that extends deep into the basin.

Wilkerson and Wellman (1993) suggested a thin triangle zone and duplex structures (Figure 42). They also included oblique ramps, tear faults and blind imbricate thrusts in their interpretation (Suneson, 1995).

Al-Shaieb et al. (1995), Cemen et al. (1994, 1997) Akhtar (1995), and Sagnak (1996), in the OCAST project, suggested imbricate thrusts within the Wilburton gas field area. They concluded that duplex structures and a triangle zone exist in the area. They proposed a triangle zone that is bounded by the Choctaw fault to the south, by the Carbon fault to the north, and that is floored by the Lower Atokan Detachment surface. They also concluded that the footwall of the Choctaw fault contains duplexes formed in a break-forward sequence of thrusting. They reported about 60% shortening of the Spiro sandstone in the Wilburton area.

This study is concerned with changes eastward from the Wilburton gas field area to the Panola and Baker Mountain quadrangles (Figures 44-48, and Plates I-V). As part of the study of structural geometry, five balanced structural cross-sections were constructed. This was done by the key-bed method, using the Spiro sandstone as the marker. The locations of the cross-secitons and seismic lines used in this study are shown in Figure 43. Cross-section D-D' (Figure 47) is based on the best well-log data control, and is positioned directly on seismic line QM5-8 (Figure 49, Plate 6). For these reasons, cross-section D-D' was used as a model to aid in the interpretation of the other four cross-sections. The cross-sections were restored to estimate the amount of shortening within the study area.

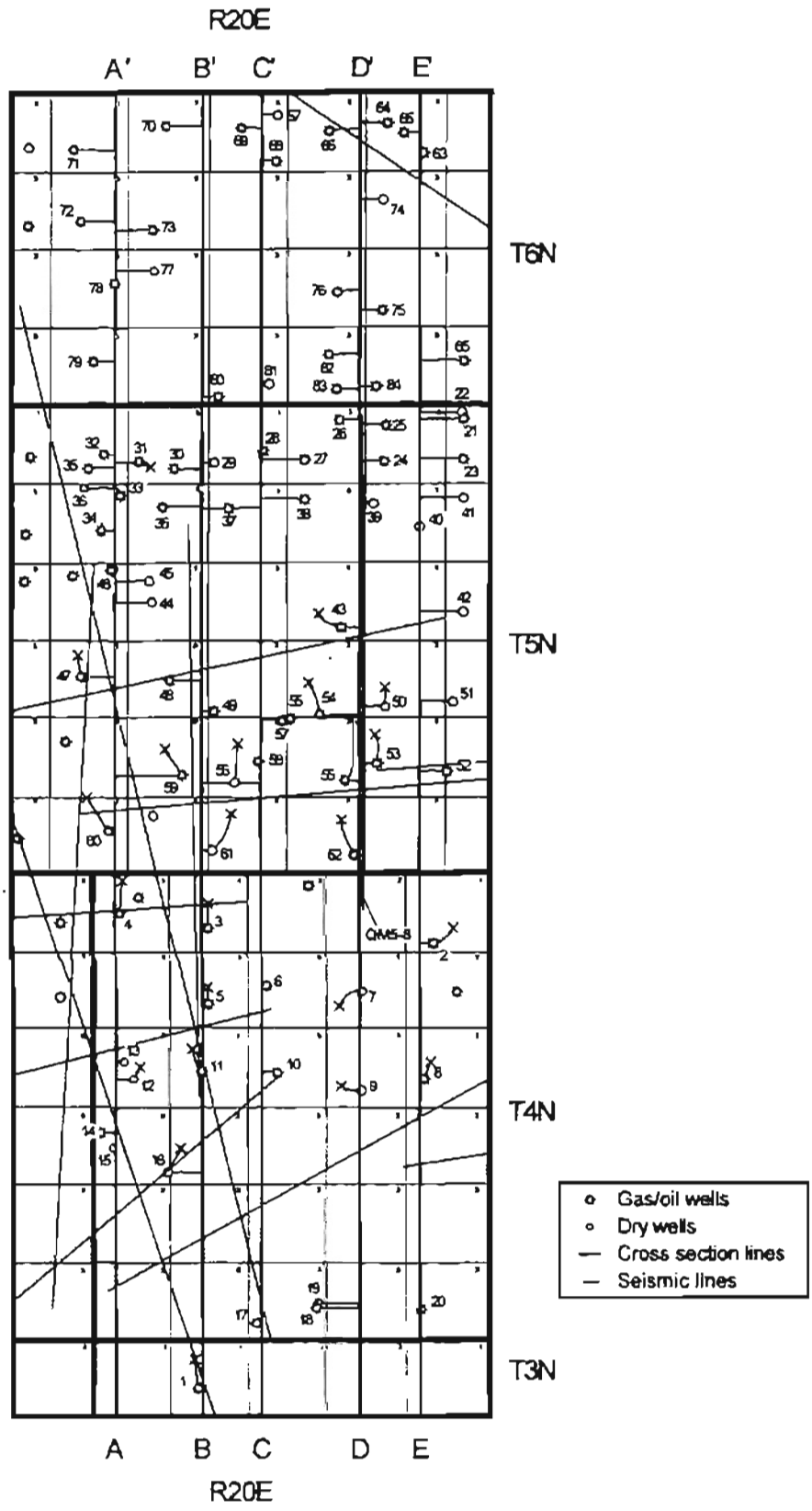

Figure 43. Map showing locations of cross-sections, seismic lines, and well locations. Well numbers reffer to Appendix I : Well log data sheets.

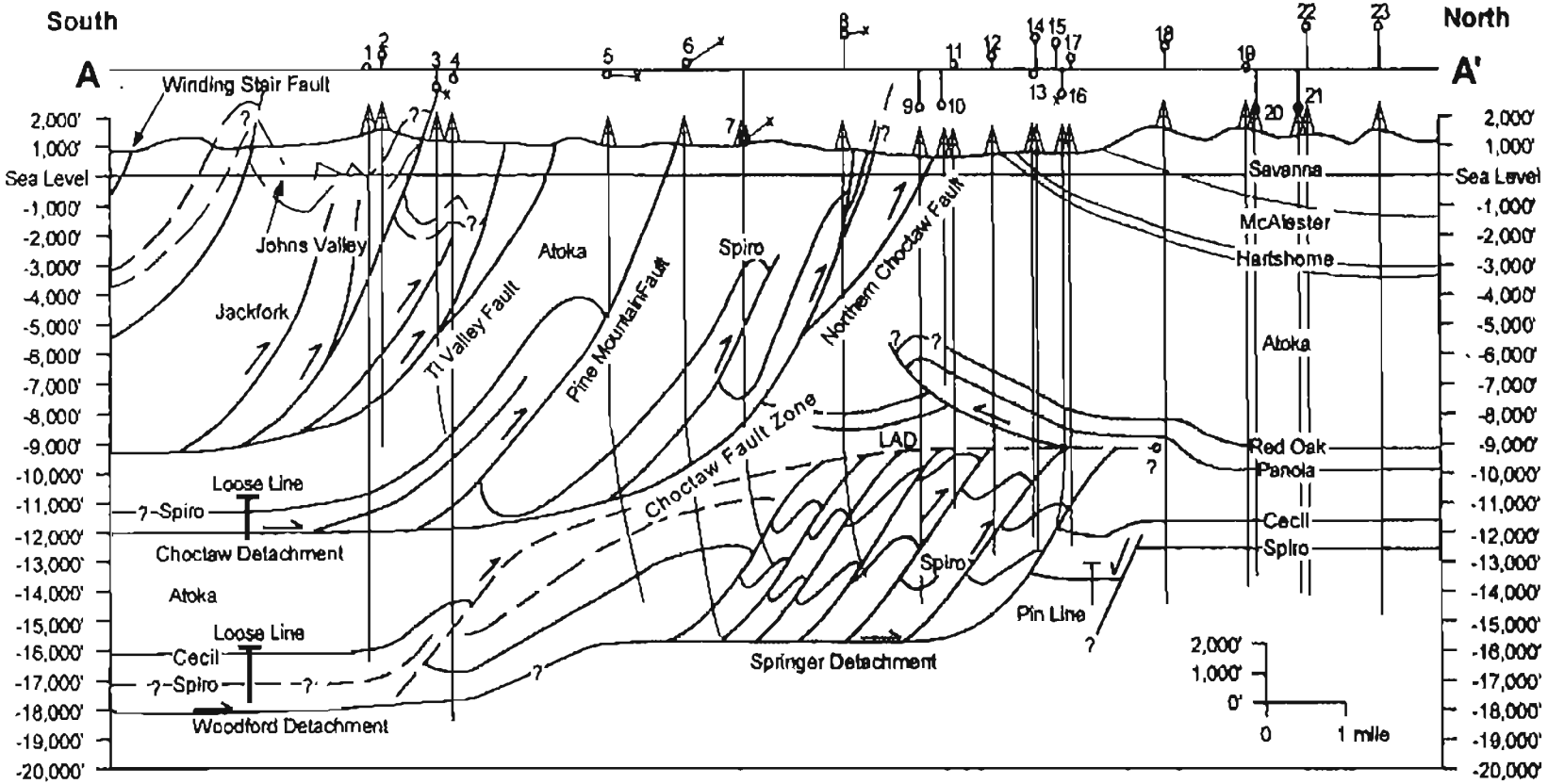

1. H&H Star Energy
   Bear Suck Knob #1-20 "A"
   20-T4N-R20E
2. H&H Star Energy
   Bear Suck Knob #1-20
   20-T4N-R20E
3. Amoco Production
   Green Bay #1-17
   17-T4N-R20E
4. Scana Exploration
   Green Bay #2-17
   17-T4N-R20E
5. H&H Star Energy
   Lucky Strike #1-5
   5-T4N-R20E
6. Anadarko Petroleum
   H&H Cattle Co. #1-31
   31-T5N-R20E
7. Anson Corp.
   Clear Creek #1-29
   29-T5N-R20E
8. Anson Corp
   Buzzard Gap #1-19
   19-T5N-R20E
9. Humble Oil & Refining Co.
   Shay #1
   17-T5N-R20E
10. Edwin L. Cox
    Shay #1
    17-T5N-R20E
11. Unit Drilling & Exploration
    Harding #1
    18-T5N-R20E
12. Williford Energy
    Butzer #1-7
    7-T5N-R20E
13. Williford Energy
    Wiginton #1-7
    7-T5N-R20E
14. Unit Drilling
    Dear #1
    8-T5N-R20E
15. Unit Drilling
    Cox #1
    8-T5N-R20E
16. Donald C. Slawson
    McKee #1-5
    5-T5N-R20E
17. Mec Inc
    Lively #2
    6-T5N-R20E
18. Leede Oil & Gas Inc
    Wilburton Mountain #1
    31-T6N-R20E
19. Santa Fe Minerals
    Pierce #1-30
    30-T6N-R20E
20. Tenneco Oil Co.
    Pierce #1-29
    29-T6N-R20E
21. Tenneco Oil Co.
    Swart #1-20
    20-T6N-R20E
22. Tenneco Oil Co.
    Cecil #1-19
    19-T6N-R20E
23. Leben Drilling
    Jankowsky #1-18
    18-T6N-R20E

Figure 44. Balanced structural cross-section A-A'. Location of cross-section shown in Figure 43.

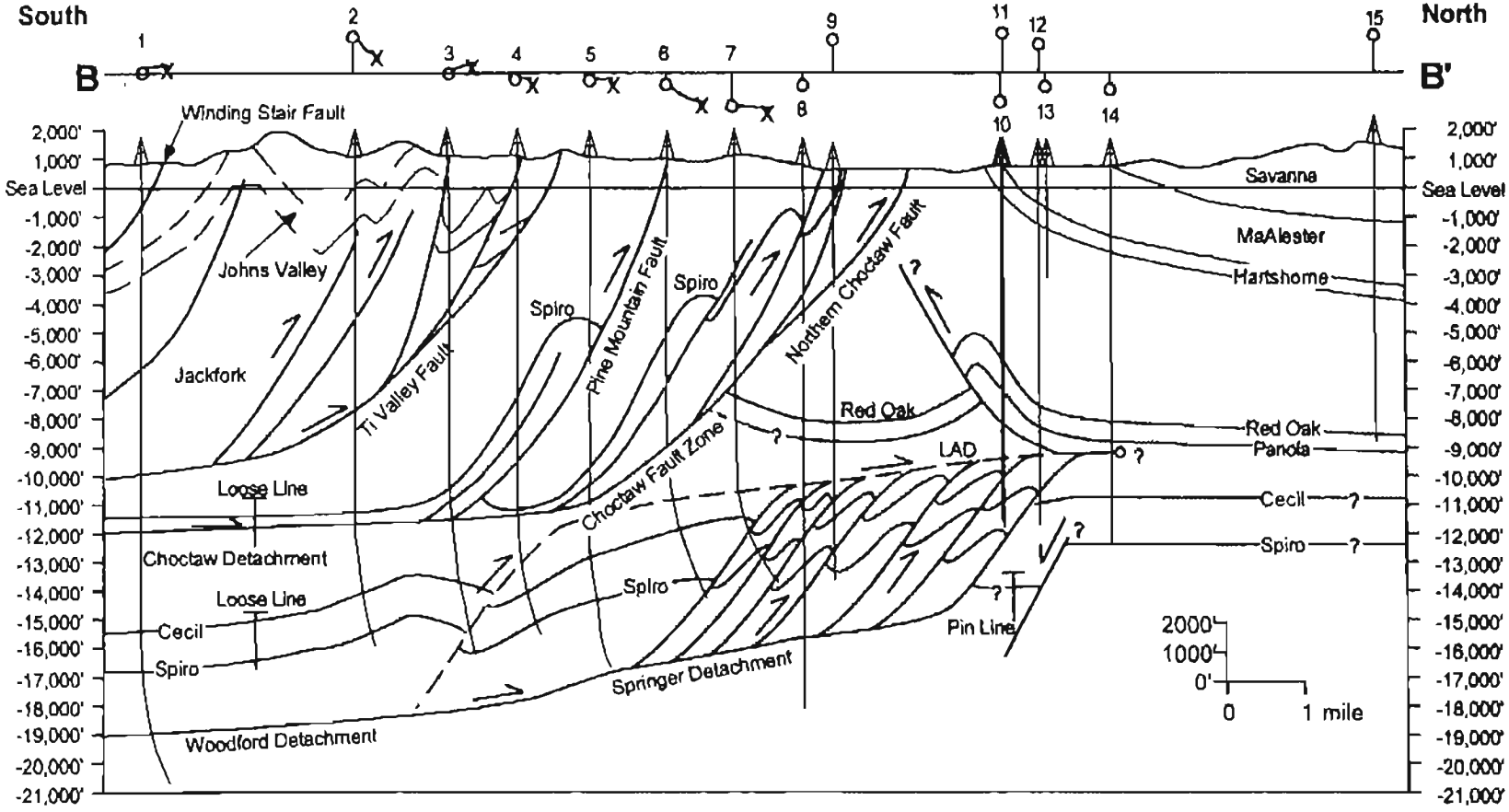

1. H&H Star Energy
   Hope #1-4
   4-T3N-R20E

2. H&H Star Energy
   Eight Mile Mountain
   21-T4N-R20E

3. H&H Star Energy
   Coppers Hollow #1-16
   16-T4N-R20E

4. Anadarko Petroleum
   Barnes #1-9 "A"
   9-T4N-R20E

5. H&H Star Energy
   Dipping Vat #1-4
   4-T4N-R20E

6. Anson Corp.
   Turner #1-33
   33-T5N-R20E

7. Anson Corp.
   Turney #1-28
   28-T5N-R20E

8. Amoco Prod.
   Cindy #1-21
   21-T5N-R20E

9. Anson Corp.
   Hardcastle #1-20
   20-T5N-R20E

10. Unit Drilling
    Go Lightly #1
    9-T5N-R20E

11. Unit Drilling
    Cox #1
    8-T5N-R20E

12. Unit Drilling
    Maxey #1-5
    5-T5N-R20E

13. Unit Drilling
    Maxey #1-4
    4-T5N-R20E

14. Mobil Oil Co.
    Parks #1
    33-T6N-R20E

15. Leben Drilling
    Parsons #1-17
    17-T6N-R20E

Figure 45. Balanced structural cross-section B-B'. Location of cross-section shown on Figure 43.

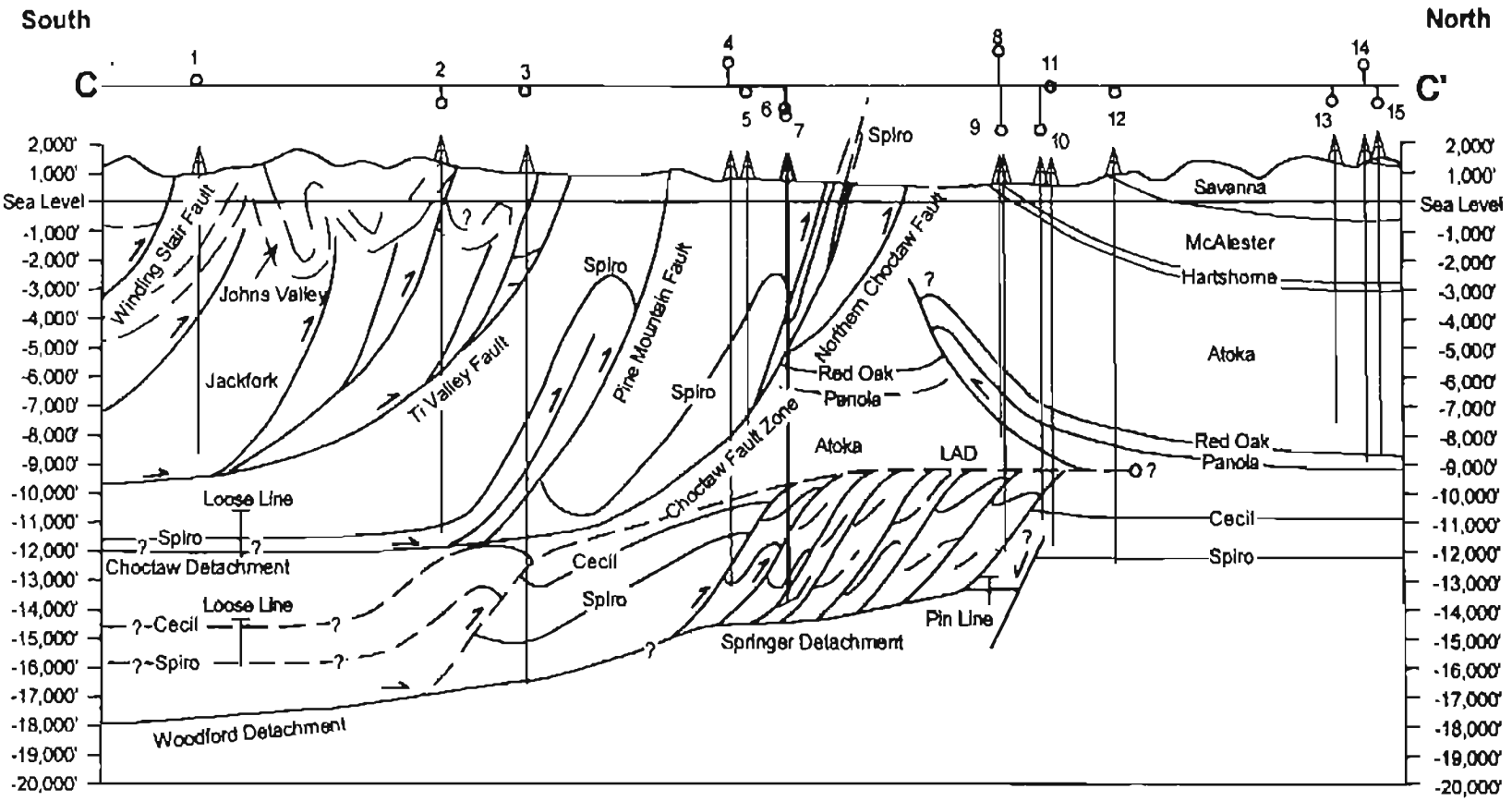

1. H&H Star Energy
   Green Bay #1-34
   34-T4N-R20E
2. H&H Star Energy
   Dipping Vat #1-15
   15-T4N-R20E
3. Anson Corp.
   Golden #1-10
   10-T4N-R20E
4. Anson Corp.
   Turney #1-28
   28-T5N-R20E
5. Anson Corp.
   Blakely #1-28
   28-T5N-R20E
6. Anson Corp.
   Cox #1-28
   28-T5N-R20E
7. Amoco Production
   Bauman Jack No. 1
   27-T5N-R20E
8. Unit Drilling Co.
   Go Lightly #1
   9-T5N-R20E
9. Austin Production
   Colvard Lm #1
   10-T5N-R20E
10. Mustang Production
    Cash-Mitchell
    3-T5N-R20E
11. Unit Drilling Co.
    Hawthorne #1
    4-T5N-R20E
12. Mustang Production
    Parks #1-33
    33-T6N-R20E
13. Texas Oil & Gas Corp.
    Parsons #1 "A"
    16-T6N-R20E
14. Shell Oil Co.
    Parsons #1-16
    16-T6N-R20E
15. Dyco Petroleum Corp.
    Parsons #A-1
    16-T6N-R20E

Figure 46. Balanced structural cross-section C-C'. Location of cross-section shown in Figure 43.

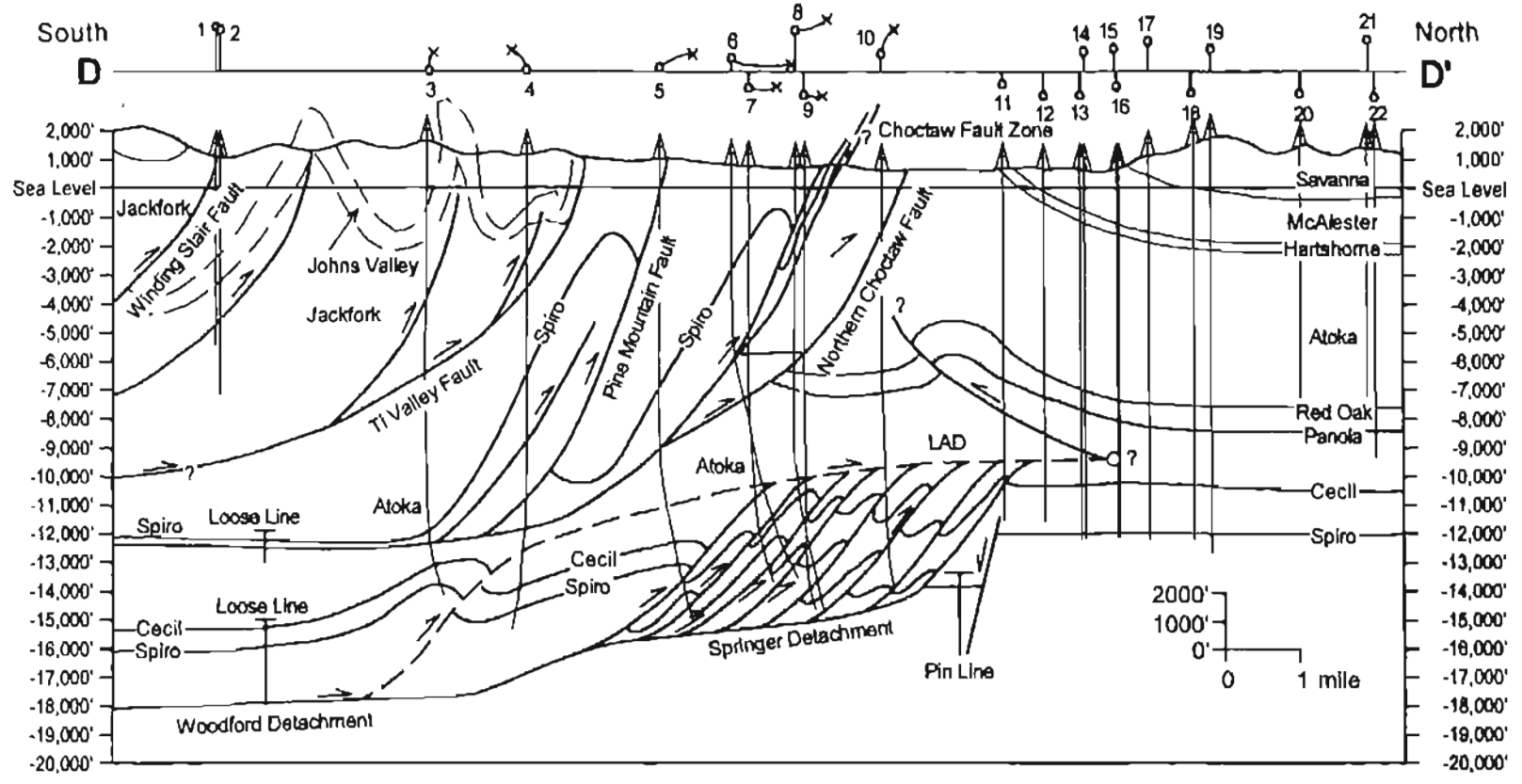

1. H&H Star Energy
   1-35 Buffalo Creek
   35-T4N-R20E
2. Chesapeake Operating Inc.
   Henry No. 1-35
   35-T4N-R20E
3. Mobil Exploration & Production
   Winding Stair No. 1A-14
   14-T4N-R20E
4. Anadarko Pet. Corp.
   Prentice "A" #1-11
   11-T4N-R20E
5. Arco Oil & Gas
   Norman 1-34
   34-T5N-R20E
6. Amoco Production
   Bauman Jack No. 1
   27-T5N-R20E
7. Amoco Production
   Raymond Smith No. 1
   26-T5N-R20E
8. Anadarko Pet. Corp.
   Nicholson "A" 1-22
   27-T5N-R20E
9. Anson Corp.
   Sinner #1-23
   23-T5N-R20E
10. ARCO Oil & Gas
    Rock Island 1-15
    15-T5N-R20E
11. Austin Production
    Robinson No. 1-11
    11-T5N-R20E
12. Mustang Production
    Adams #1-2
    2-T5N-R20E
13. Mustang Production
    Booth #1-2
    2-T5N-R20E
14. Mustang Production
    Cathey #1-3
    3-T5N-R20E
15. Mustang Production
    Metcalfe #1-34
    34-T6N-R20E
16. Mustang Production
    Foster #1-35
    35-T6N-R20E
17. Sunset Int. Pet. Corp.
    Fisherman #1
    34-T6N-R20E
18. Mustang Production
    Young & Cooper #1-26
    26-T6N-R20E
19. D. C. Slawson
    P. J. #1-27
    27-T6N-R20E
20. Dyco Petroleum
    Music #1
    23-T6N-R20E
21. Shell Oil Co.
    Foster #1-15
    15-T6N-R20E
22. Amoco Prod.
    Garrett No. 2
    14-T6N-R20E

Figure 47. Balanced structural cross-section D-D'. Location of cross-section shown in Figure 43.

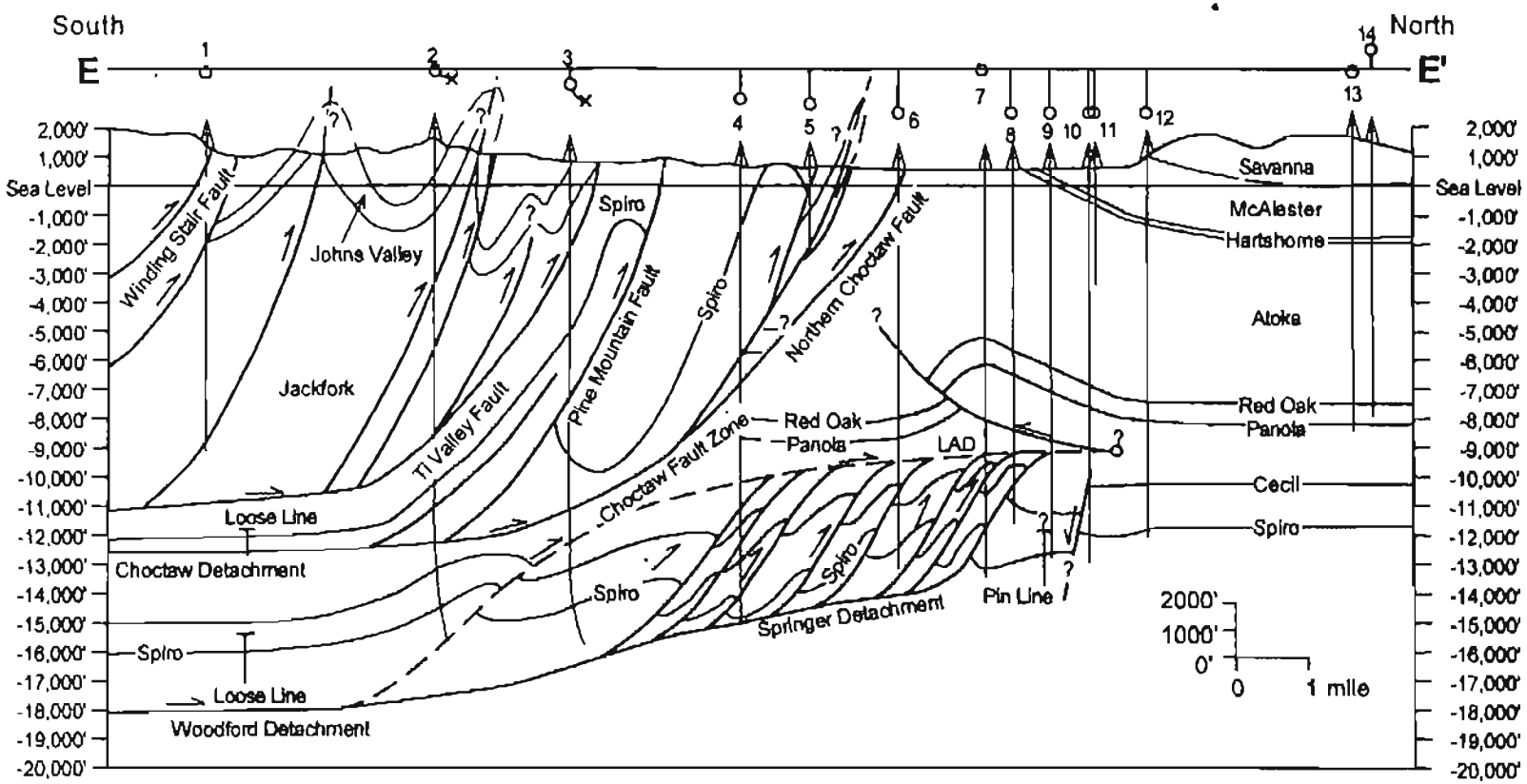

1. H&H Star Energy
   Middle Mountain #1-36
   36-T4N-R20E

2. H&H Star Energy
   Devil's Hollow #1-13
   13-T4N-R20E

3. Mobil Oil
   Long Creek #1-1
   1-T4N-R20E

4. Anson Corp.
   Long Creek #1-25
   25-T5N-R20E

5. Anson Corp.
   Boykin #1-24
   24-T5N-R20E

6. Anson Corp.
   Colley #1-13
   13-T5N-R20E

7. Mustang Production
   Robinson #1-11
   11-T5N-R20E

8. Donald C. Slawson
   Abbott #1-12
   12-T5N-R20E

9. Donald C. Slawson
   Foster #1-1
   1-T5N-R20E

10. Kaiser-Francis Oil
    Miranda #1
    1-T5N-R20E

11. Gulf Oil Co.
    Booth #1-1
    1-T5N-R20E

12. Mustang Production Co.
    Austin #1-36
    36-T6N-R20E

13. Midwest Oil Co.
    Garrett #1
    14-T6N-R20E

14. Barrett Resources
    Garrett #3
    14-T6N-R20E

Figure 48. Balanced cross-section E-E'. Location of cross-section shown in Figure 43.

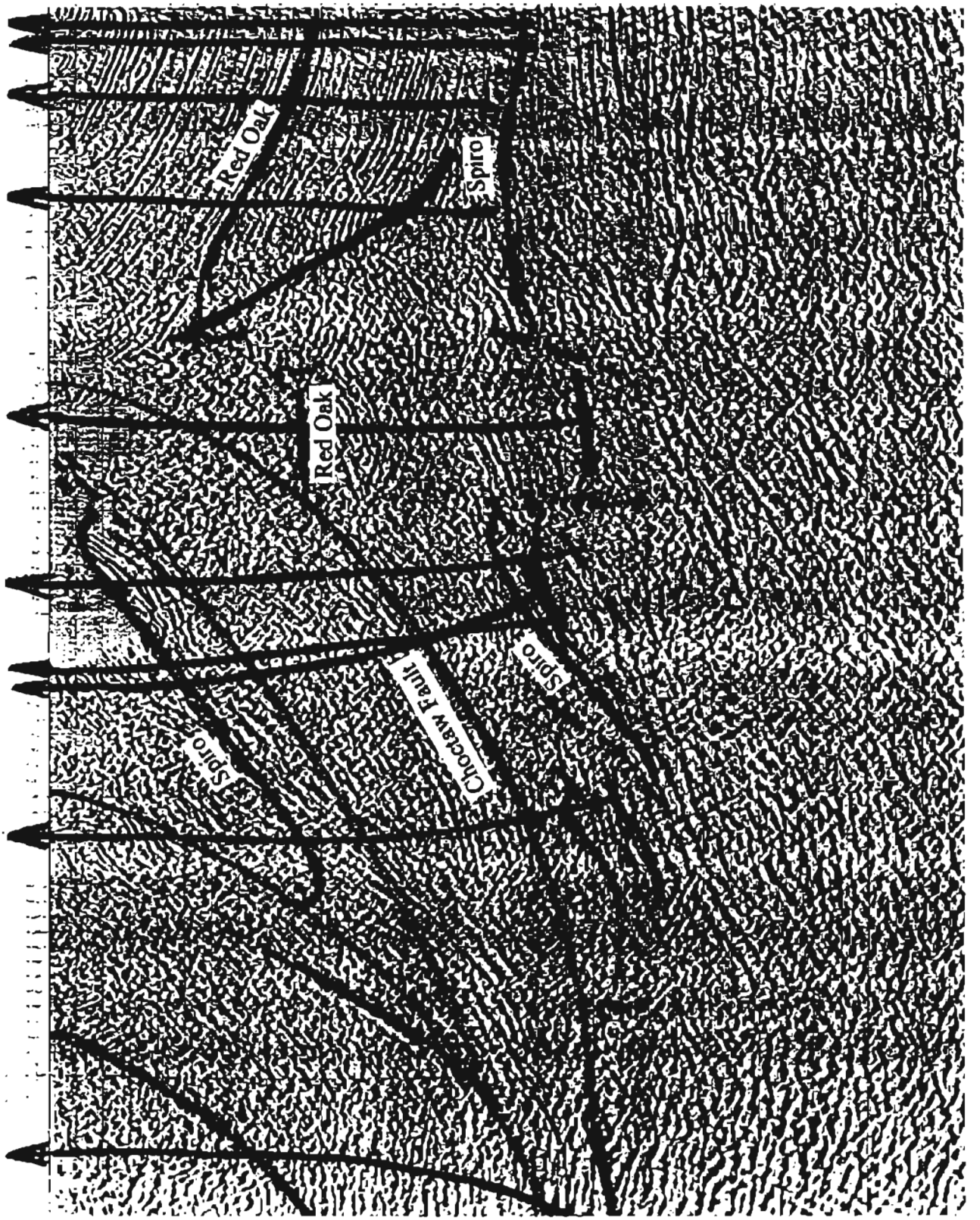

Figure 49. Seismic line QM5-8 donated by Amoco

MAJOR THRUST FAULTS

Figure 50 is a simplified geologic map of the study area that shows several south-dipping thrust faults to the southward from the trace of the Choctaw fault zone. Some of these are major thrusts, whereas others are splay faults off major faults (Figures 44-48). These faults are interpreted as branches from the Choctaw detachment (in the subsurface) (Figures 44-48, Plates I-V).

The Spiro sandstone of the subsurface is used to delineate the structural geometry of the thrust system. The Atokan Cecil, Panola, and Red Oak sandstones are also used to solve the complex geometry of the footwall of the Choctaw fault.

The Choctaw fault is the boundary between two different structural geometries. The hanging wall block has many listric thrust faults in an imbricate fan structure (Figures 44-48, Plates I-V). The footwall block contains a lower and upper detachment surface, duplex structures, normal faults, and a triangle zone.

WINDING STAIR FAULT

The Winding Stair fault is the southernmost surface fault within the study area. Areal geologic maps by Suneson, Ferguson, and Hemish (1987, 1988) indicate 70 to 80 degrees of southward dip along the fault. The Winding Stair fault juxtaposes the Jackfork Formation and the younger Atoka Formation. The amount of displacement along the fault is unknown. This is due to the lack of a piercing point, which would permit location of a bed in the hanging wall and footwall of the fault. The Winding Stair fault is located near the southern ends of the cross-sections (Figures 44-48 and Plates I-V).

CHOCTAW DETACHMENT

Cross-sections within the study area indicate that a detachment exists in the southern part of the study area. Figures 44-48 and Plates I-V show the dips of the Ti Valley fault, the Pine Mountain fault, and the Choctaw fault are less steep at depth. This variation in dip along the faults is indicated from seismic data (Figure 49). Wells in the southern part of the study area cut the Spiro sandstone at two to three places (Figures 44-48 and Plates I-V). Cross-section B-B' (Figure 45) contains two indications of horizontal Spiro sandstone; one just below the Ti Valley fault and the other at approximately -16,000 to -17,000 feet. The horizontal nature of the two Spiro units indicates that a detachment surface must cut between them. According to the interpretation of faulting in Figures 44-48 (Plates I-V), a horizontal fault would have to connect the Pine Mountain and Choctaw faults. Since the Choctaw fault is the leading thrust, the detachment is named the Choctaw Detachment. The Choctaw and Pine Mountain faults are branches from this detachment (Figures 44-48 and Plates I-V). Akthar (1995) proposed that the Ti Valley fault also branches from this detachment surface. He also proposed that the Choctaw Detachment was a branch off the Woodford Detachment. This branch occurs to the south of the study area.

TI VALLEY FAULT

The Ti Valley fault is located to the north of the Winding Stair fault. It extends about 240 miles, from near Atoka, Oklahoma to near Jacksonville, Arkansas (Suneson, 1988). The hanging wall of the Ti Valley fault contains several overturned folds within the Johns Valley Formation (Figure 50, Plate 7). Thrusts are interpreted as forming the

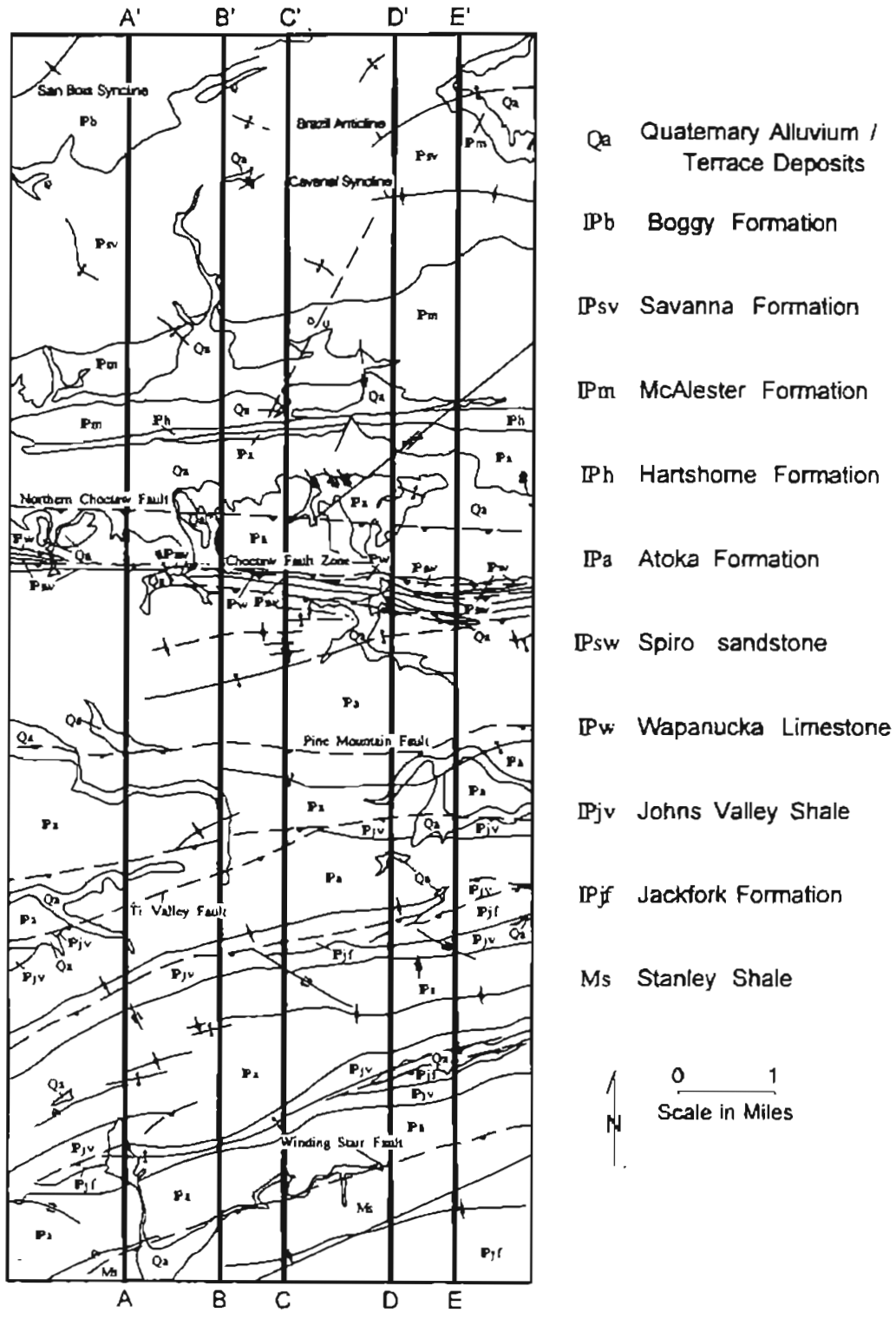

Figure 50. Generalized geology and tectonic map of the study area.

cores of these anticlines. Evidence for this is shown in cross-sections D-D' and E-E' (Figures 47-48) for the thrust cored anticline just to the north of the Winding Stair fault. Folding of the Johns Valley Formation was determined largely from surface geology.

The footwall of the Ti Valley fault contains the first identifiable location of the Spiro sandstone from the south in the subsurface. The Spiro formed a hanging wall anticline in the subsurface as it was thrust over underlying strata (Figure 19). This thrusted block was rotated as the Pine Mountain fault formed. Within the footwall of the Pine Mountain fault, the Spiro was folded as the imbricate fan propagated into the basin.

The Ti Valley fault (Figures 44-48 and Plates I-V) is a thrust fault of the leading imbricate fan in the hanging wall of the Choctaw fault. The Ti Valley fault and the blind splays to the north are the cores of anticlines (Figures 44-48 and Plates I-V). On the surface, this is manifested by the folding of the Johns Valley Shale (Figures 44-48 and Plates I-V).

At the surface, the Ti Valley fault dips about 70 to 80 degrees, based on seismic and well-log data. The fault is interpreted as having "flattened out" at depth (Figures 44-48 and Plates I-V). Hendricks (1959) estimated the "minimum displacement"along the Ti Valley fault to have been 20 miles.

Stratigraphy of the hanging wall and footwall of the Ti Valley fault is different. In the hanging-wall, the Lower Atokan is represented by the uppermost part of the Johns Valley Shale. In the footwall block, the Lower Atokan is represented by the Spiro sandstone. The transition zone between these time-equivalent units is very difficult to locate. Suneson and others believe that a surface expression of the transition zone is at

Hairpin Curve (Sec 3, T3N R19E to Sec 2, T3N R20E (Suneson, 1990). Within this study area, the hanging wall of the Ti Valley fault contains the Johns Valley Shale whereas the footwall contains the Atoka Formation (Figures 44-48 and Plates I-V). It is unclear whether the transition occurs in the extreme south end of the cross-section in the footwall block, was thrusted up and subsequently eroded or occurs to the south of the study area.

PINE MOUNTAIN FAULT

The Pine Mountain fault is located between the Ti Valley and Choctaw faults and is sub-parallel to them (Figures 44-48 and Plates I-V). The fault dips southward between 65 and 80 degrees, becoming less steep with depth. The Pine Mountain fault is interpreted as a splay from the Choctaw Detachment surface at depth (Figures 44-48 and Plates I-V). The Spiro sandstone is in the hanging wall and footwall blocks. The footwall Spiro sandstone breaches the surface in a faulted zone just south of the surface trace of the Choctaw fault (Figure 48 and Plate V).

CHOCTAW FAULT

The Choctaw fault is the boundary between the Ouachita Mountains and the Arkoma basin in Oklahoma. The fault extends more than 120 miles within Oklahoma and trends west-southwest to east-northeast. To the southwest, the Choctaw fault forms a splay, the southernmost unit of which is the main fault. This splay was named as the Choctaw fault by Suneson, Hemish, and Ferguson (1989). In the Wilburton area, Akhtar (1995) and Sagnak (1996) showed the Spiro at the surface along the Choctaw fault. In the study area, in the hanging wall of the Choctaw fault, there is a fault zone that contains an outcrop of the Spiro sandstone. This fault zone was informally named the "Ridge

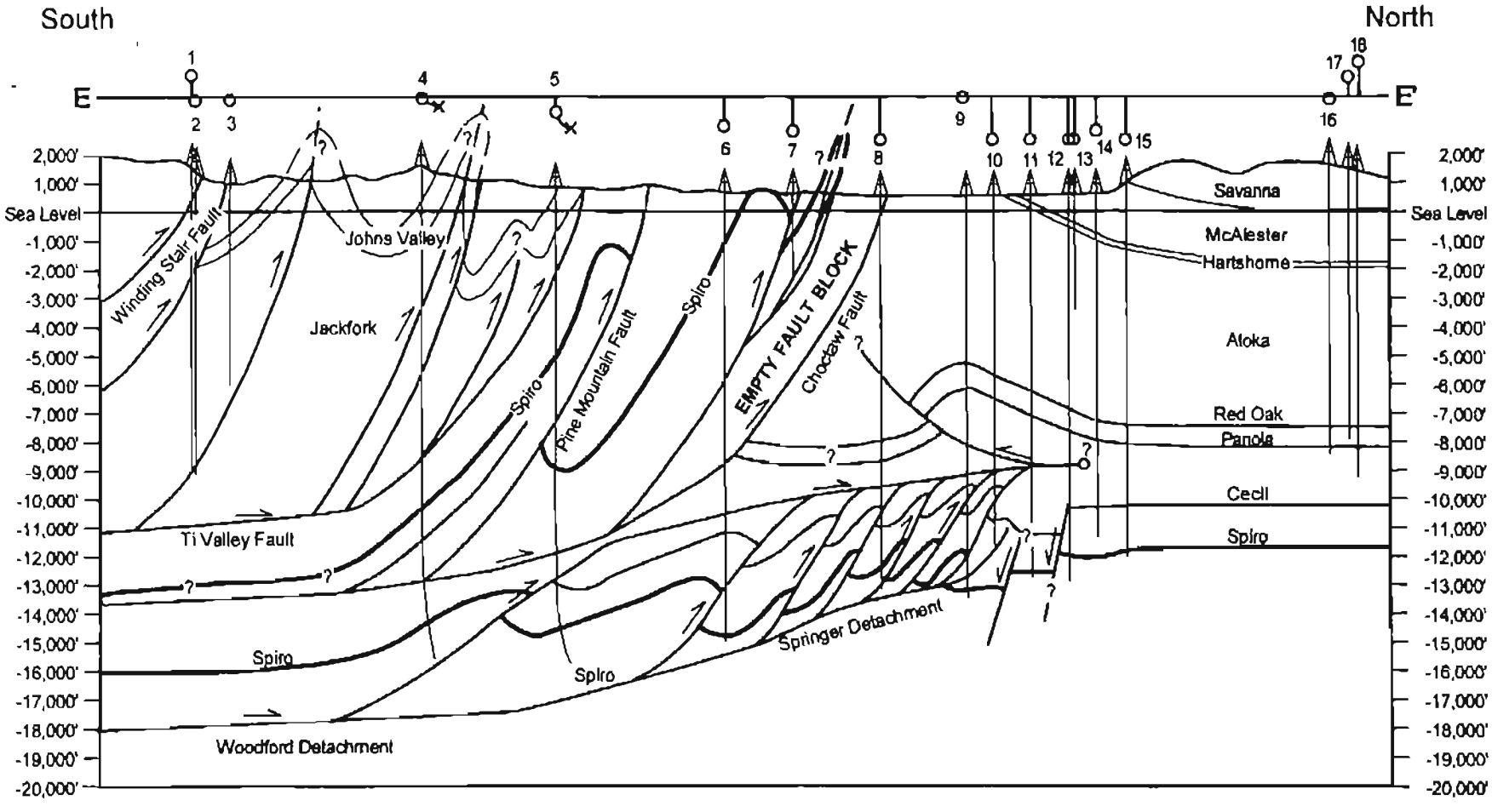

Figure 51. Interpretation of geometry using the Northern Choctaw Fault as the leading edge of the thrust system.

Thrust" by Cemen (personal comm., 1997). In this study, the "Ridge Thrust" is named the Choctaw Fault Zone and the Choctaw fault is referred to as the Northern Choctaw fault. When a cross-section is constructed using the placement of the Choctaw fault by Hemish, Suneson, and Ferguson (1988), there is a thick fault block basinward of the Choctaw Fault Zone that contains no Spiro sandstone (Figure 51). However, the fault block does contain both the Red Oak and Panola sandstones. It would be impossible to restore the cross-sections where a fault block does not contain the Spiro sandstone. The absence of the Spiro sandstone in this block suggests that the leading-edge thrust in the study area is the Choctaw Fault Zone. The splay that is now termed the Northern Choctaw Fault must be younger than the Choctaw Fault Zone since it does not cut the Spiro sandstone.

In the hanging-wall block of the Choctaw Fault Zone are several secondary thrusts. These are between the Choctaw and Pine Mountain faults. These southward-dipping thrusts are interpreted as joining the Choctaw Fault Zone where it begins to "flatten out" to the south. They form a leading imbricate fan structure with the Choctaw Fault Zone as the leading thrust. Perry and Suneson (1990) suggested about 6 miles of shortening along the Choctaw Fault.

Geometry of the footwall block of the Choctaw thrust is different from that of the hanging-wall block. Where the hanging wall had imbricate fans, the footwall block has duplexes between two main detachment surfaces, normal faults, and a triangle zone.

BASAL DETACHMENTS

The two basal detachments in the footwall block of the Choctaw fault are the Woodford and Springer Detachments. The Woodford Detachment is named for the

Woodford Shale which is the "host" for the fault (Hardie, 1988). It is a gently northward-sloping detachment that is 17,000 to 18,000 feet below sea level. In the southern areas of the cross sections (Figures 44-48 and Plates I-V), the Woodford Detachment acts as a floor thrust for a duplex system called the Gale-Buckeye thrust-system (Wilkerson and Wellman, 1993). The Woodford rises gently northward and is the detachment surface for thrusts that cut the Spiro and Cecil sandstones. Northward along the Woodford Detachment, the décollement rises to the level of the "Springer" Shale (Figures 44-48 and Plates I-V). At this location, the décollement is named the Springer Detachment. The Springer Detachment is approximately 16,000 to 17,000 feet below sea level. The Springer Detachment forms the floor thrust of a set of horses that contain the Spiro and Cecil sandstones.

The detachment that forms the roof of the horses is named the Lower Atokan Detachment (Akhtar, 1995), which is difficult to place on the cross-sections. Evidence for the detachment is in cross-sections (Figures 44-48 and Plates I-V) and on seismic line QM5-8 (Figure 49 and Plate 6). The Red Oak and Panola sandstones in the footwall of the Choctaw Fault are folded gently, as are units of the San Bois Syncline above them. Several thousand feet below this syncline, the Spiro and Cecil sandstones are included in a duplex structure (Figures 44-48 and Plates I-V). The seismic line (Figure 49 and Plate 6) also shows different attitudes in dip between the Spiro and Red Oak sandstones. This change in geometry suggests that some barrier must separate them. This proposed barrier is the Lower Atokan Detachment (LAD). The Lower Atokan Detachment branches off from the Woodford Detachment and propagates northward into the basin and thrusts

under the San Bois Syncline. The San Bois Syncline marks a change in tectonic styles in the basin from faulting to folding.

The placement of these detachments was based on available data. The Springer and Woodford Shales are at depths such that only a few well logs encountered them. Where no data were available the detachments were placed by interpolation. The vertical distance between the base of the Spiro sandstone and the top of the Springer or Woodford Shales was recorded from logs of nearby wells and extrapolated to the cross-sections to approximate the depth to detachments.

DUPLEX STRUCTURES AND THE LOWER ATOKAN DETACHMENT

In the study area, duplex structures exist in the footwall of the Choctaw fault. The floor thrust is the Springer Detachment. Correlation of the Spiro sandstone between wells in Figures 44-48 suggests that the duplexes dip to the south forming a hinterland-dipping duplex. This duplex structure results in the formation of horses (Boyer and Elliott, 1982). These horses cause repeated sections of the Cecil and Spiro sandstones that are contained in each horse. The LAD is approximately 12,000 feet below sea level. It has a gradual ramp to the north of the leading duplex and dies into a backthrust somewhere above the Cecil sandstone.

The placement of horses within this study area is inferred from cross-sections that contain many data points (A-A', B-B', D-D') (Figures 44, 45, and 47). The geometry of thrusting is slightly different from that described by Akthar (1995) and Sagnak (1996) (Figure 52). The Choctaw fault and the backthrust are much closer together in the study area than they are in the Wilburton area. This could be caused by a change in aspect of

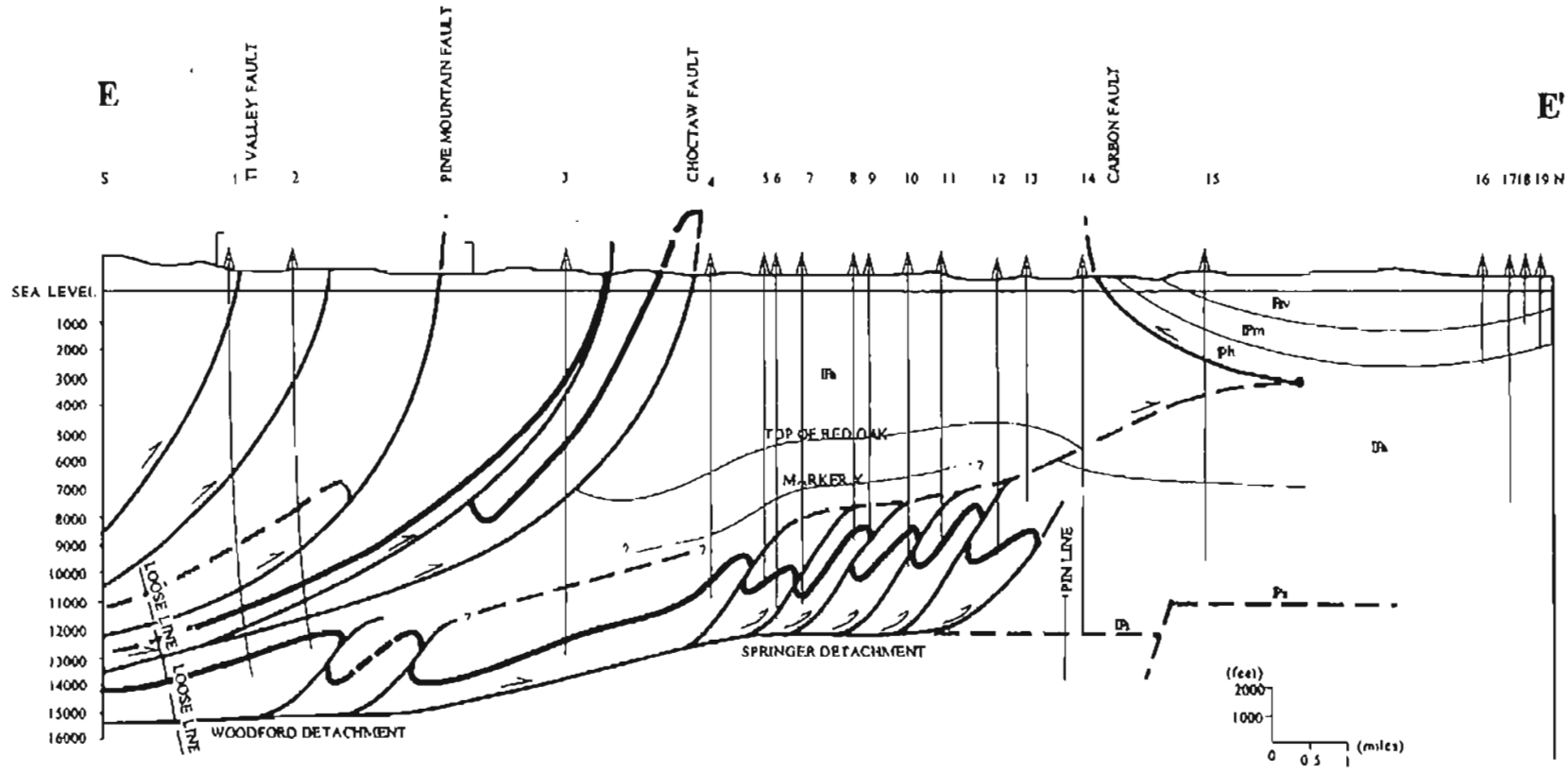

WELLS

1) EXXON
Garret No C-1
33-4N-18E (~1200W)

2) EXXON
Moore No 1
28-4N-18E (~700E)

3) TEX-PEK
A J. Mabry # 1-7
7-4N-18E (~100W)

4) KING RESOURCES
Pattison No 1-1
1-4N-17E (~200E)

5) ATLANTIC RICHFIELD
Andrew Kurilko # 1
35-5N-17E (~700W)

6) JMC EXP
Delia Holt # 1
35-5N-17E (~900E)

7) ARCO
Andrew Kurilko # 2
35-5N-17E

8) JMC EXP
Caudron # 5
26-5N-17E (~1500E)

9) SINCLAIR
Alfred Parker Unit # 1
27-5N-17E (~600W)

10) SAMSON
Sams # 1
22-5N-17E (~600E)

11) MOBIL
Boldin Sivil Unit 1
22-5N-17E (~1200E)

12) SAMSON
Bobo No 1
16-5N-17E (~1300W)

13) INTEX
Emory Estate Unit No 1
16-5N-17E (~700W)

14) GULFSTREAM
Randel No 1-9
9-5N-17E

15) COQUINA
Tobe No 1
5-5N-17E (~1000W)

16) EBERLY & MEADE
Argie Vaughn No 1
18-6N-17E

17) OXLEY
Argie Vaughn No 1
18-6N-17E

18) EBERLY & MEADE
Vaughn # 3-13
13-6N-16E (~100W)

19) EBERLY & MEADE
Vaughn # 2-13
13-6N-16E (~700W)

Figure 52: Structural cross-section E-E'. (Sagnak, 1996)

either fault. Another change from the Wilburton area is evidenced by the duplex structure in the footwall of the Choctaw fault. The duplex structure is compressed between and below the Choctaw fault and the backthrust. There are also fewer horses indicated in the Wilburton area (Figure 52) than are indicated on cross-section in the study area (Figures 44-48 and Plates I-V).

TRIANGLE ZONE

This study suggests that the triangle zone that was delineated in the OCAST project (Al-Shaieb et al., 1995, Cemen et al., 1994, 1995, 1997, Akthar, 1995, and Sagnak, 1996) continues into the study area. This triangle zone is floored by the Lower Atokan Detachment. The LAD surface propagated under the San Bois Syncline until stresses were no longer great enough to create a new fault, at which point, the detachment reached the zero displacement point and a backthrust formed. The backthrust is believed to be the subsurface equivalent to the Carbon fault that can be mapped at the surface in the Wilburton area. The presence of the backthrust is evidenced by relatively flat-lying Spiro and Cecil units and increasingly steeply dipping Panola and Red Oak sandstones above them (Figures 44-48 and Plates I-V). Cross-section B-B' and cross-section D-D' (Figures 45 and 47) indicate a flat lying Cecil sandstone below an upraised northward dipping section of Red Oak and Panola sandstones. The backthrust, along with the LAD and the leading thrust of the Choctaw Fault Zone forms a triangle zone that is similar in aspects to the ones proposed by Arbenz (1989) (Figure 35) and Camp and Ratliff (1989) (Figure 38), and is something of a hybrid between the two.

Whether this thrust intersects the Choctaw Fault is unknown. Lack of well control

in the proposed intersection zone makes it impossible to place the intersection. Likewise, the exact location of the zero displacement point along the LAD-backthrust zone is difficult to place with accuracy.

NORMAL FAULTS AND STRIKE SLIP FAULTS

Normal faults are in the footwall of the duplex structure and below the triangle zone. These normal faults are evidenced by a drop in subsea elevation of the Spiro sandstone in cross-sections A-A' and D-D' (Figures 44 and 47). The faults are interpreted to be remnant structures from the breakdown of the continental shelf during the Pennsylvanian and are therefore older than the thrust faults. Cross-sections indicate that the normal faults displace the Spiro sandstone, but their displacement does not reach into Middle Atokan units such as the Cecil. Ferguson and Suneson (1988) proposed that the growth faults acted as barriers that deflected the thrust faults upward.

Strike-slip faults are shown on the base maps (Hemish, Suneson, and Ferguson, 1988, 1989) (Figure 50). These faults have right-lateral movement and can be classified as tear faults. The tear faults are oriented in two directions. Faults in the footwall of the Choctaw Fault (Figure 50) are oriented in a northeast-southwest direction. These could be the result of differential stresses caused by the thrust sheet to the south. Faults in the hanging wall of the Choctaw Fault are oriented with a southeast-northwest trend.

RESTORED CROSS-SECTIONS AND SHORTENING

The cross-sections are restored using the key bed restoration method to calculate the amount of shortening for the Spiro sandstone (Figures 53-57). The Spiro sandstone was chosen as the key bed because it is an easily discernable and continuous unit within

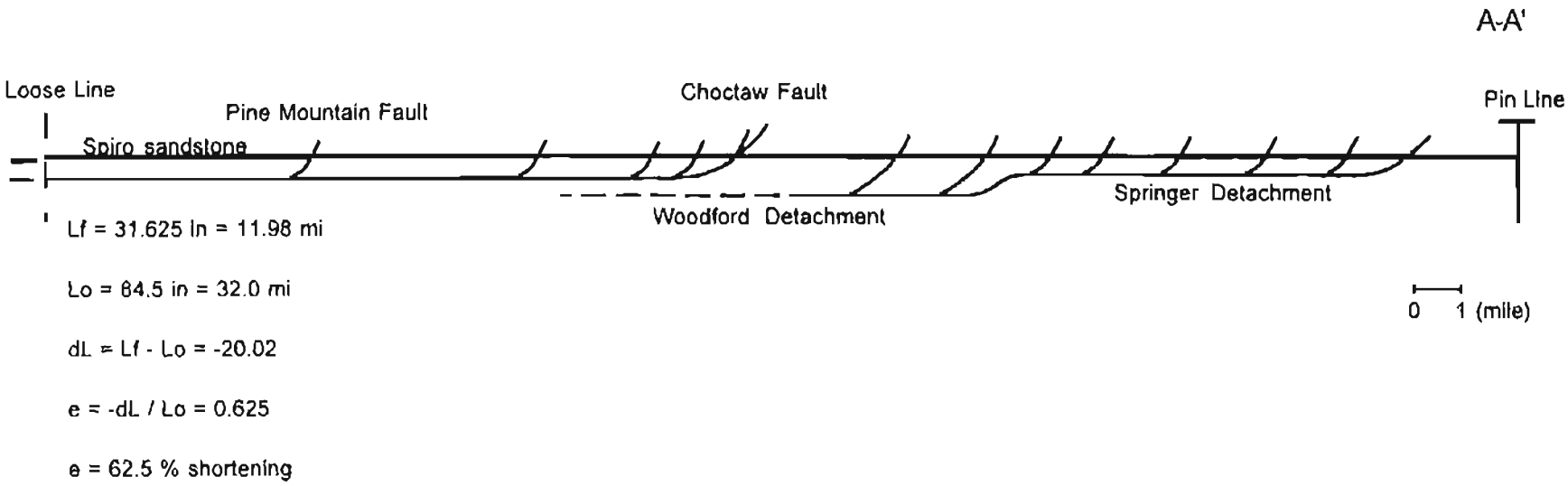

Figure 53. Restored cross-section A-A'.

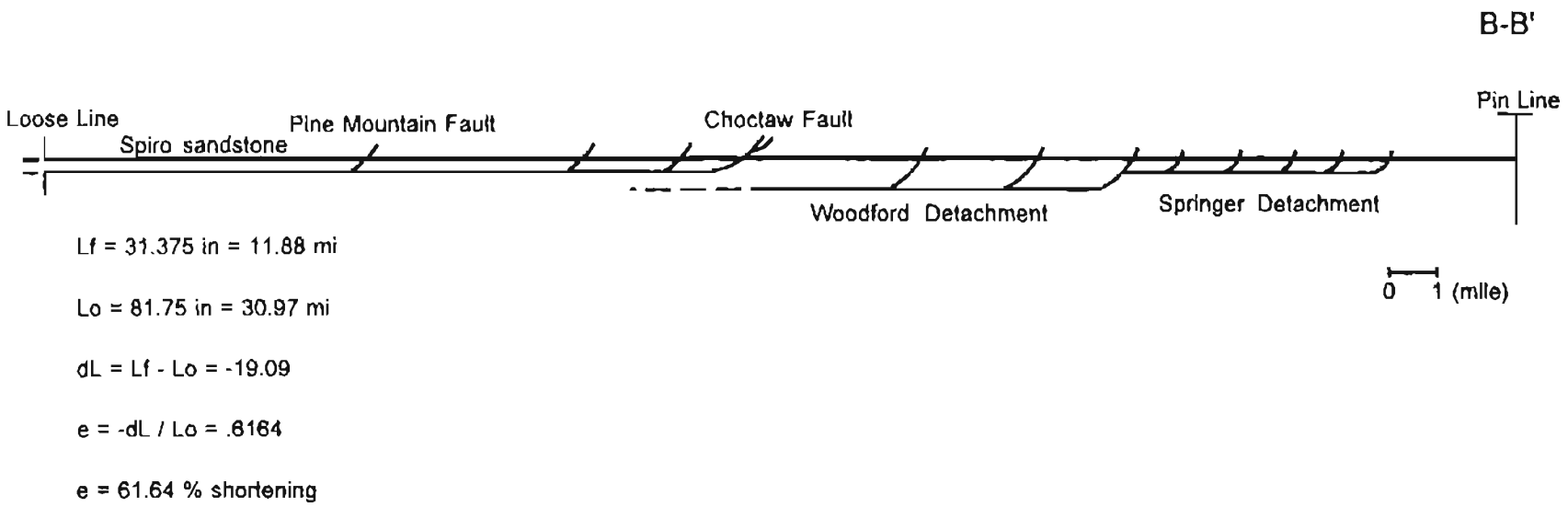

Figure 54. Restored cross-section B-B'.

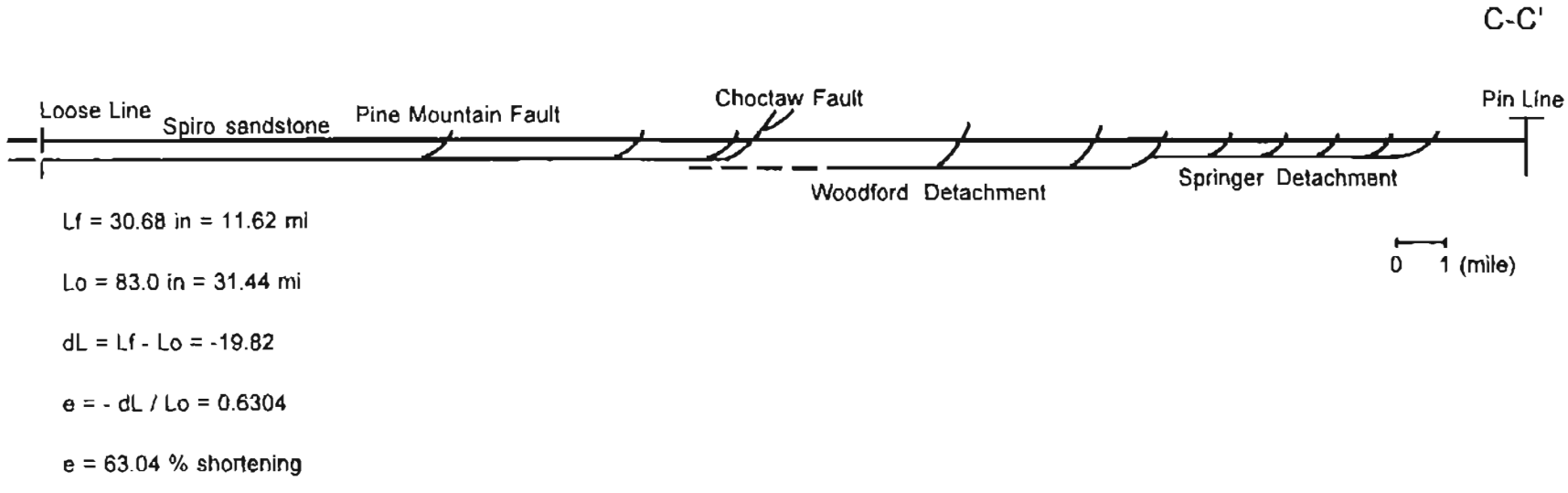

Figure 55. Restored cross-section C-C'.

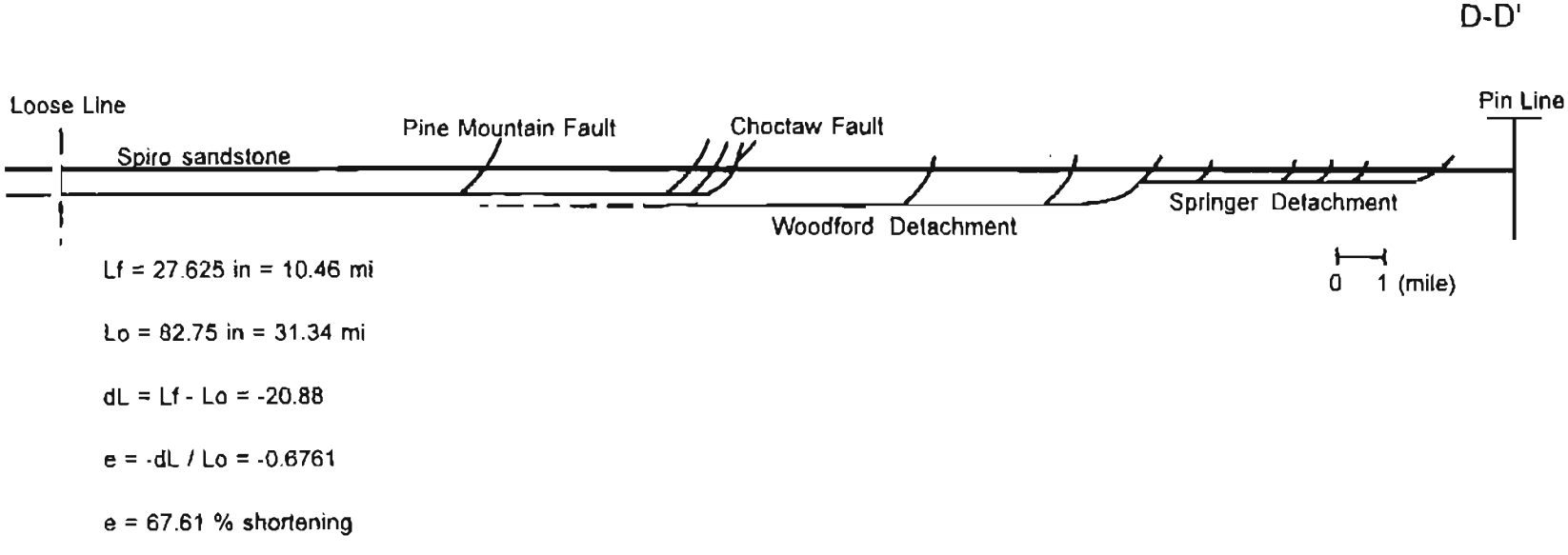

Figure 56. Restored cross-section D-D'.

E-E'

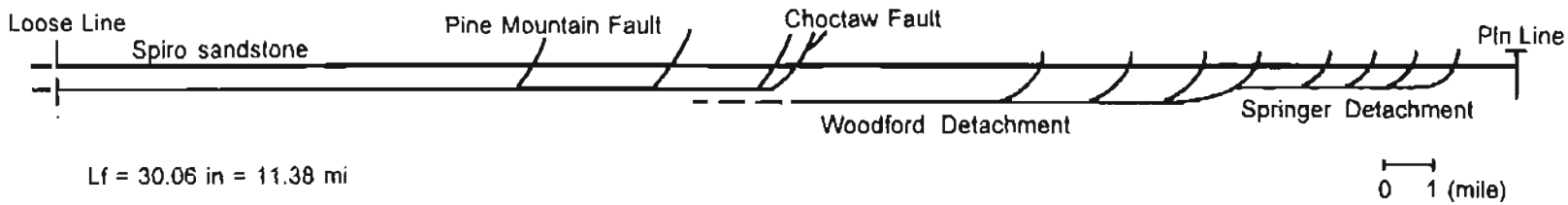

Lf = 30.06 in = 11.38 mi

Lo = 83 in = 31.44 mi

dL = Lf - Lo = -20.06

e = - dL / Lo = 0.6380

e = 63.8 % shortening

Figure 57. Restored cross-section E-E'.

the very thick Atoka Formation.

The pin lines for the restored cross-sections are located between the leading edge of the duplex structure and the normal fault where the strata was not affected by the shortening in the frontal zone. The loose lines are located in the south where there is no piercing point for the Spiro.

Calculations suggest about 63% shortening for the Spiro sandstone. Shortening amounts were calculated from 1:24,000 geologic maps. The scales for the cross-sections and the restorations are not the same. Restorations had to be scaled down in order to make them fit on the plates (Plates I-V). Lengths used in the restorations are measured lengths at the original 1:24,000 scale of the geologic maps. The calculations of shortening are as follows:

Cross-section A-A':

Lf = 31.625 in =11.98 mi

Lo = 84.5 in = 32.0 mi

dL = Lf-Lo= -20.02

e = -dL/Lo = .625

e = 62.5%

Cross-section B-B`:

Lf = 31.375 in = 11.88 mi

Lo = 81.75 in = 30.97 mi

dL = Lf-Lo = -19.09

e = -dL/Lo = .6164

e = 61.64%

Cross-section C-C':

Lf = 30.68 in = 11.62 mi

Lo = 83.0 in = 31.44 mi

dL = Lf-Lo = -19.82

e = -dL/Lo = .6304

e = 63.04%

Cross-section D-D`:

Lf = 27.625 in = 10.46 mi

Lo = 85.25 in = 32.29 mi

dL = Lf-Lo = -21.83

e = -dL/Lo = .6761

e = 67.61%

Cross-section E-E`

Lf = 30.06 in = 11.38 mi

Lo = 83.0 in = 31.44 mi

dL = Lf-Lo = -20.06

e = -dL/Lo = .6380

e = 63.8%

CHAPTER 6

CONCLUSIONS

The major accomplishments of this study are listed below.

1) The study area contains two different geometries. One above and the other below the Choctaw Fault.

2) The hanging wall of the Choctaw Fault contains a southward dipping imbricate fan complex that displaced the Spiro Sandstone.

3) The footwall of the Choctaw Fault contains a duplex structure floored by basal detachment surfaces at two different depths (Woodford-Springer Detachment).

4) A floor (Springer detachment) thrust and a roof thrust (Lower Atokan detachment) form the lower and upper boundaries of the duplex structure.

5) The leading edge of the Ouachita fold and thrust belt terminates into a shallow triangle zone that is bounded by the Choctaw fault, the Lower Atokan detachment, and the Carbon fault.

6) The average amount of shortening in the Panola and Baker Mountain quadrangles is approximately 63%.

REFERENCES

Akhtar, Saleem, 1995, The Geometry of Thrust System in the Wilburton Gas Field and Surrounding, Latimer County, Oklahoma, M.S. thesis, Oklahoma State University, Stillwater, OK, 97p.

Al-Shaieb, Z., 1988, The Spiro Sandstone in Wilburton Feild Area: Petrology, Diagenesis, Sedimentology, Porosity, and Reservoir Quality, Subnitted to Exxon Production Company, U.S.A.

Al-Shaieb, Z., I. Cemen, A. Cleaves, 1995, Overthrusted Natural Gas Reservoirs in the Arkoma Basin, OCAST Project no. AR2-025:4859, OCAST Research and Development Programs Division.

Al-Shaieb, Z., J.W. Shelton, J. Puckette, and D. Boardman, 1995. Sandstone and Carbonate Reservoirs of the Mid-Continent, Oklahoma City Geological Society - Oklahoma State University Core Workshop; Syllabus for Short Course, Oklahoma City Geological Society, Publishers, p. 59-72.

Arbenz, J. K., 1989, Ouachita Thrust Belt and Arkoma Basin: in Hatcher, R. D., Jr., W. A. Thomas, and G. W. Viele, eds., The Geology of North America, vol. F-2, The Appalachian-Ouachita Orogeny in the United States, Geological Society of America, Boulder, Colorado, p. 621-634.

Boyer, S. and D. Elliott. 1982, September. Thrust Systems. The American Association of Petroleum Geologists Bulletin: vol 66, no 9, p 1196-1230.

Butler, R.W.H. 1987. Thrust Sequences. Journal of the Geological Society, London, vol 144, p 619-634.

Cemen, I., Z. Al-Shaieb, R. Feller, and S. Akthar, 1994, Preliminary Interpretation of a Seismic Profile and the Spiro Reservoir Pressure Data in the Vicinity of the Wilburton Gas Field, Oklahoma Geological Survey Guidebook 29, p 249-251.

Cemen, I., Z. Al-Shaieb, A. Sagnak, S. Akhtar, and R. Feller, 1995, Geoletry of thrusting in Wilburton Gas Field and Surrounding Areas, Arkoma Basin, Oklahoma; Implications for Gas Exploration in the Spiro Sandstone Reserboirs; (Abstract) AAPG Bulletin. v. 79, no. 9, p. 1401.

Cemen, I., Z. Al-Shaieb, A. Sagnak, R. Feller, and S. Akhtar, 1997, Triangle Zone Geometry of the Frontal Ouachitas in the Wilburton Area, Arkoma Basin. Oklahoma: Implications for fault sealing in the Wilburton Gas Field (Abstract) AAPG Annual Convention Program with Abstracts, p. A-19.

Couzens, B.A., and D.V. Wiltschko, 1994, Some Constraints for Mechanical Models of Triangle Zones; (Abstract): Western Canadian and International Expertise, Exploration Update; A Joint Convention of CSEG and CSPG, Calgary, Alberta, 1994, p. 370-71.

Dahlstrom, C.D.A. 1969. Balanced cross sections. Canadian Journal of Earth Sciences: vol 6. p 743-757.

Ham, W. E., 1978, Regional Geology of the Arbuckle Mountains, Oklahoma: Oklahoma Geological Survey Special Publication 73-3, 61 p.

Hemish, L.A., N.H. Suneson, and C.A. Ferguson, 1988, Geologic map of the Panola Quadrangle, Latimer County, Oklahoma: Oklahoma Geological Survey, scale 1:24,000.

Hooker, E.M.O., 1998, The Distribution and Depostional Environment of the Spiro sandstone, Arkoma Basin, Haskell, Latimer, and Pittsburg Counties, Oklahoma: unpublished M.S. thesis, Oklahoma State University, Stillwater, Oklahoma, 98p.

Houseknecht, D. W., 1986, Evolution of Passive Margin to Foreland Basin: The Atoka Formation of the Arkoma Basin, South-Central U.S.A., in Allen, P. A., and Homewood, P. eds., Foreland Basins: International Association of Sedimentologists Special Publication 8, p. 327-345.

Houseknecht, D.W. and T.A. McGilvery, 1990, Red Oak Field, Structural Traps II. Traps Associated with Tectonic, AAPG Treatise of Petroleum Geology, Faulting Atlas of Oil and Gas Fields, p. 201-221.

Jamison, W.R., 1994. Triangle Zone Evolution Mechanistic Approaches, (Abstract): Western Canadian and International Expertise, Exploration Update; A Joint Convention of CSEG and CSPG, Calgary, Alberta, 1994, p. 217.

Johnson, K.S., 1988, General Geologic Framework of the Field-Trip Area, in K.S. Johnson, Editor, Shelf-to-Basin Geology and Resources of Pennsylvanian Strata in the Arkoma Basin and Frontal Ouachita Mountains of Oklahoma. Oklahoma Geological Survey Guidebook 25, p. 1-6.

Jones, P.B., 1994, Triangle Zone Geometry and Terminology, (Abstract): Western Canadian and International Expertise, Exploration Update; A Joint Convention of CSEG and CSPG, Calgary, Alberta, 1994, p. 69-70.

Keller, G. R. and S. E. Cebull, 1973, Plate Tectonics and the Ouachita System in Texas, Oklahoma, and Arkansas, Geological Society of America Bulletin, v. 83, p. 1659-1666.

Marshak, S. and G. Mitra. 1988. Basic Methods of Structural Geology. Prentice Hall Publishers, Englewood Cliffs, NJ.

Mazengarb, C., 1995, Interpretation of Structure from Surface Geology, Frontal Ouachitas, Southeastern Oklahoma: in K.S. Johnson, Editor. Structural Styles in the Southern Midcontinent, 1992 Symposium: Oklahoma Geological Survey Circular 97, p. 26-31.

McBee, William, Jr., 1995, Tectonic and Stratigraphic Synthesis of Events in the Region of the Intersection of the Arbuckle and Ouachita Structural Systems, Oklahoma; in Johnson, K.S., Editor, Structural Styles in the Southern Midcontinent, 1992 Symposium, Oklahoma Geological Survey Circular 97, p. 45-81

Price, R.A., 1994, "Triangle zones" as Elements in a Temporal and Spatial Spectrum of Tectonic Wedging and Delamination, (Abstract): Western Canadian and International Expertise, Exploration Update: A Joint Convention of CSEG and CSPG, Calgary, Alberta, 1994, p. 208.

Sagnak, Ata. 1996, Geometry of Late Paleozoic Thrusting Between Wilburton-Hartshorne Area, Arkoma Basin, Southeast Oklahoma. M.S. thesis, Oklahoma State University, Stillwater, OK, 131 p.

Shelton, J.W., 1974, Depositional Framework of the Atoka Formation in Eastern Oklahoma; in J. W. Shelton and T. L. Rowland Editors, Guidebook to the Depositional Environments of Selected Pennsylvanian Sandstones and Carbonates of Oklahoma. Oklahoma Geological Survey Special Publication 74-1, p.8-9.

Suneson, N.H., 1988. The Geology of the Ti Valley Fault in the Oklahoma Ouachita Mountains, in K.S. Johnson, Editor, Shelf-to-Basin Geology and Resources of Pennsylvanian Strata in the Arkoma Basin and Frontal Ouachita Mountains of Oklahoma, Oklahoma Geological Survey Guidebook 25, p. 33-48.

Suneson, N.H., 1990. Hairpin Curve Locality-Johns Valley Shale and Atoka Formation: Geology and Resources of the Frontal Belt of the Western Ouachita Mountains; Oklahoma Geological Survey Special Publication 90-1. Stop 3, p. 19-31.

Suneson, N.H., 1995, Structural Interpretations of the Arkoma Basin-Ouachita Mountains Transition Zone, Southeastern Oklahoma; A Review: in K.S. Johnson, Editor, Structural Styles in the Southern Midcontinent, 1992 Symposium, Oklahoma Geological Survey Circular 97, p. 259-263.

Suneson, N.H., J.A. Campbell, and M J. Tillford, 1990, Geologic Setting and Introduction: Geology and Resources of the Frontal Belt of the Western Ouachita Mountains; Oklahoma Geological Survey Special Publication 90-1, p 1-4.

Suneson, N.H. and C.A. Ferguson, 1987. Geologic map of the Baker Mountain Quadrangle, Latimer County, Oklahoma: Oklahoma Geological Survey, scale 1:24,000.

Suppe, John. 1983, September. Geometry and Kinematics of Fault-Bend Folding. American Journal of Science: vol 283, p 684-721.

Sutherland, P.K., 1982. Lower and Middle Pennsylvanian Stratigraphy, in South-Central Oklahoma, Oklahoma Geological Survey Guidebook 20, 42 p.

Tearpock, D. and R.E. Bischke. 1991. Applied Subsurface Geological Mapping. Prentice Hall Publishers. Englewood Cliffs, NJ.

Twiss, Robert, and E.M. Moores. 1992. Structural Geology. W. H. Freeman and Company, New York.

Valderrama, M.H., K.C. Nielsen, G.A. McMechan, and Holly Hunter, 1994, Three-Dimensional Seismic Interpretation of the Triangle Zone of the Frontal Ouachita Mountains and Arkoma Basin, Pittsburg County, Oklahoma, Oklahoma Geological Survey Guidebook 29.

Wilkerson, M.S., and P.C. Wellman, 1993, Three-Dimensional Geometry and Kinematics of the Gale-Buckeye Thrust System, Ouachita Fold and Thrust Belt, Latimer and Pittsburg Counties, Oklahoma. AAPG Bulletin, v. 77, no. 6, p. 1082-1100.

Woodward, N.B., S. Boyer, and J. Suppe. 1985. An Outline of Balanced Cross-Sections. Short Course Textbooklet produced by the Geological Society of America.

APPENDIX I

WELL LOG DATA SHEETS

Well Log Data

	Operator	Well	Location	Sec.	Field	K.B.	Top R O	Top Spiro	X-Section
	3N-20E								
1	H&H Star Energy	Hope #1-4	E/2 W/2 SE	4	Buffalo Mountain	785		18736	B-B'
	4N-20E								
2	Mobil Expl. & Prod.	Long Creek #1-1	500 FSL 2240 FWL	1	Wildcat	867	NR	NR	E-E'
3	H&H Star Energy	Dipping Vat #1-4	C SE	4	Damon East	1028		10620 / 16060	B-B'
4	H&H Star Energy	Lucky Strike #1-5	SE NE SW	5	Panola South	902	NR	14112	A-A'
5	Anadarko Pet.	Barnes #1-9 "A"	SE NW SE	9	Damon South	1145	12280	16286	B-B'
6	Anson Corp.	Golden #1-10	NW NE SW	10	Dipping Vat	1061		14914	C-C'
7	Arco Oil & Gas	Prentice "A" #1-11	N/2 N/2 S/2	11	Panola South	1245		15910	D-D'
8	H&H Star Energy	Devils Hollow #1-13	NE SE SW	13	Panola South	1618		16147	E-E'
9	Mobil Oil	Winding Stair #1A-14	SW SW SE	14	Panola South	1582		14745 / 16234	D-D'
10	H&H Star Energy	Dipping Vat #1-15	NW NE SW	15	Panola South	1385		11300	C-C'
11	H&H Star Energy	Coopers Hollow #1-16	NE NW SE	16	Panola South	1232		17197	B-B'
12	Amoco Prod.	Green Bay #1-17	1840 FSL 1600 FWL	17	South Wilburton	1224		17992	A-A'
13	Scana Exploration	Green Bay #2-17	565 FSL 840 FWL SE	17	South Wilburton	1188	NDE	NDE	A-A'
14	H&H Star Energy	Bear Suck Knob #1-20	SW NE SW	20	Eight Mile Mountain	1486	NR	NDE	A-A'
15	H&H Star Energy	Bear Suck Knob #1-20 "A"	SW NE SW	20	Eight Mile Mountain	1532	NR	11200	A-A'
16	H&H Star Energy	Eight Mile Mntn. #1-21	NW SE NW	21	Wildcat	1512		17600	B-B'
17	H&H Star Energy	Green Bay #1-34	SE SW NE	34	Wildcat	1135		NDE	C-C'
18	H&H Star Energy	Buffalo Creek #1-35	SW NW SE	35	Buffalo Mountain	976	NR	NR	D-D'
19	Chesapeake Oper. Inc.	Henry #1-35	2400 FNL 2100 FWL	35	Wildcat	1119	NR	NR	D-D'
20	H&H Star Energy	Middle Mountain #1-36	SW SE NW	36	Winding Stair	1045	NDE	NDE	E-E'

	5N-20E								
21	Kaiser-Francis Oil	Miranda #1	SW NE NW	1	Atoka	622	NDE	NDE	E-E'
22	Gulf Oil Expl. & Prod Co.	Booth #1-1	C NW	1	Panola	625			E-E'
23	D. C. Slawson	Foster #1-1	C SW	1	Panola	650	7351	13188	E-E'
24	Mustang Production	Adams #1-2	W/2 E/2 SW	2	Panola	607	7101	NDE	D-D'
25	Mustang Production	Booth #1-2	NW NW SE NW	2	Panola	610	7553	12540	D-D'
26	Mustang Production	Cathey #1-3	NE NE SW NE	3	Panola	596	7828	12646	D-D'
27	Mustang Production Co.	Cash-Mitchell #1-3	C SW	3	Panola	601	7290	NDE	C-C'
28	Unit Drilling	Hawthorne #1	E/2 E/2 NW SE	4	Panola	623	7987	NDE	C-C'
29	Unit Drilling	Maxey #1-4	SW SE	4	Panola	653	NDE	NDE	B-B'
30	Unit Drilling	Maxey #1-5	1090 FSL 1725 FWL SE	5	Panola	648	8305	NDE	B-B'
31	D.C. Slawson	McKee	N/2 SW SW	5	Panola	659	8542	NDE	A-A'
32	Mec Inc.	Lively #2	C SE SW	6	Panola	616	8472	NDE	A-A'
33	Williford Energy	Wiginton #1-7	SW NE NE	7	Panola	675	7550	NDE	A-A'
34	Williford Energy	Butzer #1-7	C SE	7	Panola	574	6090	NDE	A-A'
35	Unit Drilling	Cox #1	NW NE SW NE	8	Panola	659	6774	NDE	B-B'
36	Unit Drilling	Dear #1	SE NW NW	8	Panola	697	7490	NDE	A-A'
37	Unit Drilling	Go Lightly #1	N/2 SE NW	9	Panola	648	6339	14320	B-B' / C-C'
38	Austin Production Co.	Colvard Lm #1	C NW	10	Panola	626	6525	NDE	C-C'
39	Austin Production Co.	Robinson #1-11	NE SW NW	11	Panola	672	6200	NDE	D-D'
40	Mustang Production Co.	Robinson #1-11	C N/2 SE	11	Panola	585	6420	13710	E-E'
41	D. C. Slawson	Abbott #1-12	NW SE NW	12	Panola	764	6508	NDE	E-E'
42	Anson Corp.	Colley #1-13	SE SW SW	13	Panola	640	9100	10600 / 12750	E-E'
43	Arco Oil & Gas	Rock Island #1-15	SW SE SE	15	Panola South	613	7296	NDE	D-D'
44	Humble Oil & Refining	Shay #1	SW NE SW	17	Wildcat	626	6250	14348	A-A'
45	Edwin L. Cox	Shay #1	C S/2 NW	17	Wildcat	616	6356	NDE	A-A'
46	Unit Drilling	Harding #1	E/2 NE	18	Panola	575	6855	NDE	A-A'
47	Anson Corp.	Buzzard Gap #1-19	SE NE SW	19	Panola South	833	8889	13790	A-A'
48	Anson Corp.	Hardcastle #1-20	N/2 N/2 SE	20	Wildcat	684	8350	13940	B-B'

49	Amoco Production	Cindy #1-21	SE SW SW	21	Panola South	717		2160 / 13546	B-B'
50	Anson Corp.	Sinner #1-23	SW SE SW	23	Panola South	683		15253	D-D'
51	Anson Corp	Boykin #1-24	SE SW SW	24	Panola South	652		160	E-E'
52	Anson Corp.	Long Creek #1-25	1050 FSL 270 FWL	25	Panola South	861		15580	E-E'
53	Amoco Production	Raymond Smith #1	SE NE SW	26	Bear Suck Knob	710		13286 / 13740 / 14086	D-D'
54	Anadarko Petroleum	Nicholson "A" #1-22	300 FNL 2400 FEL	27	Cravens	748		1986 / 13920 / 15378	D-D'
55	Amoco Production	Jack Bauman #1	SE SE SE	27	Wilburton	N/A	5774	3945 / 13750 / 13840	D-D'
56	Anson Corp.	Turney #1-28	SE NW SW	28	Wildcat	1111		4310 / 14173 / 15000	B-B'
57	Anson Corp.	Cox #1-28	520 FNL 310 FEL	28	Panola South	887		14200	C-C'
58	Anson Corp.	Blakely #1-28	NE NE	28	Panola South	992	4700	NDE	C-C'
59	Anson Production	Clear Creek #1-29	190 FSL 1570 FWL	29	Cravins	876		8260 / 13253	A-A'
60	Anadarko Petroleum	H&H Cattle Co. #1-31	N/2 SE SE	31	Wilburton East	869	7900	15248	A-A'
61	Anson Corp.	Turner #1-33	NW SE SE	33	Panola South	1048		5614 / 15344	B-B'
62	Arco Oil & Gas	Norman #1-34	SE SE SE	34	Wilburton East	941		14500 / 15360 / 15955	D-D'
	6N-20E								
63	Midwest Oil Corp.	Garrett#1	SE NW SE	14	Red Oak-Norris	1019	9034	NDE	E-E'
64	Amoco Production	Garrett #2	SW SE NW	14	Red Oak-Norris	N/A			E-E'
65	Barrett Resources	Garrett #3	SW SW NE	14	Red Oak	1468	9032	NDE	E-E'
66	Shell Oil Co.	Foster #1-15	SE SW NE	15	Red Oak-Norris	1327	8927	NDE	D-D'
67	Dyco Petroleum Corp.	Parsons #A-1	C E/2 NE	16	Red Oak	1554	10050	NDE	C-C'
68	Texas Oil & Gas Corp.	Parsons #A-1	C NW SE SE	16	Red Oak-Norris	1416	9070	NDE	C-C'
69	Shell Oil Co.	Parsons #1-16	S/2 S/2 N/2	16	Red Oak-Norris	1497	10110	NDE	C-C'
70	Leben Drilling Inc.	Parsons Unit #1-17	E/2 W/2 E/2	17	Red Oak-Norris	1344	9961	NDE	B-B'
71	Leben Drilling Inc.	Jankowsky #1-18	1000 FEL 1300 FSL	18	Red Oak-Norris	1298	9842	NDE	A-A'
72	Tenneco Oil Co.	Cecil #1-19	SW SW NE SW	19	Panola	1058	NDE	13600	A-A'
73	Tenneco Oil Co.	Swart #1-20	C SW	20	Kinta	1210	10212	13858	A-A'
74	Dyco Petroleum	Music #1	W/2 W/2 E/2 NW	23	Red Oak-Norris	1513	NDE	NDE	D-D'

75	Mustang Production	Young & Cooper #1-26	C SW	26	Panola	1663	9335	13645	D-D'
76	D. C. Slawson	PJ #1-27	C E/2	27	Panola	1570	9330	13571	D-D'
77	Tenneco Oil Co.	Pierce #1-29	S/2 N/2 S/2 NW	29	Panola	1156	10235	13480	A-A'
78	Santa Fe Minerals	Pierce #1-30	E/2 NE	30	Panola	1500	10520	14103	A-A'
79	Leede Oil & Gas Co.	Wilburton Mountain #1	NE NW NW SE	31	Wildcat	1498	9400	13940	A-A'
80	Mobil Oil Co.	Parks #1	SE SW SW	33	Wildcat	672	8380	13080	B-B'
81	Mustang Production Co.	Parks #1-33	W/2 W/2 E/2 SE	33	Panola	1068	8750	13290	C-C'
82	Sunset Int. Petroleum Co.	Fisherman #1	1000' NE of Center	34	Red Oak	977	8704	13042	D-D'
83	Mustang Production	Metcalfe #1-34	N/2 N/2 S/2 SE	34	Red Oak	654	8274	12642	D-D'
84	Mustang Production	Foster #1-35	1170' S 820' W SW	35	Panola	652	8215	12630	D-D'
85	Mustang Production	Austin #1-36	SW SW SE NW	36	Panola	695	8260	12542	E-E'

Plates 1, 2, 3 , 4, 5,

There is a Plate 6 listed, but it was not accompanying the other plates; however, there are two Plate 7's and they are both represented here as:

7 and 7a.

South

A

North

A'

H&H Star Energy
Bear Suck Knob #1-20
20-T4N-R20E

H&H Star Energy
Bear Suck Knob #1-20
20-T4N-R20E

Amoco Production
Green Bay #1-17
17-T4N-R20E

Scana Exploration
Green Bay #2-17
17-T4N-R20E

H&H Star Energy
Lucky Strike #1-5
5-T4N-R20E

Anadarko Petroleum
H&H Cattle Co. #1-31
31-T5N-R20E

Anson Corp.
Clear Creek #1-29
29-T5N-R20E

Anson Corp
Buzzard Gap #1-19
19-T5N-R20E

Unit Drilling
Harding #1
18-T5N-R20E

Humble Oil & Refining Co.
Shay #1
17-T5N-R20E

Edwin L. Cox
Shay #1
17-T5N-R20E

Williford Energy
Butzer #1-7
7-T5N-R20E

Unit Drilling
Dear #1
8-T5N-R20E

Williford Energy
Wiginton #1-7
7-T5N-R20E

Unit Drilling
Cox #1
8-T5N-R20E

Donald C. Slawson
McKee #1-5
5-T5N-R20E

Wec Inc
Lively #2
6-T5N-R20E

Leede Oil & Gas Inc
Wilburton Mountain #1
31-T6N-R20E

Tenneco Oil Co.
Pierce #1-29
29-T6N-R20E

Santa Fe Minerals
Pierce #1-30
30-T6N-R20E

Tenneco Oil Co.
Swart #1-20
20-T6N-R20E

Tenneco Oil Co.
Orell #1-19
19-T6N-R20E

Leben Drilling
Jankowsky #1-18
18-T6N-R20E

Winding Stair Fault

Ti Valley Fault

Pine Mountain Fault

Choctaw Fault Zone

Northern Choctaw Fault

2, 000'
1, 000'
Sea Level
-1, 000'
-2, 000'
-3, 000'
-4, 000'
-5, 000'
-6, 000'
-7, 000'
-8, 000'
-9, 000'
-10, 000'
-11, 000'
-12, 000'
-13, 000'
-14, 000'
-15, 000'
-16, 000'
-17, 000'
-18, 000'
-19, 000'
-20, 000'

Johns Valley

Jackfork

Atoka

Spiro

Loose Line

Cecil

Woodford Detachment

Springer Detachment

Red Oak

Panola

LAD

Pin Line

Savanna

Macalester

Hartshorne

2000'
1000'
0'
0
1 mile

A-A'

Loose Line

Spiro sandstone

Pine Mountain Fault

Choctaw Fault Zone

Pin Line

Springer Detachment

Woodford Detachment

Lf = 31.625 in = 11.98 mi

Lo = 84.5 in = 32.0 mi

dL = Lf - Lo = -20.02

e = -dL / Lo = 0.625

e = 62.5 % shortening

0 1 (mile)

South-North
Balanced and Restored Cross-Section
A-A'

Justin Evans Plate I

South

North

B

B'

H&H Star Energy
Hope #1-4
4-T3N-R20E

H&H Star Energy
Eight Mile Mountain
21-T4N-R20E

H&H Star Energy
Coppers Hollow #1-16
16-T4N-R20E

Anadarko Petroleum
Barnes #1-9 "A"
9-T4N-R20E

H&H Star Energy
Dipping Vat #1-4
4-T4N-R20E

AnSon Corp.
Turner #1-33
33-T5N-R20E

AnSon Corp.
Turney #1-28
28-T5N-R20E

Amoco Prod.
Cindy #1-21
21-T5N-R20E

AnSon Corp.
Hardcastle #1-20
20-T5N-R20E

Unit Drilling
Cox #1
8-T5N-R20E

Unit Drilling
Go Lightly #1
9-T5N-R20E

Unit Drilling
Maxey #1-5
5-T5N-R20E

Unit Drilling
Maxey #1-4
4-T5N-R20E

Mobil Oil Co.
Parks#1
33-T6N-R20E

Leben Drilling
Parsons #1-17
17-T6N-R20E

Winding Stair Fault

Ti Valley Fault

Pine Mountain Fault

Choctaw Fault Zone

Northern Choctaw Fault

2,000'
1,000'
Sea Level
-1,000'
-2,000'
-3,000'
-4,000'
-5,000'
-6,000'
-7,000'
-8,000'
-9,000'
-10,000'
-11,000'
-12,000'
-13,000'
-14,000'
-15,000'
-16,000'
-17,000'
-18,000'
-19,000'
-20,000'
-21,000'

Savanna

Macalester

Hartshorne

Red Oak

Panola

Cecil

Spiro

Johns Valley

Jackfork

Spiro

Spiro

Red Oak

LAD

Loose Line

Loose Line

Cecil

Spiro

Spiro

Spiro

Pin Line

Springer Detachment

Woodford Detachment

2000'
1000'
0'
0
1 mile

B-B'

Loose Line

Spiro sandstone

Pine Mountain Fault

Choctaw Fault Zone

Pin Line

Woodford Detachment

Springer Detachment

0 1 (mile)

Lf = 31.375 in = 11.88 mi

Lo = 81.75 in = 30.97 mi

dL = Lf - Lo = -19.09

e = -dL / Lo = .6164

e = 61.64 % shortening

South-North
Balanced and Restored Cross-Section
B-B'

Justin Evans

Plate II

South

North

C

C'

H&H Star Energy
Green Bay #1-34
34-T4N-R20E

AnSon Corp.
Golden #1-10
10-T4N-R20E

AnSon Corp.
Tunney #1-28
28-T5N-R20E

AnSon Corp.
Cox #1-28
28-T5N-R20E

AnSon Corp.
Blakely #1-28
28-T5N-R20E

Amoco Production
Bauman Jack No. 1
27-T5N-R20E

Unit Drilling Co.
Go Lightly #1
9-T5N-R20E

Unit Drilling Co.
Hawthorne #1
4-T5N-R20E

Austin Production
Colvard Ln #1
10-T5N-R20E

Mustang Production
Cash-Mitchell
3-T5N-R20E

Mustang Production
Parks #1-33
33-T5N-R20E

Texas Oil, & Gas Corp.
Parsons #1 "A"
16-T6N-R20E

Shell Oil Co.
Parsons #1-16
16-T6N-R20E

Dyco Petroleum Corp.
Parsons #A-1
16-T6N-R20E

H&H Star Energy
Dipping Vat #1-15
15-T4N-R20E

Winding Stair Fault
Ti Valley Fault
Pine Mountain Fault
Choctaw Fault Zone
Northern Choctaw Fault
Spiro
Johns Valley
Jackfork
Spiro
Spiro
Red Oak
Panola
Atoka
L A D
Loose Line
Spiro
Cecil
Loose Line
Cecil
Spiro
Spiro
Loose Line
Pin Line
Springer Detachment
Woodford Detachment
Savanna
Macalester
Hartshorne
Atoka
Red Oak
Panola
Cecil
Spiro

2, 000'
1, 000'
Sea Level
-1, 000'
-2, 000'
-3, 000'
-4, 000'
-5, 000'
-6, 000'
-7, 000'
-8, 000'
-9, 000'
-10, 000'
-11, 000'
-12, 000'
-13, 000'
-14, 000'
-15, 000'
-16, 000'
-17, 000'
-18, 000'
-19, 000'
-20, 000'

2000'
1000'
0'
0
1 mile

Loose Line
Pine Mountain Fault
Choctaw Fault
Woodford Detachment
Springer Detachment
C-C'
Pin Line

0 1 (mile)

Lf = 30.68 in = 11.62 mi

Lo = 83.0 in = 31.44 mi

dL = Lf - Lo = -19.82

e = - dL / Lo = 0.6304

e = 63.04 % shortening

South-North
Balanced and Restored Cross-Section
C-C'

Justin Evans | Plate III

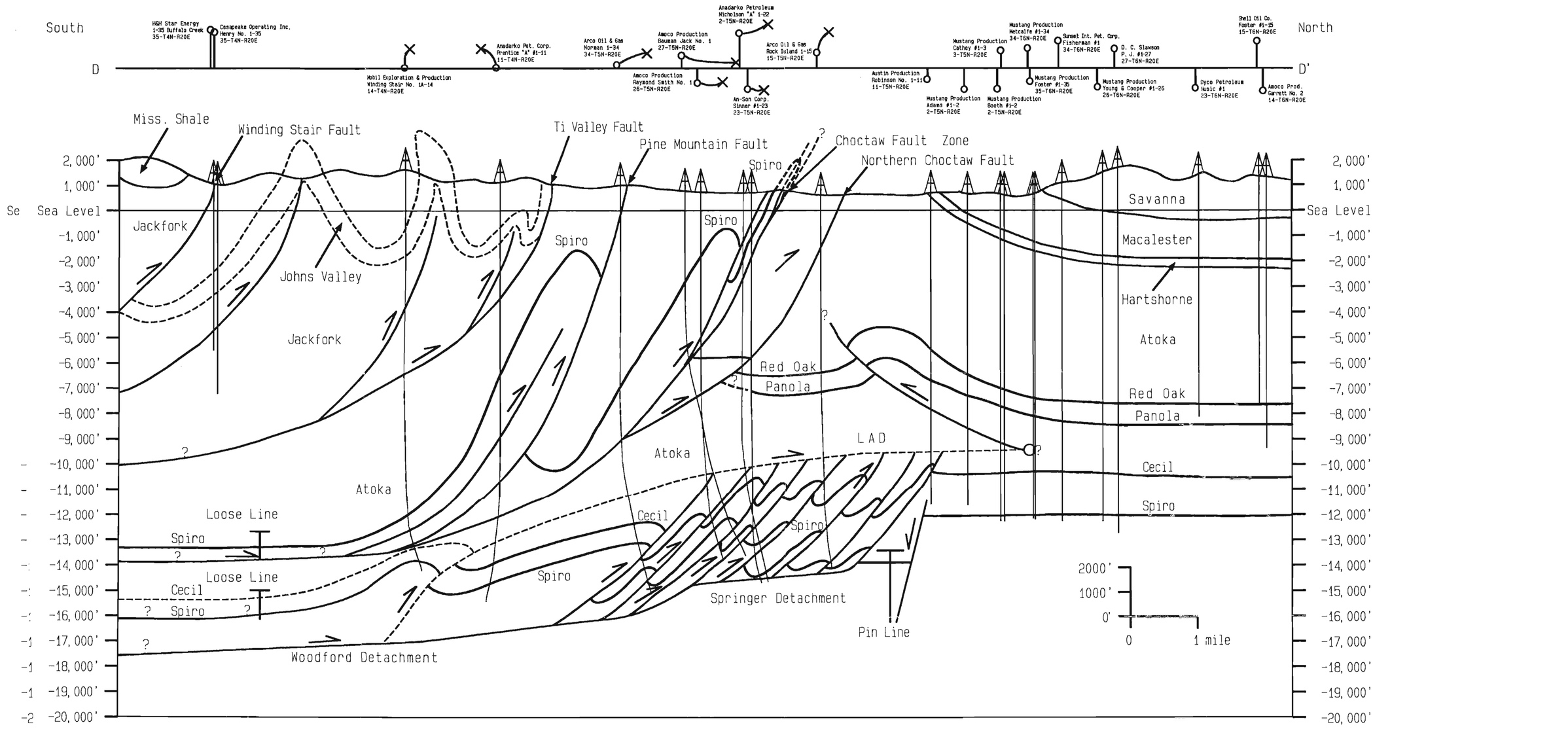

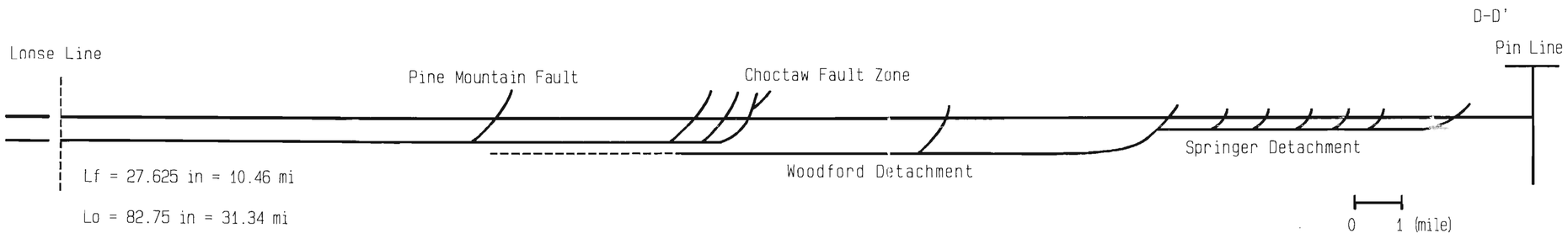

Lf = 27.625 in = 10.46 mi

Lo = 82.75 in = 31.34 mi

dL = Lf - Lo = -20.88

e = -dL / Lo = -0.6761

e = 67.61 % shortening

South-North
Balanced and Restored Cross-Section
D-D'

Justin Evans — Plate IV

South

North

E

E'

H&H Star Energy
Middle Mountain #1-36
36-T4N-R20E

H&H Star Energy
Devil's Hollow #1-13
13-T4N-R20E

Mobil Oil
Long Creek #1-1
1-T4N-R20E

AnSon Corp.
Long Creek #1-25
25-T5N-R20E

AnSon Corp.
Boykin #1-24
24-T5N-R20E

An Son Corp.
Colley #1-13
13-T5N-R20E

Mustang Production
Robinson #1-11
11-T5N-R20E

D. C. Slawson
Abbott #1-12
12-T5N-R20E

Kaiser-francis Oil
Miranda #1
1-T5N-R20E

D. C. Slawson
Foster #1-1
1-T5N-R20E

Gulf Oil Co.
Booth #1-1
1-T5N-R20E

Mustang Production Co.
Austin #1-36
36-T6N-R20E

Barrett Resources
Garrett #3
14-T6N-R20E

Midwest Oil Co.
Garrett #1
14-T6N-R20E

2, 000'
1, 000'
Sea Level
-1, 000'
-2, 000'
-3, 000'
-4, 000'
-5, 000'
-6, 000'
-7, 000'
-8, 000'
-9, 000'
-10, 000'
-11, 000'
-12, 000'
-13, 000'
-14, 000'
-15, 000'
-16, 000'
-17, 000'
-18, 000'
-19, 000'
-20, 000'

Winding Stair Fault
Ti Valley Fault
Choctaw Fault Zone
Northern Choctaw Fault
Johns Valley
Jackfork
Spiro
Savanna
Macalester
Hartshorne
Atoka
Red Oak
Panola
Cecil
Loose Line
Woodford Detachment
Springer Detachment
Pin Line
LAD

2000'
1000'
0'
0
1 mile

Loose Line
Spiro sandstone
Pine Mountain Fault
Choctaw Fault
E-E'
Pin Line
Springer Detachment
Woodford Detachment
0 1 (mile)

Lf = 30.06 in = 11.38 mi

Lo = 83 in = 31.44 mi

dL = Lf - Lo = -20.06

e = - dL / Lo = 0.6380

e = 63.8 % shortening

South-North
Balanced and Restored Cross-Section
E-E'

Justin Evans Plate V

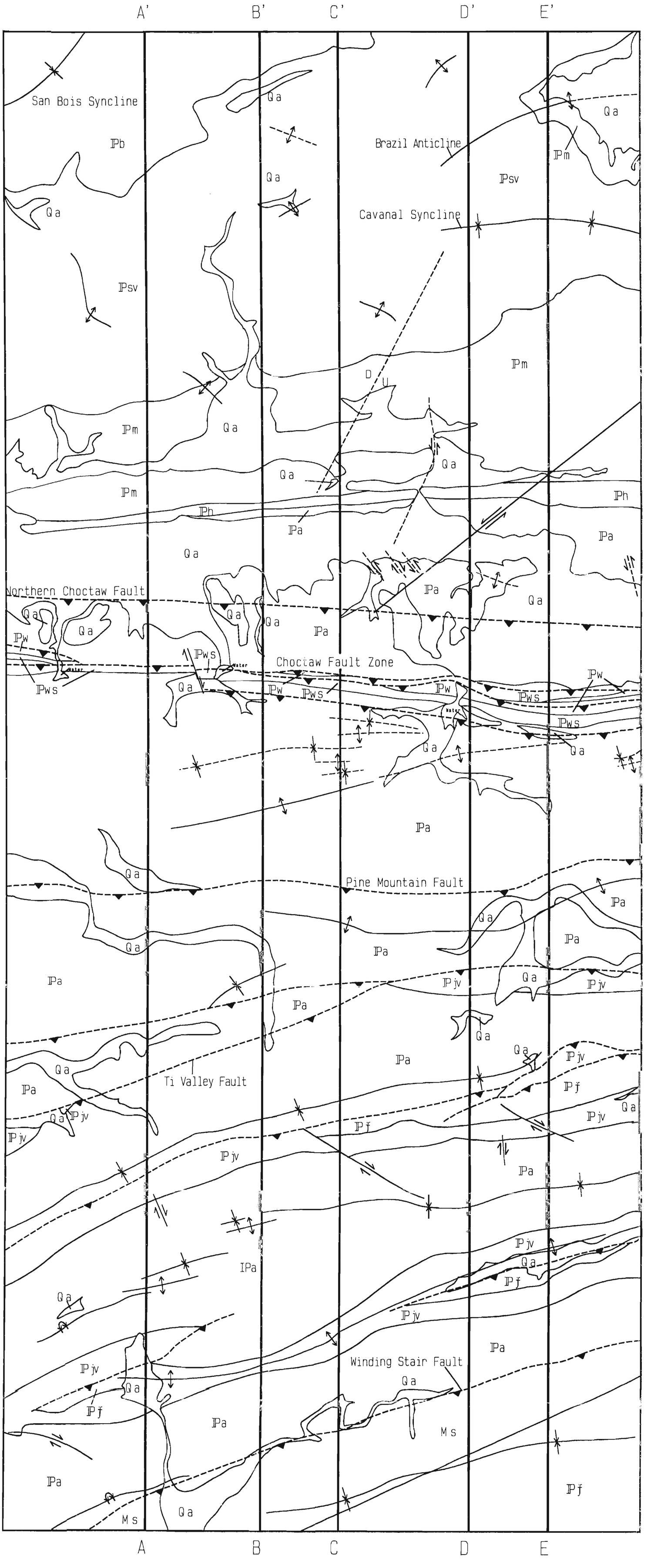

Qa Quaternary Alluvium / Terrace Deposits

Pb Boggy Formation

Psv Savanna Formation

Pm McAlester Formation

Ph Hartshorne Formation

Pa Atoka Formation

Pws Spiro sandstone

Pw Wapanucka Limestone

Pjv Johns Valley Shale

Pf Jackfork Formation

Ms Stanley Shale

N

0 1

Scale in Miles

Generalized Geologic Map
of Panola and Baker Mountain
7.5 Minute Quadrangles

Justin Evans Plate VII

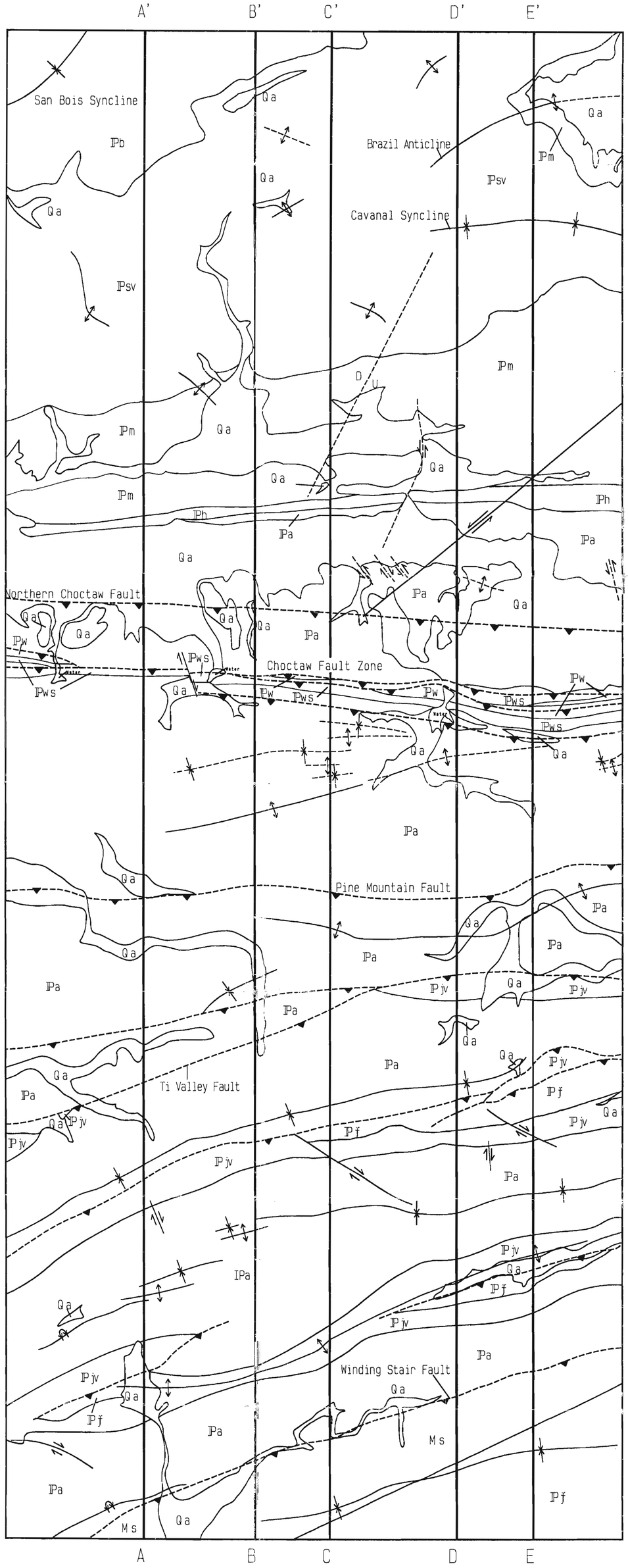

Qa Quaternary Alluvium / Terrace Deposits

Pb Boggy Formation

Psv Savanna Formation

Pm McAlester Formation

Ph Hartshorne Formation

Pa Atoka Formation

Pws Spiro sandstone

Pw Wapanucka Limestone

Pjv Johns Valley Shale

Pf Jackfork Formation

Ms Stanley Shale

N

0 1

Scale in Miles

Generalized Geologic Map
of Panola and Baker Mountain
7.5 Minute Quadrangles

Justin Evans Plate VII

VITA

Justin Evans

Candidate for the Degree of

Master of Science

Thesis: STRUCTURAL GEOMETRY OF THRUST FAULTING IN THE BAKER MOUNTAIN AND PANOLA QUADRANGLES, SOUTHEASTERN OKLAHOMA

Major Field: Geology

Biographical:

Education: Graduated from Shattuck High School. Shattuck, Oklahoma in May of 1990; received Bachelor of Science degree in Geology from Oklahoma State University, Stillwater, Oklahoma in December of 1994. Completed the requirements for the Master of Science degree with a major of Geology at Oklahoma State University in July. 1997.

Professional Experience:

Teaching Assistant: Department of Geology, Oklahoma State University
Summer Geologist Internship: Exxon Exploration Company: Houston Production Organization, Houston, Texas

Professional Memberships: American Association of Petroleum Geologists